COMPARISON OF LOW VOLTAGE RIDE THROUGH CAPABILITIES OF SYNCHRONOUS GENERATOR WITH STATCOM AND DFIG BASED WIND FARMS

PREPARED BY:

Kulisha W. APPADOO

University of Cape Town

This thesis was submitted to the University of Cape Town in the fulfillment of the academic requirements for the Master of Science degree in Electrical Engineering.

PREPARED FOR:

Dr S. Chowdhury

Department of Electrical Engineering

University of Cape Town

February 2015

DECLARATION

I declare that this Master's thesis, Comparison of Low Voltage Ride Through Capabilities of Synchronous Generator with STATCOM and DFIG based wind farms, is my own work. All sources that I have used or quoted have been indicated and acknowledged in the references. This work has not been submitted to any other university for any other degree or examination.

Signed by candidate

APPADOO Kulisha W.

Date

ACKNOWLEDGEMENTS

I would like to express my greatest and most sincere appreciation and thankfulness to the following people, who have helped me during the course of this thesis.

My supervisor, Dr. S. Chowdhury, for her continuous effort and help in providing the appropriate guidance and support during the development of this thesis.

My parents, sisters and fiancé for their infinite love and continuous support for my success in life.

My Friends, specially Shameem, Femi and Risha for their concerned help during the course of this thesis.

The department of Postgraduate Electrical Engineering in guiding me throughout the duration of this thesis.

TERMS OF REFERENCE

This thesis is submitted in the fulfillment of the academic requirements of a Masters of Science in Electrical Engineering at the University of Cape Town. The topic of this thesis was proposed by Dr. Chowdhury, from the Department of Electrical Engineering at the University of Cape Town, whose area of research is based mainly on Power systems and renewable energy scheme. Dr S. Chowdhury major aim of this thesis is to find a more effective low-voltage-ride-through design as per the new grid code requirement. The supervisor recommended the thesis to focus on the following requirements:

- Write a comprehensive literature review on the low-voltage-ride-through condition with respect to the new grid code requirement, the synchronous generator with compensation from STATCOM and the doubly fed induction generator.

- Develop an integrated model of a synchronous generator with STATCOM based wind system based and compare its efficiency with a built-up doubly fed induction generator with crowbar based wind farm.

- Perform simulations in MATLAB® / SIMULINK software version 7.6 to analyse the dynamic performance for the two different operating case study scenarios.

- Discuss and analyse obtained results

- Conclude and suggest recommendations for future work to be done based on this topic.

SYNOPSIS

Background to the thesis:

Increase in wind generation and grid-integration of wind energy technologies has resulted from an increasing demand of cheap and clean electricity across the globe. Wind generators are available as small, medium and large scale electric generators, usually in the range of 1kW to 100MW and are usually installed in areas rich in wind resource which may or may not be located close to the load centres.

Wind energy penetration has increased since the 1970s with the total worldwide capacity of installed wind power reaching about 282,275 MW. Apart from technical issues of grid-integration, research is also being done to investigate the participation of wind energy systems to enhance grid performance through fault ride-through capabilities, providing voltage control and power quality improvement etc. The goal of a Fault Ride Through (FRT) or Low Voltage Ride Through (LVRT) system is to enable a wind farm (WF) to withstand a severe voltage dip at the connection point and still stay connected to the power system as long as the fault persists. Wind turbine designs are required to incorporate LVRT capability as per Grid Code's requirements only if they are technically needed for a reliable and secure power system operation. The basic requirement for LVRT is that the wind turbines must maximise their reactive power injections to the network without exceeding the turbine limits. The maximisation of reactive current must continue for at least 150ms after the fault clearance or until the grid voltage is recovered within the normal operation range.

It is important here to discuss here the immediate impact of the voltage dip on the wind farm (WF) operation. During the voltage dip caused by the fault, the active power provided to the grid by the WF is instantaneously reduced. This power becomes at least temporarily lower than the mechanical power available at the rotor*;* hence the rotor speed of the wind generator increases. It is required for the LVRT capability of the WF, that the wind generators of the WF must not disconnect from the grid during fault persistence, either due to over-speeding or under voltage protections. After the clearing of the fault that led to the voltage dip, the voltage at the wind turbine bus would increase. It is also required that the wind generators should resume their power supply to the network without losing stability. However, the stability response of wind generators will vary according to their types. The risk of a loss of stability after the fault clearing is very limited for induction or synchronous generators with full power electronic converters such as STATCOM, and limited for DFIG type wind generators, thanks to the control. As the penetration of wind energy increases, the need to address the LVRT capability issues becomes more critical. Earlier, the wind turbines were allowed to trip when a voltage dip occurred. However, due to improved controls, now the wind turbines are expected to remain connected to the grid both during and after a fault. Upon voltage recovery,

the wind turbines must not consume excessive reactive power when re-exciting the generator, as this may result in a further voltage dip.

This thesis reports on results of the modelling and simulation studies carried out to demonstrate the compliance of a wind farm to meet the fault ride-through requirements of the National Grid Code in South Africa.

Summary of Research

This investigates the behaviour of different grid-integrated wind energy technologies during grid fault events and compares their fault ride through capabilities in relation to existing grid codes and power system stability. The research work focuses mainly on wind turbines using synchronous generators with STATCOM as the controller for the reactive power compensation. Static Synchronous Compensator (STATCOM) is a FACTS device which plays a vital role in controlling the reactive power in a power network. The main purpose of the STATCOM is to produce variable reactive shunt impedance that can be adjusted continuously in order to meet the compensation requirements of the power system. Mention may be made that the basic reactive power compensation is required to provide direct voltage support and transient and dynamic stability improvements while specific type of voltage support is needed in intermediate points and specific load terminals of a power system which feed voltage-sensitive loads. Thus STATCOM is installed to mitigate voltage variation, prevent voltage collapse and increase transient stability limits of a power system. Proper variation in the terminal voltage can further enhance transient stability and dynamic stability.

During the past years, the requirements were mainly focused on protecting the wind turbines without considering the impacts on the power system operation or parameters. Wind turbines were allowed to be disconnected in case of disturbances, and no contribution to power system stability was required from them. Nevertheless, different problems experienced by some transmission system operators in countries with high penetration levels of wind power have led to a general re-evaluation of grid requirements around the world. As a consequence, the immediate disconnection of wind turbines in case of voltage dips is usually not admitted anymore and voltage stability support is in some cases also required. Although most modern wind turbines are able to fulfil restrictive technical requirements through modification in their designs, wind turbines on their own are not able to “ride through” voltage dips or faults on the system. Additional control strategies must be added to the system for a reliable and secure power system operation. Also rigorous requirements do not allow the integration of low cost technologies based on fixed speed induction generators without additional investments in dynamic reactive power support devices like Static VAr Compensators (SVC) or Static Synchronous compensators (STATCOM). Hence, through costly and technically challenging, wind turbine design currently need to

incorporate features such as voltage stability support or Fault Ride Through capability if they are to technically contribute to a reliable and secure power system operation.

In this work, modelling and simulation studies are carried out to compare the Low Voltage Ride Through (LVRT) behaviour of two different types of wind turbine generators, such as the synchronous generator (SG) and without using the STATCOM and the doubly-fed induction generator (DFIG) with crowbar as the controller.

The Static Synchronous Compensator or STATCOM is a shunt connected FACTS device used for reactive power compensation as mentioned earlier and it is important to understand its role in being used in conjunction with a wind turbine generator. STATCOM is a shunt-connected reactive power compensation device that is capable of generating or absorbing reactive power. The reactive power of a STATCOM is produced by means of power electronic equipment such as a voltage source converter (VSC). The interaction between the AC system voltage and the voltage at the STATCOM terminals controls the reactive power flow. If the system voltage is less than the voltage at the STATCOM terminals, the STATCOM acts as a capacitor and reactive power is injected from the STATCOM to the system. On the other hand, if the system voltage is higher than the voltage at the STATCOM terminal, the STATCOM behaves as an inductor and the reactive power transfers from the system to the STATCOM terminal, the STATCOM behaves as an inductor and the reactive power transfers from the system to the STATCOM. STATCOM can enhance the transient stability and significantly minimize the blade-shaft torsion oscillation of wind turbine generators.

STATCOM has no long term energy support on the DC side and it cannot exchange real power with the AC system. In the transmission systems, STATCOMs basically can handle only fundamental reactive power exchange by providing voltage support to busses through modulation of bus voltages during dynamic disturbances. This improves transient stability margins and damp out system oscillations. In terms of Two AC sources, having the same frequency and connected through series inductance, active power flows from the leading source to the lagging source whereas the active power goes from the leading source to the lagging source. This results in the reactive power flowing from the higher voltage magnitude source to the lower voltage magnitude source. The phase angle difference between the two sources determines the active power flow and the voltage magnitude difference between the sources determine the active power flow and the voltage magnitude difference between the sources determines the reactive power flow. The STATCOM is used to regulate the reactive power flow by changing the magnitude of the VSC voltage with respect to the source bus voltage.

In this thesis, the control strategy used for the STATCOM is the phase angle δ. The modulation index variable, m, and the fundamental voltage component of the STATCOM is controlled by changing the DC link voltage. On the one hand, the DC voltage can be increased by further charging the DC link capacitor, thus increasing the reactive power delivered or absorbed by the STATCOM. On the other hand, the reactive power delivered is decreased in capacitive operation mode or the reactive power absorbed by the STATCOM in an induction power mode increases through the discharging of the DC link.

The STATCOM thus can provide reactive power compensation to the wind farm system during low voltage conditions. The reactive power compensation is set up according the grid code.

As mentioned earlier, DFIG with crowbar control is used to compare results from synchronous generator with STATCOM control. DFIG with crowbar control is a mainstream type of generator because of its variable speed operational capability, active and reactive power decoupling control, low cost and simple structure amongst others.

This thesis investigates and compares the LVRT behaviour of two types of wind generators under voltage dip condition caused by grid faults in order to comply with the grid codes. Two types of cases have been considered as follows:

- Case 1A - Synchronous Generator Based Wind Turbine with STATCOM (FACTS devices used for LVRT)
- Case 1B - Synchronous Generator Based Wind turbine without controller (No LVRT capability)
- Case 2 - DFIG with Crowbar controller

The output waveforms from the different case scenarios indicate that the synchronous generator with STATCOM based wind farm provide a better LVRT condition than the DFIG based wind farm. The STATCOM provide a reactive power compensation which enables the synchronous generator to stay connected to the network during system faults as per the grid code.

Studies assume large scale synchronous generator based wind farms to be cost effective. This thesis aims to show the viability of the synchronous generator with STATCOM to ride through system faults and thus the stability of the wind farm system is achieved.

TABLE OF CONTENTS

LIST OF FIGURES

LIST OF TABLES

NOMENCLATURE

WECS	Wind Energy Conversion System
D-axis	Direct Axis
Q-axis	Quadrature axis
r.m.s	Root Mean Square
Rpm	Revolutions per minute
PWM	Pulse Width Modulation
MPPT	Maximum Power Point Tracking
TSR	Tip Speed Ratio
SG	Synchronous Generator
DFIG	Doubly Fed Induction Generator
LVRT	Low Voltage Ride Through
PCC	Point of Common Coupling

1 INTRODUCTION

1.1 Research Summary

This research work, in the context of grid-integration of wind farms, investigates and compares the Low Voltage Ride through (LVRT) behaviour of two types of wind generators under different grid fault scenarios – a synchronous generator with and without static synchronous compensator (STATCOM) and a doubly-fed induction generator (DFIG) with crowbar protection in compliance to the grid codes in South Africa. The study is based on modelling and simulation of various case studies using Matlab and the results have been interpreted in order to highlight the key points of comparison. The research work aims to aid the utilities and wind energy stakeholders to plan and execute grid-integration of wind farms for a more economic and reliable operation of the power system.

1.2 Background of Research

The global electrical energy consumption has been constantly increasing bringing about a need for augmenting power generation capacity and investment in new grid infrastructure for the utilities to keep pace [1]. Just as energy demand continues to soar, supplies of fossil fuels are dwindling and prices are at their most volatile state [1, 2]. As a result, studies on alternative energy production are flourishing. Wind energy, however, is a massive indigenous power source which is available virtually everywhere in the world, though with varying wind velocity profiles. There are no fuel costs and no supply import dependency involved apart from environmental/social impact issues in installing an wind farm. Moreover, by not emitting dangerous air pollutants and any toxic waste, it has a positive effect on air pollution, which is choking cities around the world. At many sites, wind power is already competitive with new-built conventional technologies and in some cases much cheaper. While counter balancing the price of carbon, wind power represents a legitimate and attractive source of energy. Like all renewable sources it is based on capturing the energy from natural forces and has none of the polluting effects associated with ‘conventional’ fuels [2]. Hence, this makes wind generation a matured and well-accepted clean and emissions-free power generation technology today

Wind power as a generation source has specific characteristics, which include variability and geographical distribution. These raise challenges for the integration of large amounts of wind power into electricity grids. In order to integrate large amounts of wind farms successfully, a number of issues need to be addressed, including design and operation of the power system, grid infrastructure issues and grid connection points and voltage levels for the wind farms and the wind farm capacities.

The present levels of wind power connected to electricity systems already show that it is feasible to integrate the technology to a significant extent. Experiments with almost 60 GW installed in Europe, has shown where areas of high, medium and low penetration levels take place in different conditions.

A grid code covers all material technical aspects relating to connections to, and the operation and use of, a country's electricity transmission system. They lay down rules which define the ways in which generating stations connecting to the system must operate in order to maintain grid stability. Specific requirements for wind power generation are changing as penetration increases and as wind power is assuming more and more power plant capabilities, i.e. assuming active control and delivering grid support services. This has motivated a lot of research into the fields of renewable energy generation, energy management and obtaining grid support from the renewable technologies during faults and contingencies; hence the focus of this thesis is the Low Voltage Ride Through (LVRT) capability of wind turbine generators for providing reactive power support to mitigate voltage drop caused by grid faults.

1.3 Low Voltage Ride Through Capability of Wind Farms and their Role in Voltage Dip Mitigation

Currently research is being carried out to investigate how voltage or reactive power support could be obtained from wind farms during grid faults or contingencies for voltage dip mitigation, instead of disconnecting the wind farms during fault. The

main purpose is to encourage participation of wind farms in enhancing grid performance, providing voltage control and power quality improvement. The wind generators considered for comparison are firstly, the synchronous generator with STATCOM and secondly, the DFIG with crowbar protection.

The goal of a LVRT system is to enable a wind farm (WF) to withstand a severe voltage dip at the connection point and still stay connected to the power system as long as the fault persists. Wind turbine design is required to incorporate LVRT capability as per Grid Code's requirements only if they are technically needed for a reliable and secure power system operation. The basic requirement for LVRT is that the wind turbines must maximize their reactive power injections to the network without exceeding the turbine limits. The maximization of reactive current must continue for at least 150ms after the fault clearance or until the grid voltage is recovered within the normal operation range.

In response to increasing demands from the network operators, for example to stay connected to the system during a fault event, the most recent wind turbine designs have been substantially improved. The majority of MW-size turbines being installed today are capable of meeting the most severe grid code requirements, with advanced features including fault-ride-through capability. This enables them to assist in keeping the power system stable when disruptions occur [3].

During the past years, the requirements were mainly focused on protecting the wind turbines without considering the impacts on the power system operation. Wind turbines were allowed to be disconnected in case of disturbances, and no contribution to power system stability was required. However, there were some problems encountered by electrical operators in regions with high penetration levels with respect to wind energy and this required a development in the grid requirements of the system. As a result, voltage stability is now required and disconnection of the turbines in the event of voltage dips is no longer allowed. Wind turbines were re-designed and are now capable to achieve those grid requirements. However, it is not possible for the Wind turbines to ride through faults and voltage dips without any additional control system. Flexible Alternating Current Transmission

System (FACTS) devices in terms of STATCOM are used to provide support to Wind Turbines for a reliable and secure power system operation.

A major part of this thesis is involved in investigating the role of STATCOM in assisting a synchronous generator based wind turbine during its LVRT. A Static Synchronous Compensator (STATCOM) is a shunt connected FACTS device whose main purpose is to control the reactive power in power system by generating and absorbing reactive power as per necessity. The STATCOM produces variable reactive shunt impedance which is constantly adjusted for compensation of the power system as per the standard requirements; in this dissertation, compensation refers to direct voltage support for transient and dynamic stability improvements. Voltage Support usually mitigates voltage variation, thus preventing voltage collapse and increase transient stability limits which can trigger enhanced dynamic stability [4].

STATCOM works by generating a balanced set of three phase sinusoidal voltages at the fundamental frequency, with rapidly controllable amplitude and phase angle. It enhances transient stability and can produce reactive power by using power electronic equipment similar to voltage source converter type. Though a STATCOM can have different topologies, the three main components of any STATCOM are the Voltage Source Converter (VSC), the coupling transformer and the control circuit [4].

The reactive power of a STATCOM is produced by means of power electronic equipment of a voltage source converter (VSC) type. STATCOM is a shunt-connected reactive power compensation device that is capable of generating or absorbing reactive power. Irrespective of the different topologies, The STATCOM has three main components: voltage source converter (VSC), coupling transformer and the control circuit. The VSC is modelled as a six-pulse Pulse-Width Modulator Gate Turn-Off (PWM GTO) converter with a DC Link capacitor. The interaction between the AC system voltage and the voltage at the STATCOM terminals controls the reactive power flow. If the system voltage is less than the voltage at the STATCOM terminals, the STATCOM acts as a capacitor and reactive power is injected from the STATCOM to the system. On the other hand, if the system voltage

is higher than the voltage at the STATCOM terminal, the STATCOM behaves as an inductor and the reactive power transfers from the system to the STATCOM terminal. Under normal operating conditions, both voltages are equal and there is no reactive power exchange between the STATCOM and the AC system [4].

It can be commented that in the transmission systems, STATCOMs handle fundamental reactive power exchange by providing voltage support to buses through modulation of bus voltages during dynamic disturbances. This improves transient stability margins and damp out system oscillations. In case of two AC sources, having the same frequency and connected through a series inductance, active power flows from leading source to lagging source. This results in the reactive power flowing from the source of higher voltage magnitude to the source of lower voltage magnitude. The phase angle difference between the two sources determines the active power flow and the voltage magnitude difference between the sources determines the reactive power flow. The STATCOM is used to regulate the reactive power flow by changing the magnitude of the VSC voltage with respect to the source bus voltage.

As already mentioned at the beginning of this section, the thesis will compare the LVRT behavior of synchronous generator-based wind generation with and without STATCOM with DFIG-based wind generation with crowbar protection. The reason is that DFIG with crowbar protection is the most commonly used and classical solution to achieve LVRT requirements nowadays. This is why the synchronous generator with STATCOM wind system is compared to the DFIG with crowbar protection. The crowbar protection provides feed-forward transient current control scheme for the rotor side converter of a DFIG. By injecting additional feed-forward transient compensation, in the outputs of the Rotor Side Convertor (RSC) current controller, the RSC AC-side output voltage will be aligned with the transient induced voltage resulting in minimum transient rotor current and minimum occurrence of crowbar interruptions. However, DFIG with crowbar has a major disadvantage when it loses its controllability due to resulting overcurrent once the crowbar is triggered. This is because the rotor side convertor is deactivated and the DFIG absorbs a high amount of reactive power from the grid, which leads to further grid voltage drop.

Thus an alternative to DFIG wind farm should be considered taking into account its cost effectiveness [5].

1.4 Objectives and Research Methodology

The main objective of this thesis is to investigate the application of STATCOM (Static Synchronous Compensator) on a Synchronous Wind based Generator to achieve the LVRT as per compliance with the South African grid code and compare its effectiveness to the LVRT behaviour of a DFIG-based wind turbine under the same grid fault occurrences.

To ensure stability of the system, with respect to power quality and voltage level, all the grid codes demand that the wind farms must be able to produce reactive power at the point of common coupling (PCC), i.e. the point of its integration to the grid. When dealing with wind farms, adding the reactive power capability of each individual wind turbine may not be sufficient to comply with grid codes. This is due to the losses in connection cables and line losses between wind farm and the PCC. One solution is to use an external reactive power compensation device. The work presented in this thesis involves the application of STATCOM which has been selected as a control device to implement LVRT condition on synchronous generator-based wind turbines and its performance comparison with respect to a DFIG wind generator with built-in LVRT characteristics (using Crowbar protection for reactive power compensation). The crowbar includes a set of thyristors that usually short circuit the rotor windings when triggered. Thus limiting the rotor voltage and providing the additional path for the rotor current. Using the crowbar for reactive power compensation, DFIG can ride through low voltage conditions or resume operation as soon as the voltage is resettled.

In the light of the aforesaid research objective, modelling and simulation of the following case studies have been performed as listed below:

- Case 1A – Synchronous generator based wind turbine with STATCOM controller for achieving LVRT
- Case 1B - Synchronous generator based wind turbine without any STATCOM controller and without any LVRT capability

- DFIG with Crowbar controller and built-in LVRT capability

Research methodology steps followed in this work are listed below:

a) A review of the LVRT scenarios for synchronous generators with STATCOM and DFIG including crowbar control
b) Mathematical Modelling of the test systems: synchronous generator, STATCOM and DFIG
c) Simulation of the test scenarios using Matlab®/Simulink®
d) Case study 1A: A salient pole synchronous generator based Wind Energy Conversion System (WECS) with STATCOM
e) Case study 1B: A salient pole synchronous generator based WECS without STATCOM
f) Case study 2: Doubly Fed Induction Generator based WECS
g) Comparison of the LVRT characteristics

Comparison of the two case studies has been done in context of the following parameters:

- The voltage and current profile (phase A only) at bus 1(120kV), which depicts the voltage drop at the grid.
- The voltage profile (phase A only) at bus 2 (25kV) and bus 3 (575V). The profiles at bus 2 and bus 3 show the voltage characteristics (p.u.) at the transmission line and generator respectively.
- The active and reactive power measured at the output from the generator to show the variation in the power generated from the generator.
- The reactive power profile from the STATCOM showing the reactive power compensation from the STATCOM.

1.5 Limitations and scope of this project

The report focuses on the modelling and performance of the STATCOM implemented as a control system for Ride Through Conditions on a Synchronous Wind Generator. The simulated model only considers one Strategy - STATCOM and does not consider alternative control to monitor the Ride Through Conditions of

the generator. The simulated model is then compared to the Integrated Fault Ride Through control on a DFIG system. The scope of this thesis includes the modelling of the STATCOM and its performance and the comparison of the output results to those of the DFIG Fault Ride Through control Strategy. The limitations of this project arises out of the limited information available with respect to the implementation of STATCOM with synchronous generator based WECS for ride through conditions as STATCOM is a relatively new device.

1.6 Plan of development

This thesis is organized as follows:

Chapter One introduces the research topic, gives the background and objective of the research, and summarises the research methodology and clearly presents the organization of the thesis including the brief summary of the rest of the chapters.

Chapter Two presents the review of existing literature relevant to this research.

Chapter Three describes the research method including all mathematical modelling and simulation steps, description of the case studies and basis of comparison of the cases studies.

Chapter Four presents the results of all the simulation studies carried out along with the interpretation of results and comparison of the two case studies.

Chapter Five summarises the results and draws the conclusion there from. This chapter also presents the recommendations for the utilities in matters of LVRT capability of wind farms, based on the interpretation of the results and suggestions for further work.

2 LITERATURE REVIEW

This chapter reviews relevant existing research literature in the field of low voltage ride through (LVRT) performance of wind farms which forms the basis of the work presented in this thesis. The main objective of this thesis is to analyse and compare the efficiency of LVRT behaviour of two different types of wind generators (along with their protection and control) in providing grid voltage support during faults or contingencies leading to voltage dip. The fault considered here is a three-phase to ground fault which is considered to the most severe of faults in terms of magnitude of fault current and voltage dips. One wind generator investigated in this work is a salient pole synchronous generator with a STATCOM as the controller providing the necessary reactive power compensation to achieve the LVRT; the other wind generator investigated is a Doubly Fed Induction Generator (DFIG) with crowbar protection and built-in LVRT characteristic. Though the DFIG is the most commonly used generator nowadays due to its various advantages such as reduced inverter and output filter costs due to low rotor and grid side power conversion ratings (25% - 30%), yet it is expected that with improvement in control system, the salient pole synchronous generator can prove to be competitive to DFIG in matters of efficiency, controllability.

2.1 Basics of Wind Energy

Challenges such as pollution, global warming, and energy supply preservation has brought about various efforts in the development of renewable energy sources including wind energy. Wind power has realized the fastest growth in all renewable energy sources with a 20% annual growth rate since the past five years. It has been predicted that in the next 8 years, it will supply about 12% of the world's electricity [1].

During the 1990's, several developed countries deployed grid-integrated distributed generation (DG). As a consequence, new problems on distribution networks occurred in relation to grid connection of DGs. Therefore, authorities and governments were urged to implement new technical requirements or amend existing rules for grid connections of DG units. When wind generation was first

introduced, the network requirements for wind farms were less arduous than traditional generators. However, with the increasing development in wind power generation, the grid rules had to be redefined to suit the new wind generation - grid connection. Thus, more complex, yet more expensive, reliable and refined solutions are applied [2, 3].

Wind farms are now required to meet rigorous connection requirements including reactive power support, transient recovery, system stability and voltage/frequency regulation [2]. These requirements constitute the main challenges for the wind generation industry. One of the major changes is the ride-through capacity of the wind turbines which implies that the latter must stay connected to the grid during grid disturbances. They should continuously feed the reactive power in addition to limited active power. New scenarios include the use of power electronic devices to control the behaviour of wind generation system during faulty periods [2].

2.2 Low Voltage Ride Through

It is important to discuss here the immediate impact of the voltage dip on the wind farm operation. During the voltage dip, the active power provided to the grid by the wind farm is instantaneously reduced at least temporarily to a value lower than the mechanical power available at the rotor; hence the rotor speed of the wind generator increases. It is required for the LVRT capability of the wind farm, that the wind generators must not be disconnected from the grid during fault persistence, either due to over-speeding or under voltage protections. After the clearing of the fault that led to the voltage dip, the voltage at the wind turbine bus increases. It is also required that the wind generators should resume their power supply to the network without losing stability. Upon voltage recovery, the wind turbines must not consume excessive reactive power when re-exciting the generator, as this may result in a further voltage dip. This is most commonly known as Fault Ride Through or Low Voltage Ride through (LVRT). LVRT characteristic, as shown in Figure 2-1, is usually described by a Voltage v/s Time graph, depicting the minimum required protection characteristics of the wind farm [6].

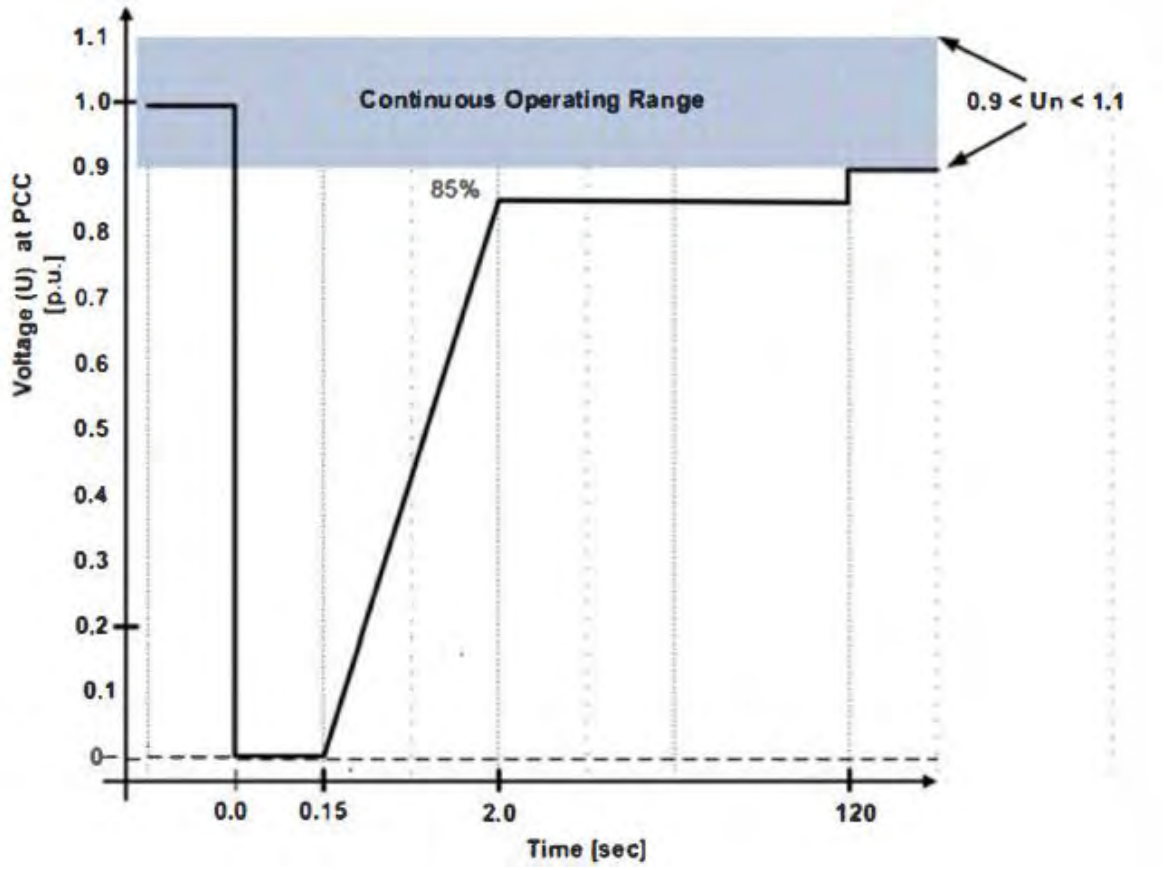

Figure 2-1: Characteristics of Low Voltage Ride Through [7]

The operational requirements of a wind farm to provide LVRT is to supply additional reactive power to mitigate the voltage dip during a fault or contingency condition within the framework of the grid codes [7].

Most grid codes around the world demand active power curtailment upon request from the network operator, at a specified set-point. This is done either by disconnecting wind turbines or by controlling the pitch angle of the blades in order to limit the power extracted from the wind. Some grid codes also impose limitations on the rate of change of active power, with maximum and minimum ramp-up and ramp-down rates. These limitations aim to suppress large frequency fluctuations caused by extreme wind conditions and to avoid large voltage steps and in-rush currents during wind farm start-up and shutdown [8].

Under normal conditions many grid codes require a ramp-down rate of <10% of per minute. The most demanding requirements of both ramp-up and ramp-down rates under normal conditions are in Denmark where wind farms must always be able to vary their active power ramp-rates in the range 10%–100% of per minute upon request. The fastest ramp-up rate of active power output after a fault back to the

prefault value is that of Ireland and the UK (>90% of /s), where due to the isolated nature of their electrical grids the wind farms must provide fast active power support to assist in the grid voltage recovery [8].

In general, the most demanding requirements regarding active power control are found in the Danish grid code where wind farms must be equipped with and apply active power control functions with set-points and ramp-rates set by the system operator as shown in Figure 2-2. The “Delta” control function is particularly demanding, as the active power output of wind farms with capacity greater than 25 MW must be constrained to a required constant value in proportion to the available active power. This reserve power can be used in fast grid frequency control, similar to the spinning reserves in conventional power plants [8].

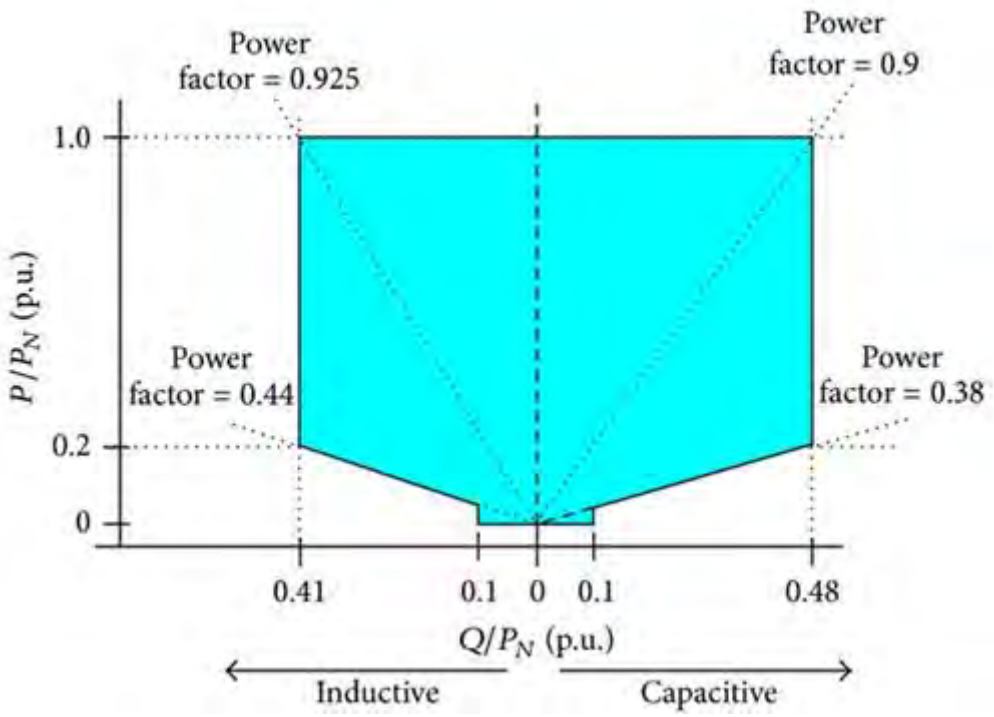

Figure 2-2: P-Q Profile to satisfy all grid codes [8]

South African Grid codes require that wind farms must withstand voltage dips to a certain percentage of the nominal voltage, down to 0% voltage drop in some cases, and for a specified duration [9].

The required fault behaviour of a wind generation system is characterized as follows [2]:

- For system faults that last up to 140 ms the wind farm has to remain connected to the network. For supergrid voltage dips of duration greater

than 140 ms the wind farm has to remain connected to the system for any dip-duration [3,9].

- During system faults and voltage sags a wind farm has to supply maximum reactive current to the grid system without exceeding the transient rating of the plant [9].
- For system faults that last up to 140ms upon the restoration of voltage to 90% of nominal a wind farm has to supply active power to at least 90% of its pre-fault value within 0.5 sec. For voltage dips of duration greater than 140 ms a wind farm has to supply active power to at least 90% of its pre-fault value within 1 sec of restoration of voltage to 90% of nominal [9].
- During voltage dips lasting more than 140ms the active power output of a wind farm has to be retained at least in proportion to the retained balanced voltage [9].

It should be noted that, in cases where less than 5% of the turbines are running or under very high wind speed conditions where more than 50% of the turbines have been shut down, a wind farm is permitted to trip [9].

During period of voltage dip, active power provided by the wind generator is immediately reduced, which makes it lower than the mechanical power generated. Thus there is an increase in rotor speed of the generator. The LVRT feature will not trigger the wind turbine generator to disconnect during this period, in cases of overspeed or under voltage. However after the clearing of the fault or low voltage condition, the voltage of the wind generator increases, enabling the wind turbine generator to resume the power supply to the network grid and recover stability. Control capabilities in various generators such as synchronous generators, and doubly-fed induction generators limits the risk of loss of stability. The control capabilities include mainly power electronics devices to achieve reactive power compensation in the system [6, 10].

Moreover, for wind turbine generators to adhere to grid connection codes, the following points need to be considered [11]:

- to limit the increase of the rotor speed so that it doesn't exceed the maximal permitted value,
- to keep the voltage at the generator bus in the permissible range,
- Not to lose stability so as to be able to resume the power supply after the fault clearing.

Nowadays, wind turbine generators are likely to include Ride Through capabilities in their control strategies, taking into account the wind turbine technology. These may include: [11]

- mechanical active power limitation with pitch control,
- Use of capacitor or breaking resistance on the DC bus of the back-to-back converter (connected at the stator or the rotor) to stock or dissipate the active power during the voltage dip.
- Disconnection and reconnection of stator.

However, solutions based on additional devices may be proposed to enable LVRT of wind farms. The principle of these devices is generally to support the voltage at the generator terminals during the voltage sag by injecting reactive power into a decoupling reactance that could be permanently or temporarily connected.

2.3 Reactive Power Compensation Devices for Voltage Control

On transmission system, various types of components such as transmission line, transformers and power loads, usually consume reactive power. The reactive power consumed should be compensated and thus reactive power is supplied by plants and other devices. Various control strategies are used to enable reactive power compensation. Voltage control is accomplished by controlling the production, absorption and flow of reactive power at all levels in the system.

2.3.1 Role of reactive power compensation in voltage control and LVRT of wind farms

Depending on the technology, the wind turbines can directly participate in the reactive compensation and voltage control. More precisely, DFIG wind turbines connected to the grid through power electronic interfaces can be used to control the reactive power and the voltage at the point of connection. The reactive power

provided or consumed by these wind generators is limited by the current limitation of the converters and hence their rating. Depending on the technology, it generally enables to produce or consume a reactive power up to 30% of the nominal active power. In order to perform the grid voltage control at the connection point of the wind farm, a coordinated voltage control strategy between the different wind turbines in the wind farm has to be defined [12,13].

Classical squirrel cage induction wind generators and induction wind generators with dynamic slip control can only consume reactive power. They need additional devices to perform the reactive compensation and possibly contribute to the grid voltage control.

There are several additional devices that can provide reactive power compensation and voltage control [13].

Growing capabilities of power electronic components resulted in creation of controllers with much faster response times, due to their lack of mechanical switch inertias. Lower transient over voltages are accomplished when using semiconductor devices, also a smooth, gradual changes in VAR output are made, compared to the large discrete steps that arise from mechanically switching in capacitor and/or reactor banks. FACTS controllers using semiconductor devices are the fastest option for obtaining maximum system benefits. Also the usage of semiconductor switches instead of mechanical switches, which led to an increased life-time of the system by less maintenance. However, the drawback of this technology is that it is more expensive than the traditional methods.

2.3.2 Flexible AC Transmission Systems (FACTS)

The basic limitations in power system transmission such as distance, stability, effective power flow and cable loading limits led to the investigation of power electronic devices into power systems and their impact on reactive power compensation. Thus FACTS devices were introduced as a solution for ameliorating the power system performance. Development of this technology was based on the same principle as in traditional power system controllers (i.e. phase shifting transformers, passive reactive compensation, synchronous condensers etc.) [14].

FACTS devices can be divided into two subgroups: Old generation was based on thyristor valve idea and the new generation focuses on using the voltage source converter (VSC) [14]. In both cases, corresponding solutions provide similar services. The main difference between those two categories is that VSC technology is much faster and has a wider range of control [14]. Figure 2-3 shows the basic principle of FACTS devices on the wind farm system:

where:

TSC: Thyristor-Switched Capacitor

SVC: Static VAR Compensator

STATCOM: Static Synchronous Compensator

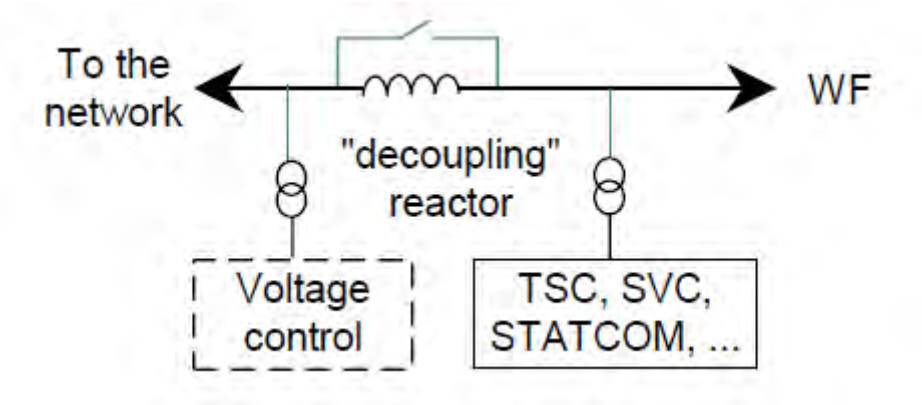

Figure 2-3: general principle of compensation during FRT [15]

Eventually FACTS devices found their applicability in the wind power industry. It was discovered that by providing earlier wind farms with some external reactive compensation devices such as SVC or STATCOM, the grid compliance can be met, and thus the wind farms could remain connected to the power system without stability risks [8, 14].

A different approach to categorize the FACTS controllers is to group them in a way in which they are connected to the power system, such as, shunt, series or shunt-series connected. This research deals with shunt-connected FACTS device applicable for LVRT of wind farms and hence the following sections review different shunt-connected FACTS controllers used for wind generators [8, 14].

		CHARACTERISTICS OF COMMON VAR COMPENSATORS		
		TSC	**SVC Including TSC**	**STATCOM**
1	**Compensation Accuracy**	Very Good	Good	Excellent
2	**Control Flexibility**	Very Good	Good	Excellent
3	**Reactive Power Capability**	Lagging/Leading Indirect	Leading/Lagging Indirect	Leading / Lagging
4	**Control**	Continuous	Discontinuous	Continuous
5	**Response Time**	Fast 0.5 to 2 Cycles	Fast 0.5 to 2 Cycles	Very Fast
6	**Harmonics**	Very High	Good	Good, but depends on switching pattern
7	**Losses**	Good, but increase in lagging mode	Good but increase in leading mode	Very Good, but increase with switching frequency
8	**Phase Balancing**	Good	Limited	Very Good with 1_{φ} units, limited with 3_{φ} units
9	**Cost**	Moderate	Moderate	Low to Moderate

Table 2-1: Comparison between SVC and STATCOM [7]

The growing penetration of produced wind power (size growth of wind farms) forced the Transmission System Operator (TSO) and Distribution System Operator (DSO) to develop more strict and detailed grid codes for wind turbines. The new grid codes specify new requirements for wind farms regarding such issues as frequency control, voltage control and fault ride-through behaviour. Table 2.1 depicts the main characteristics of the most important shunt VAR compensators. The significant improvements observed in the STATCOM devices, makes them a first choice for improving the performances in AC power systems [13].

Thyristor-Switched Capacitor (TSC)

TSCs are designed to insert the appropriate number of multi-stage power capacitors into the network, without transient effects. For that purpose, capacitors are switched into the circuit when the grid voltage and the capacitor voltage are both equal to the positive or negative peak voltage. Two types of TSC systems are used: the first one is based on 2 thyristors connected in back to back and the second one consists of a thyristor and diode connected in antiparallel for each valve. A microprocessor-based system manages the measurements, calculates the amount of reactive power to compensate and the gating signals to the thyristors. Figure 2-4 illustrates the control mechanism in the Thysristor Switched Capacitor. TSCs are often used to regulate voltage especially when it fluctuates slowly. The dynamic of a TSC is limited, as in any device, including line commutated thyristors, at the double of the 50 Hz network frequency, i.e. 10ms. Practically, one should add to this time interval, the computation delay of the regulator (typically some milliseconds). Therefore the typical response time of a TSC is about 20 milliseconds [8, 13].

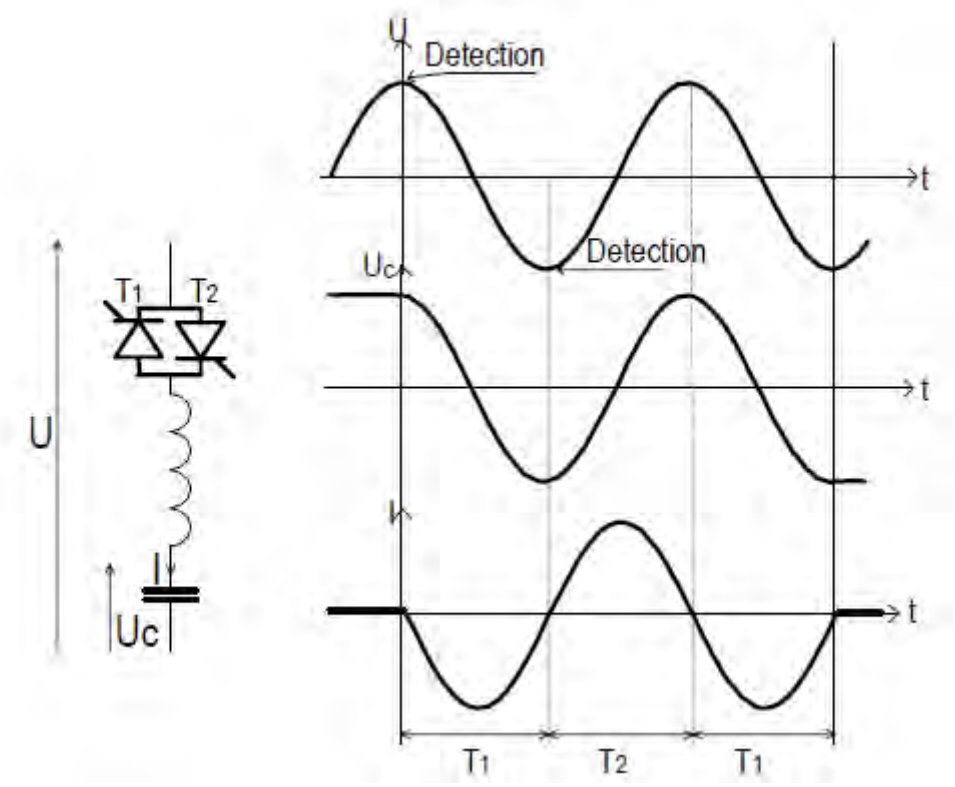

Figure 2-4: Illustration of control mechanism in Thyristor-Switched Capacitor [13]

Static VAR Compensator (SVC)

SVC's being dated from early 70's, have the largest share among FACTS devices. They consist of conventional thyristors which have a faster control over the bus voltage and require more sophisticated controllers, compared to the mechanical switched conventional devices. SVC's are shunt connected devices capable of generating or absorbing reactive power. By having a controlled output of capacitive or inductive current, they can maintain voltage stability at the connected bus.[14,15]

Usually SVC's are connected to the transmission lines, thus having high voltage ratings. Therefore the SVC systems have a modular design with more thyristor valves connected in series/ parallel for extended voltage level capability [16].

Over the last three decades, utilization of large pulsed type loads such as arc furnaces, welding equipment, rolling mills has increased with the growing need of steel. The increasing number and size of those fluctuating loads caused power quality problems such as flicker, harmonics and unbalance. Static VAR Compensators have been used in the factories to reduce flicker and unbalance.

Some 900 SVC applications are running to date around the world. The technology, based on Thyristor-Controlled Reactors (TCR) is matured and its exploitation to improve reactive compensation and grid voltage control in wind farms can be envisaged [14,15,16].

Figure 2-5 illustrates a SVC system that has been implemented between the grid and a wind farm, which can be seen from the grid as a fluctuating user. The device utilizes a TCR and a Fixed Capacitor (C).

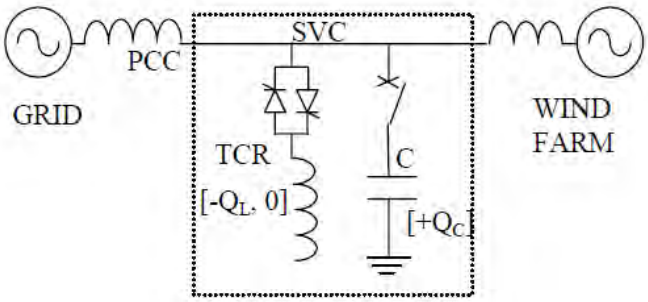

Figure 2-5: SVC system, implemented between the grid and a wind farm [16]

The semi-conductors allow the three branches of the TCR to be delta-connected to form a 3-phase variable inductance, capable of absorbing continuously an amount of reactive power from -QL to QC in Figure 2.5 [16].

One of the main characteristics of static VAR compensators is that the amount of reactive power interchanged with the system depends on the applied voltage, as shown in Figure 2-6. This Figure displays the steady state Q-V characteristics of a combination of fixed capacitor - thyristor controlled reactor (FC-TCR) compensator [16,17].

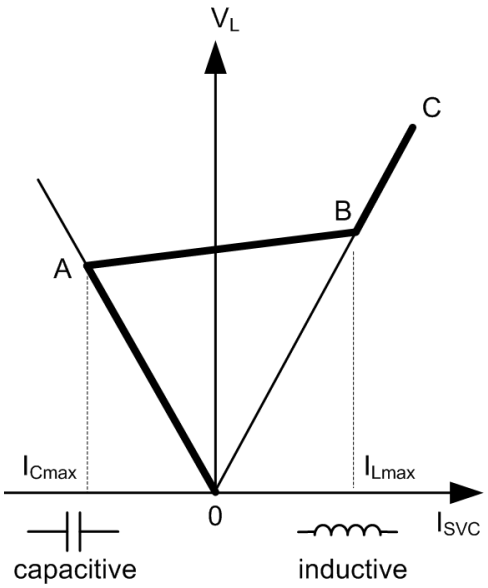

Figure 2-6: SVC configurations and its I V characteristic.[17]

To provide the needed reactive power generation/consumption in the network, SVC's adjust the conduction periods of each thyristor valve. For an SVC consisting of one TCR and one TSC, assuming that both reactor and capacitor have same p.u. ratings, the following scenarios can occur:

• Reactive power is absorbed when the thyristor valve on the reactor leg is partially or fully conducting and the capacitor leg switch is off.

• Reactive power is generated when the thyristor valve on the reactor leg is in partial or no conduction mode and the capacitor leg switch is on.

• No reactive power is generated/absorbed if both the thyristor valve is not conducting and the capacitor switch is off [17].

The technology of SVC with thyristor valves is becoming *outdated m*ainly, due to the slow time responses, of injected current dependence on bus voltage and low dynamic performance. Their replacements are called Static Synchronous Compensator's (STATCOM) and will be discussed in the following section.

Static Synchronous Compensation - STATCOM

The STATCOM (static compensator) and its variant, the Distribution Static Compensator (D-STATCOM), are based on voltage sourced converters (VSC), and

so are voltage sources where amplitude, phase and frequency are entirely controllable. STATCOM applications include the following: [17]

- Stabilization of weak system voltage
- reduced transmission losses
- enhance transmission capacity
- power oscillation damping
- improve power factor
- reduce harmonics
- flicker mitigation
- assist voltage after grid faults

STATCOM can be widely used for retrofitting old wind turbines or wind farms which are not able to comply with new strict grid codes. This can be done by adding static synchronous compensation alone or with battery storage. In case of new wind farms, reactive power control can be done to some extend by single wind turbines [17].

However, even new designs are limited with respect to the newest requirements given in grid codes. Therefore some additional reactive power compensation is needed. STATCOM is a good example of such additional control [17].

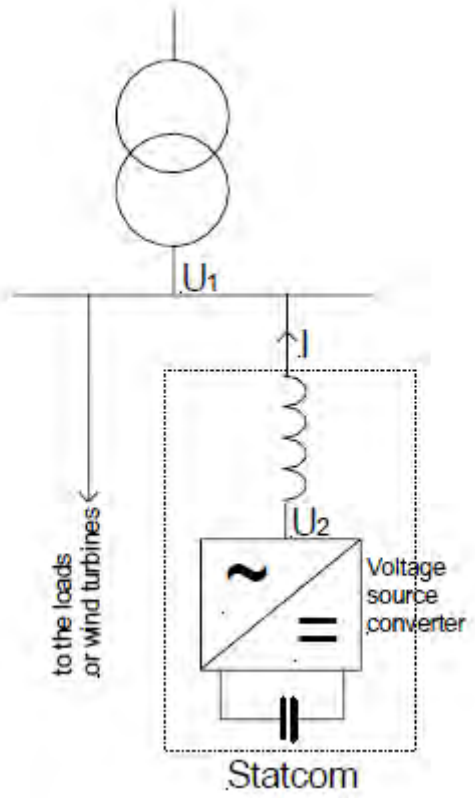

Figure 2-7: Working Principle of STATCOM [2]

Figure 2-7 shows the working principle of the STATCOM. The DC bus capacitor applies a DC voltage at the input of the inverter. Its output is connected to the AC grid via an inductance. While adjusting the converter voltage (U2) with respect to the network voltage (U1), the converter can very quickly supply or absorb reactive power thanks to the gating signals set to the switches of the converter. The response time is mainly influenced by the switching frequency (typically 1 to 2 kHz) and by the size of the inductance [17, 18].

Thus, the STATCOM can help mitigating the flicker due to variations of reactive power absorbed by induction machine-based wind farms. The reactive power required by the farm is evaluated and a controller drives the STATCOM inverter so as to generate the adequate quantity, permitting to reduce drastically reactive power flows towards the grid and therefore, the associated flicker. Unlike thyristor based solutions (TSC and SVC), VSC power electronic systems are based on IGBT (Insulated Gate Bipolar Transistor) technology, intrinsically faster than thyristors. Continuous progress in the semi-conductor industry now makes it possible to build and operate high power STATCOM (about a few tens of MVA), with a very good dynamic response, i.e. time constants in the millisecond range. Among the available products and wind farm references the following can be mentioned [18].

Another way to provide an wind farm with the ability to deliver or absorb reactive power from the grid is to use Static Synchronous Compensation. STATCOM can be treated as a solid state synchronous condenser connected in shunt with the AC system. The output current of this controller is adjusted to control either the nodal voltage magnitude or reactive power injected at the bus. STATCOM is a new breed of reactive power compensators based on VSC. It has a characteristic similar to a synchronous condenser, but because it is an electrical device it has no inertia and it is superior to the synchronous condenser in several ways. Lower investment cost, lower operating and maintenance costs and better dynamics are the major advantages of this technology [17,18].

STATCOM consists of one VSC with a capacitor on a DC side of the converter and one shunt connected transformer. Voltage Source Converter is usually built with thyristors with turn-off capability like Gate Turn-Off (GTO) or Integrated Gate Commutated Thyristors (IGCT) or Insulated Gate Bipolar Transistors (IGBT) based converters. Configuration of the STATCOM circuit is shown in Figure 2-8 [17, 18].

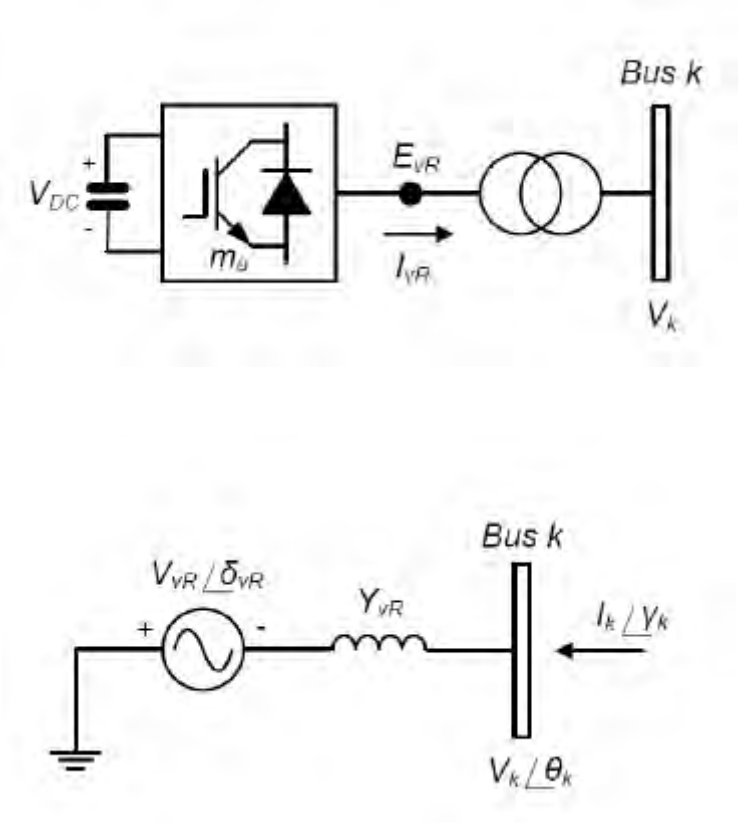

Figure 2-8: STATCOM scheme with equivalent circuit representation.[17]

Operating principles and control modes of the STATCOM are discussed in the following sections.

Operating principle of STATCOM

The working principle of the STATCOM is schematically depicted in Figure 2-9. As it is mentioned earlier, STATCOM can be treated as a synchronous voltage source, because its output voltage can be controlled as desired. Assuming that no active power is exchanged between STATCOM and the grid (lossless operation), the voltage of the controller is in phase with the grid voltage. If the magnitude of the output voltage rises above the voltage value of the AC system voltage, current will flow from the STATCOM to the grid through the coupling reactance. In this case, the reactive power will be generated. This is usually called the over-excited operation mode. However, if the situation is opposite: the magnitude of the voltage output is smaller than the voltage at the connection node, the reactive current flows from the grid to the inverter, and the STATCOM consumes reactive power , thus the voltage is decreased; this is usually referred to as the under-excited operation mode [13].

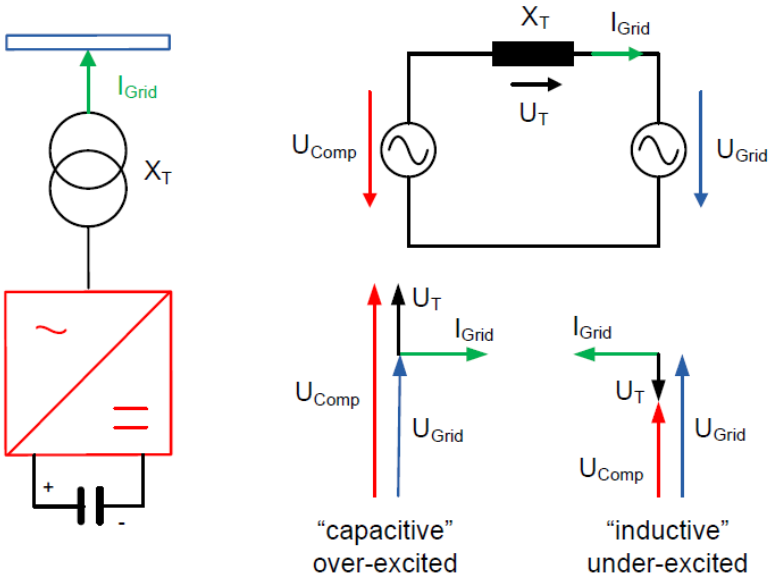

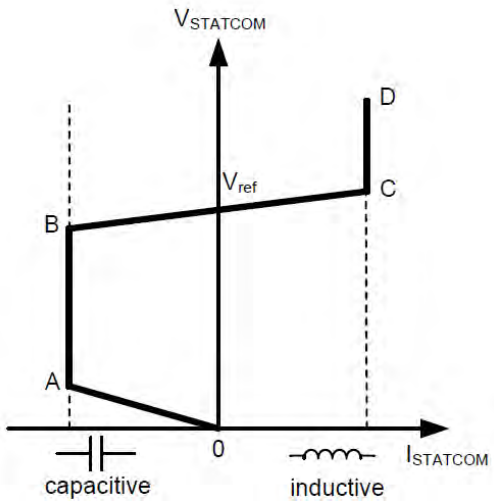

Figure 2-9: Schematic representation of working principle of STATCOM.[17]

Reference [19] reports that STATCOM has played a major role in maintaining the transient voltage stability of the power system and has also improved the LVRT capability of DFIG-based WECS. It can be seen that the speed, active and reactive power of DFIG and power quality can well be controlled well by using converters [12]. When faults occur, in order to maintain voltage stability of grid, the induction generators have to be disconnected from the grid, but LVRT requires that the DFIG wind farm needs to remain connected during a grid fault event. In such cases, the LVRT capability of induction generators can be improved by using STATCOM. When the grid faults happen, STATCOM can provide plenty of reactive power into the wind farm. With the compensation of reactive power from STATCOM, the output voltage of induction generators can be recovered to normal level immediately after grid fault. Thereby, the ability of LVRT of wind farm and the stability of grid can be greatly enhanced with the help of STATCOM [17]. In the light of this project, a salient pole synchronous generator with STATCOM for reactive power compensation is studied and compared to DFIG with crowbar with built-in LVRT feature. The DFIG with crowbar control is discussed in the next paragraph.

The other type of wind generator considered in the thesis for comparison is DFIG with crowbar protection. The reason is that DFIG with crowbar protection is the most commonly used and classical solution to achieve LVRT requirements nowadays. This is why the synchronous generator with STATCOM wind system is compared to the DFIG with crowbar protection. The crowbar protection provides feed forward

transient current control scheme for the rotor side converter of a DFIG. By injecting additional feed-forward transient compensation, in the outputs of the Rotor Side Convertor (RSC) current controller, the RSC AC-side output voltage will be aligned with the transient induced voltage resulting in minimum transient rotor current and minimum occurrence of crowbar interruptions. However, DFIG with crowbar has some disadvantages. One of which is the loss of its controllability once the crowbar is triggered. This is because the RSC is deactivated and the DFIG absorbs a high amount of reactive power from the grid, which leads to further grid voltage drop. Thus an alternative to DFIG wind farm should be considered taking into account its cost-effectiveness [12].

Control modes

The control of reactive power flow provided by STATCOM can be realized in one of the following control modes.

Reactive power control strategy based on STATCOM focuses on reactive power injection to the local bus, to which the STATCOM is connected, according to a reference from the wind park controller.

In this type of operation, STATCOM works in a way to fulfil a voltage/reactive power slope characteristics. This is done by setting a target voltage accepted from wind park controller at the Point of Common Coupling (PCC) [17].

2.3.3 Synchronous Condenser

Synchronous condensers are synchronous generators without prime mover, that can be controlled to absorb or to provide reactive power that can perform a voltage control. They have been partly supplanted by static compensators. However, developments, for example on superconductor synchronous condensers, can make them interesting for reactive compensation and voltage control of wind farms [11].

2.4 Types of Wind generators and their controls

The function of a wind generator is to achieve the mechanical to electrical energy conversion between the wind turbine and the electrical loads. Types of AC

generators that are commonly used in modern wind turbine systems are as follows: [20]

- Squirrel-Cage rotor Induction Generator (SCIG);
- Wound-Rotor Induction Generator (WRIG);
- Doubly-Fed Induction Generator (DFIG);
- Synchronous Generator (With external field excitation); and
- Permanent Magnet Synchronous Generator (PMSG).

Selection of a particular type of generator depends on operational characteristics, weight of active materials, system cost, maintenance aspects, reliability and the appropriate type of power electronic converters. The following sections review the different types of wind generators, mentioned in this section.

2.4.1 Squirrel-Cage and Wound-Rotor Induction Generators

Historically, induction generator (IG) has been extensively used in commercial wind turbine units. Asynchronous operation of induction generators is considered an advantage for application in wind turbine systems because it provides some degree of flexibility when the wind speed is fluctuating. There are two main types of induction machines: squirrel cage induction generator (SCIG), and wound rotor induction generator (WRIG).

SCIG is a very popular because of its low price, mechanical simplicity, robust structure and resistance against disturbance and vibration. The WRIG is suitable for speed control purposes. By changing the rotor resistance, the output of the generator can be controlled and also speed control of the generator is possible. Although wound rotor induction generator has the advantage described above, it is more expensive than SCIG. However, there are various disadvantages which make them not so popular. These disadvantages are listed below: [20]

Disadvantages of SCIG: [20]

- The speed can be varied over a short range only
- SCIG consists of higher slip, which means a higher electrical energy in rotor bars.
- Wind speed fluctuations are directly transferred into electromechanical torque due to fixed speed strategy, thus creating higher mechanical stress and fatigue on system components.

- Higher flicker is experienced in SCIG
- SCIG does not provide continuous speed variations

Disadvantages of WRIG: [20]

The main characteristics of the WRIG are that the stator of the generator is directly connected to the grid, and the rotor winding is connected in series with a controlled resistor.

- Variable speed operation can be achieved by controlling the energy extracted from the rotor [20]. However, this energy is dissipated in the external resistor.
- As the variable speed increases, the higher the slip and the higher the power extracted by the rotor. Thus the efficiency of the generator is lower and the rating of the resistor is higher.
- The energy extracted from the external resistor is lost as heat in the controllable rotor resistance.

2.4.2 Doubly Fed Induction Generator

Another category of induction generator is the doubly fed induction generator (DFIG). The DFIG may be based on the squirrel-cage or wound-rotor induction generator.

The Doubly-Fed Induction Generator (DFIG) is a kind of induction machine in which both the stator windings and the rotor windings are connected to the source. The rotating winding is connected to the stationary supply circuits via power electronic converter. The advantage of connecting the converter to the rotor is that variable-speed operation of the turbine is possible with a much smaller and therefore much cheaper converter. The power rating of the converter is often about 1/3 the generator rating [12, 21].

LVRT Strategies of Doubly Fed Induction Generators

DFIG has various ways through which it can ride through the low voltage condition. Though the most common one is the crowbar method, other methods exist and are discussed in the following subsections.

Behaviour of DFIG exposed to Voltage Sags

Several Studies have shown that the influence of sag has a direct relation to the ride through characteristics of the generator [15]. A simple control algorithm is considered in [12]. The mechanism, which is assumed as ideal, is depicted as follows: the rotor current, I_r, in the synchronous reference frame is kept constant. This hypothesis allows the electrical transient to be solved analytically, providing a comprehensive description of DFIG behavior under symmetrical sags. The fault-clearing physics of symmetrical sags is also analyzed. That is, the fault is cleared in the successive natural fault-current zeros, leading to a voltage recovery in one, two, or three steps. This clearing process, called *discrete* fault clearing, results in a more accurate sag modeling than the *abrupt* or instantaneous fault clearing (the usual modeling in the literature). The fault-clearing process has a strong influence on the rotor voltage required to control the rotor current after fault clearing. To compare the effects of both *abrupt* and *discrete* sags, different wind turbine operating points, which determine different generated powers, are considered. This study helps in the understanding of WT fault ride-through capability [12,21].

Ride Through with Passive Impedance Network

A DFIG wind turbine provides electrical power to the grid which may be equivalently considered as a power source connected to an infinite-bus system. According to [16], if a three-phase fault occurs at the PCC, the system can be divided into two-parts as if the generator is being short circuit through transformer Z_t and part of Line Z_l. In that case, the Stator Flux, λ, changes fully and the transient value of stator current, L_s and rotor current, L_r change to almost 4 times its nominal value, driver shaft Torque, Te, changes to almost 7 times the nominal value.. One solution is to stabilise the stator flux, λ, currents I_s and I_r, and torque, T_e by placing an equivalent impedance between the generator and the grid. The following equations (2.1) and (2.2) are used to stabilise the system from the equivalent circuit of passive impedance network as shown in Figure 2-10: [22]

$$Zeq\ Is = Vg - Zg\ Is \qquad (2.1)$$

$$Zeq = \frac{Vg}{Is} - Zs \qquad (2.2)$$

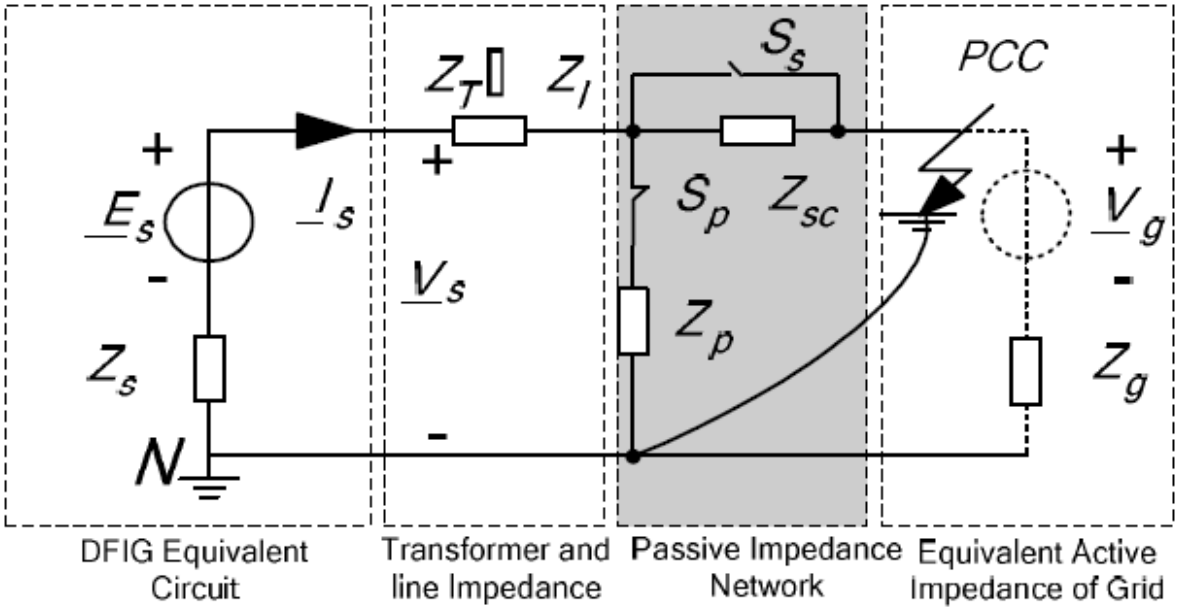

Figure 10: Topology circuit of passive impedance network [22]

In the ideal case scenario, the equivalent impedance Z_{eq} can be placed into the system [22].

Crowbar Method

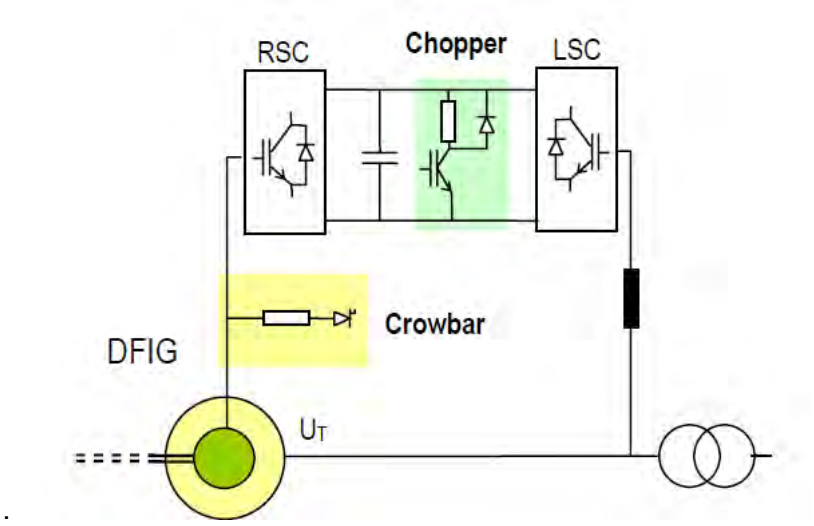

Figure 2-11: DFIG with Crowbar [23,24]

Figure 2-11 shows the schematic diagram of a DFIG with a crowbar system. The crowbar circuit is used to prevent the overvoltage condition from damaging the system. The crowbar method mainly improves the LVRT of DFIG by protecting the

converter as mentioned in [25]. For deep voltage sags, the crowbar short-circuits the rotor and the system goes into an asynchronous machine operating mode, in which the DFIG is not controlled by the rotor-side converter (RSC). The crowbar firing is triggered by the DC-voltage which rises due to the first rotor current peal. The IGBT's are usually stopped by the protection but the current and thus the energy continues to flow into the DC-link through the freewheeling diodes leading to a very fast voltage increase. When the crowbar is switched on, the converter is separated from the rotor circuits. The characteristic operating modes of the rotor converter and the crowbar during LVRT are shown in Figure 2-12.

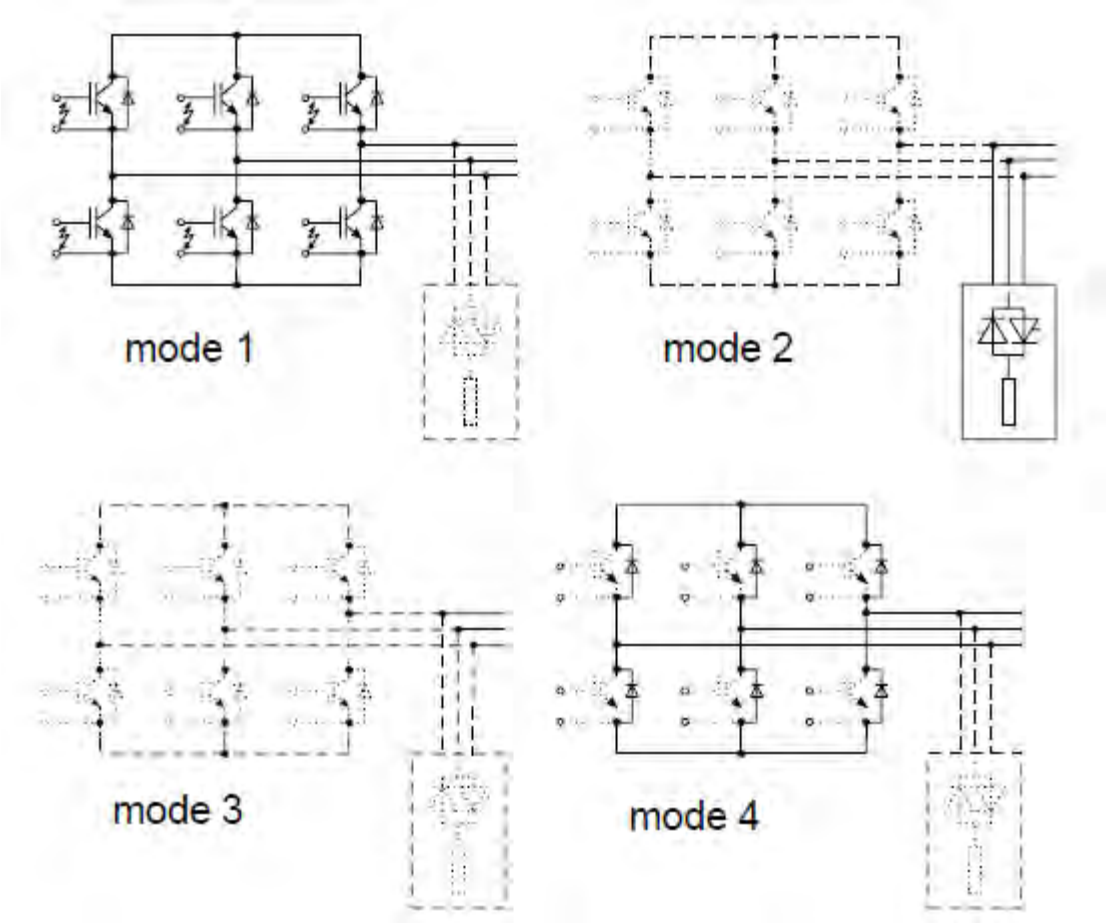

Figure 2-12: Operating mode of the DFIG rotor side converter [25]

Following the short circuit, the system goes first from normal mode 1 into mode 4 as depicted in Figure 2-12. Then, mode 2 follows which is called the crowbar mode. After a short delay of about 60 – 120ms during which the flux transients in the machine die down, the converter resynchronises and the system goes back into controlled DFIG operation. Because the crowbar thyristor switches used in many applications will not interrupt the current before their zero-crossing, the exact

interruption time is not predictable. Therefore, between crowbar interruption and converter resynchronisation is a possible time slot with open rotor circuits characterised as mode 3 in Figure 2-12. When the converter is started again, the DFIG can provide reactive power support to the grid and thus help stabilising the grid voltage. To avoid overload, active power generated by the DFIG will be reduced automatically when the converter current reaches its rated level. Additionally reactive power is dynamically provided by the grid side converter even during the period of crowbar firing. The results from [23] clearly show that the RSC has been successfully protected against overload during the grid low voltage. The RSC is separated from the DFIG in mode 3 after the low voltage condition. After 60ms the RSC is resynchronised and the wind turbine starts to supply active and reactive currents to the grid although the grid fault is still not cleared. To avoid overload, the rotor current limiter is active during this period. Following voltage recovery, the system experiences a similar disturbance as at the beginning of the fault. However, in this case the DC-link voltage is kept within limit by another protection scenario [25].

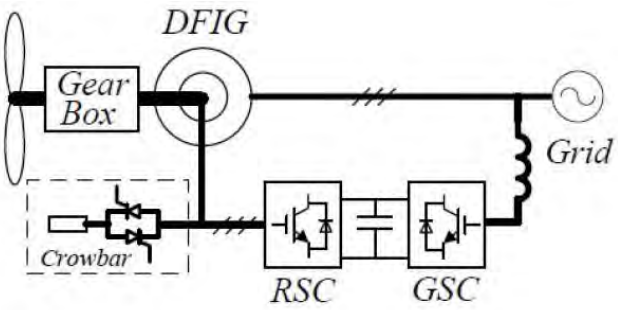

Figure 13: Topology of a DFIG based wind generation system with a typical crowbar protection circuit

Reference [23] presents a DFIG system shown in Figure 2.13 in which the RSC currents rise rapidly, following deep voltage sags caused by grid short circuits the rotor currents and the DFIG system is extended for improved fault ride through capability. The DC Short circuit component on the stator side appears on the rotor side as an alternating current with high initial peak. It contains two protection circuits, a DC Chopper and an AC crowbar to avoid DC Link over voltages during grid faults. The crowbar provides a lower impedance path for the rotor currents during the fault. When the rotor current exceeds a certain limit the IGBTs will be stopped to protect the converter but the rotor current and thus the energy continues to flow into the DC-Link through the freewheeling diodes leading to fast voltage

increase. This fast increase in voltage and continuous energy flow short circuit the rotor windings, preventing the rotor currents from being fed to the converter. The crowbar is activated either by high rotor currents or over voltage on the DC bus. To keep the DC Voltage below the upper threshold, first the chopper is switched on by IGBT switches. The crowbar used in [23] consists of resistors connected in parallel with the rotor converter as shown in [25]. The crowbar switches are force-commutated in order to interrupt the currents flowing through them at will, allowing return to normal operation. Depending on the level of energy flow into the DC Link and the chopper design, this measure may be successful in most cases. When the DC Voltage is maintained by the chopper, the RSC goes back into operation following a few milliseconds and the DFIG can be controlled again even if it is operating on a low voltage level. Using force commutated devices provides an advantage over naturally commutated devices as they can break DC current, hence their designation as active crowbar. This solution is relatively simple and cost effective. As the next line of protection, the crowbar is fired and the rotor is short-circuited. The crowbar firing is triggered by the DC Voltage. When the crowbar is switched on, the wind turbine operates as a slip-ring asynchronous machine. After a short transient period, the generator becomes a reactive power consumer which is counterproductive in respect of the grid voltage support as required by the grid codes. However, the crowbar is switched on only for a time period of 60-120 ms. Because the crowbar thyristor switches used in many applications will not interrupt the currents before their zero-crossing, the exact interruption time is not predictable. Therefore, between crowbar interruption and RSC resynchronisation, a possible time slot with open rotor circuits, can exist. However, upon activation of the crowbar, the control over the machine is lost, and the DFIG behaves as a squirrel cade induction machine. The return to normal operating conditions at grid recovery can lead to further crowbar activation if proper control is not set in place to ensure a smooth transition [17, 23, 24, 25].

When the rotor side converter is started again, the DFIG can provide reactive power support to the grid and thus help stabilising the grid voltage. During LVRT, the limitation of the RSC excitation current is switched from active current priority to reactive current priority. As a result, the active power will be reduced automatically when the magnitude of the converter current reaches its threshold. The maximum current allowed for short time is usually approximately the steady state nominal

current and adapted to the loading conditions of the semiconductors dynamically [22, 24].

Additionally, the RSC and the GSC can also be used for reactive current supply. For this temporary overloading of the LSC during FRT is possible so that 30-50% of the 1.0p.u. reactive current, can usually be supplied by the LSC. However, the primary task of LSC comprises the control of DC Link voltage which is performed by the active current control loop. Therefore, the active current has always priority when the magnitude of the LSC reference current has to be limited [24].

DC Converter with Energy Storage

The DC converter with energy storage is used for DFIG. During the grid fault, the rotor current increases, and large current flows across the rotor side converter which remains connected to the grid as shown in Figure 2-12. If the active power reaches its limit or if the terminal voltage is too low, the grid side converter is not able to transmit active power to the grid, then the DC link voltage will increase. To maintain the DC-link Voltage to its rated value, the two quadrants converter is used in combination with an energy storage system (ESS) to control the DC bus voltage [26]. The LVRT capability maintains the DC bus voltage within its limits and allows the rotor converter to control the machine during the fault [23,24].

Reference [24] presents a combined protection and control strategy to improve the transient performance of the DFIG. A wind farm including six 1.5MW wind turbines is simulated to verify the effectiveness of this method. Each DFIG is equipped with an active crowbar and a battery energy storage device. A control scheme which is auto-switching the crowbar according to the size of rotor current is adopted for the crowbar protection to decrease the adverse effects on the system caused by the crowbar. A cascaded control scheme is applied for the battery energy storage devices to attenuate the transient DC voltage ripple in the DC bus when voltage sags in power failure situations.

During LVRT, the wind turbine is commonly equipped with the crowbar connected to the rotor windings and acted to short circuit it in the abnormal rotor current or DC

bus voltage. The rotor speed is then not controlled by the converter during crowbar operation. The work proposed in [26] is the DC converter using battery energy storage system (BESS) for the DC link voltage control in normal and fault conditions. At high wind speed, the BESS absorbs the energy and return it at low wind speed. The DC converter consists of two quadrants DC converter in such a manner to maintain the DC Link voltage constant. The proposed scheme is shown in Figure 2-14 [27].

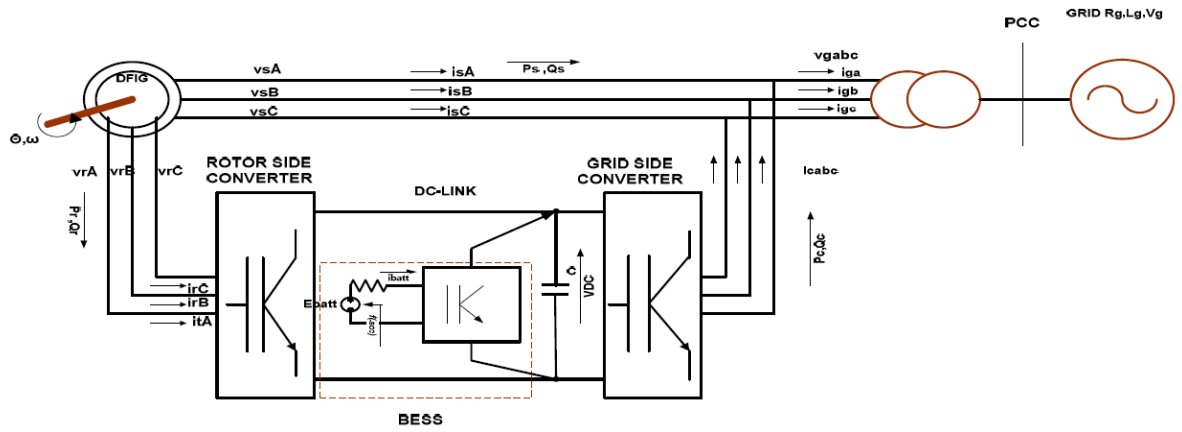

Figure 2-14: Wind Energy Conversion System using Doubly Fed Induction Generator and Battery Energy Storage [27].

The mathematical model of the converter control strategy as depicted in [26, 27] is as follows:

Rotor Side Converter Control

The current hysteresis PWM is chosen to control the rotor side converter and to mitigate harmonic current.

Speed Control

The Generator rotor speed controller can be expressed by equation (2.3) below:

$$P^*_s = \left(K_{wp} + \frac{K_{wt}}{s}\right)(\omega^*_g - \omega_g) \quad (2.3)$$

Where ω is the angular velocity in rad/s of the DFIG.

Power control

The rotor q-axis reference current can be written as equation (2.4) below

$$i^*_q = \left(K_{dp} + \frac{K_{dt}}{s}\right)(P^*_S - P_s) \quad (2.4)$$

Where P_s is the active power delivered by the stator

K_{dp} and K_{dt} are constants

and the rotor d-axis reference circuit can be written as equation (2.5) below:

$$i^*_d = \left(K_{qp} + \frac{K_{qt}}{s}\right)(Q^*_S - Q_s) \quad (2.5)$$

Where Q_s is the reactive power delivered by the stator

Grid Side Converter control

The converter reference voltages V^*_{cd} and V^*_{cq} can be obtained by the following feedback loops and PI controller as shown in equations (2.6) and (2.7) below: [26,27]

$$V^*_{cd} = \left(K_{gdp} + \frac{K_{gdl}}{s}\right)(i^*_{gd} - i_{gd}) - \omega_s L_g i_{gq} + V_s \quad (2.6)$$

$$V^*_{cq} = \left(K_{gqd} + \frac{K_{gql}}{s}\right)(i^*_{gq} - i_{gq}) - \omega_s L_g i_{gd} \quad (2.7)$$

Ignoring the power losses and maintaining Vs constant, the d-axis grid side converter reference current can be obtained by equation (2.8);

$$i^*_{gd} = \left(K_{gdp} + \frac{K_{gdl}}{s}\right)(P^*_g - P_g) \quad (2.8)$$

and the q-axis grid side converter reference current can be obtained by equation (2.9).

$$i^*_{gq} = \left(K_{gqp} + \frac{K_{gql}}{s}\right)(Q^*_g - Q_g) \quad (2.9)$$

The grid side converter reactive power reference can be expressed by the following feedback loops and PI controller as in equation (2.10):

$$Q^*_g = \left(K_{gQ} + \frac{K_{gQl}}{s}\right)(V^*_s - V_s) \quad (2.10)$$

The power in the capacitor is expressed as in equation (2.11):

$$P_{dc} = P_b - P_g - P_r \approx CV_{dc}\frac{dv_{dc}}{dt} \quad (2.11)$$

Where P_{dc} is the capacitor power

P_r is the rotor side converter power

P_g is the grid side converter power

P_b is the battery power

The battery reference current I^*_b can be generated using a voltage feedback control and a PI control scheme as per equation (2.12): [26,27]

$$I^*_b = \left(K_{vp} + \frac{K_{vl}}{s}\right)(V^*_{dc} - V_{dc}) \quad (2.12)$$

The battery current is forced to follow reference current as given by the equation (2.13):

$$S_b = \left(K_{bp} + \frac{K_{bl}}{s}\right)(I^*_b - I_b) \quad (2.13)$$

The battery model used in [23] consists of a DC dependent voltage current controlled source in series with resistor with the following parameters:

V_{batt} – battery voltage

r_{batt} – battery resistance

If battery current I_{batt} > 0 this is the discharge mode then E_{batt} is as per equation 2.14,

$$E_{batt} = f_1(SOC) \quad (2.14)$$

If I_{batt} < 0 this is the charge mode then E_{batt} is as per equation 2.15

$$E_{batt} = f_2(SOC) \quad (2.15)$$

where SOC is the battery state of charge, and is given as per equation 2.16:

$$SOC = 1 - \frac{1}{Q_n}\int_0^t I_{batt}(t)dt \quad (2.16)$$

Braking resistors on DFIG

Reference [28] reports on a DFIG control scheme using braking resistors. As per [28] the control scheme works according to the following steps:

1. Detect the grid fault.
2. Connect the braking resistors by opening the switches; simultaneously inject demagnetizing currents through the rotor converter.
3. Activate the DC link chopper when DC voltage is over 1.1 p.u.
4. Generate reactive power when natural flux decays to a certain small value.
5. Steps 2 and 3 are repeated upon the detection of voltage recovery.
6. Normal operation is then resumed.

The braking resistors have two functions: accelerates the decay of the natural flux and balance active power of wind turbine. When the braking resistors are placed in series with the stator winding, the time constant of stator natural flux evolution is given as per equation 2.17: [28]

$$t_s = (L_T + \sigma L_s)/(R_s + R_B) \quad (2.17)$$

Since the braking resistance is much larger than stator resistance, inserting braking resistors will be able to significantly reduce the time constant. If R is selected to be 0.3pu, time constant T_s will be reduced from 34ms to 1.5ms and then the flux transient will last less than 5ms. The wind turbine can start injecting reactive current

almost immediately after the beginning of the fault. It should be noted that, the required demagnetizing current, may still be higher than two times of the rated current which is normally not acceptable. Thus, it is required to limit the injecting current reference to an acceptable value and simultaneously reduce the steady state current reference when the demagnetizing current is high. On the other hand, insufficient demagnetizing current cannot weaken the natural flux sufficiently to ensure the converter is fully controllable. Then the converter may be saturated in the beginning of the fault and current will go throw the diode to charge DC-link capacitor. Therefore a DC chopper is required here to limit the DC-link voltage. Since the natural flux decay very fast with the help of braking resistors, the activation time of the chopper is very short and the energy required to dissipate on the chopper resistor is very small. During fault, the breaking resistors may stay connecting in series with the stator such that they can be used for dissipating energy of wind turbine. This will help reduce the acceleration of the rotor speed since the pitch control system cannot response that fast during fault. In addition, this will also reduce the low frequency shaft oscillation caused by fault since wind turbine shaft-blades systems are considered as 'soft' mechanical system [28].

2.4.3 Salient pole synchronous generator

Another type of generator that has been proposed for wind turbines in several research articles is a salient pole synchronous generator. This type of generator has the capability of direct connection (direct-drive) to wind turbines with no gearbox. This advantage is favourable with respect to lifetime and maintenance. Synchronous machines can use either electrically excited or permanent magnet (PM) rotor [29].

In this thesis, the performance of a salient pole synchronous generator with STATCOM control is investigated. Control systems proposed by authors are mainly related to Permanent Magnet Synchronous Generators (PMSG) elaborated in section 2.4.4.

In [30], two control systems have been implemented for a Direct Drive Synchronous Generator (DDSG) - one type of synchronous generator. In the scheme, the control is achieved through the DC TO DC boost converter, the average model of the DC to DC boost converter was used as per the equations (2.18) and (2.19): [30]

$$\frac{dU_{dc}}{dt} = \frac{1-D}{C_{dc}}.i_L \quad (2.18)$$

$$\frac{di_L}{dt} = -\frac{1-D}{L_c}.U_{dc} + \frac{1}{L_c}U_0 \quad (2.19)$$

where the duty cycle D is given by equation (2.20):

$$D = 1 - \frac{U_0}{U_{dc}} \quad (2.20)$$

The notations of currents and voltages are explained in Figure 2-15:

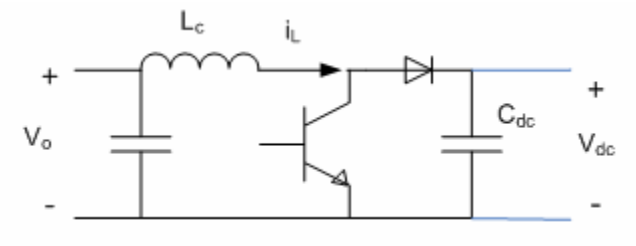

Figure 2-15: Average model of the DC to DC boost converter [31]

The power control via the DC to DC boost converter is implemented through the control of the duty cycle as shown in Figure 2-16:

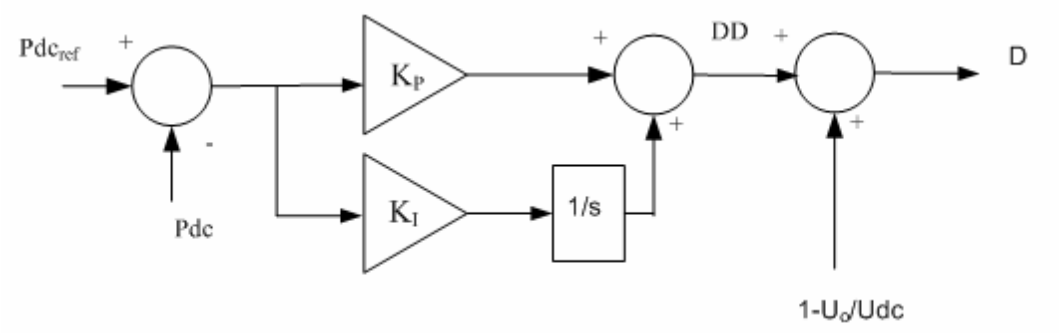

Figure 2-16: Diagram of the power control via the DC to DC boost converter [31]

The DC voltage is kept to equal its nominal value (1.0 p.u.) through the automatic voltage regulator (AVR) due to the algebraic relation between the generator terminal voltage and the output voltage of the rectifier. The differential describing the dynamics of the capacitor in the DC-link connecting the rectifier and the grid side converter was added to the model and is given in equation (2.21) below: [31]

$$C_{dc} = \frac{dU_{dc}}{dt} = \frac{\Delta P_{conv}}{V_{dc}} \qquad (2.21)$$

where $\Delta P_{conv} = P - P_{Grid}$, the difference between the active power supplied from the stator circuit and the active power exchanged between the GSC and the grid. The control of the GSC follows the same principles as those shown in Figures 2-17a and 2-17b below: [30]

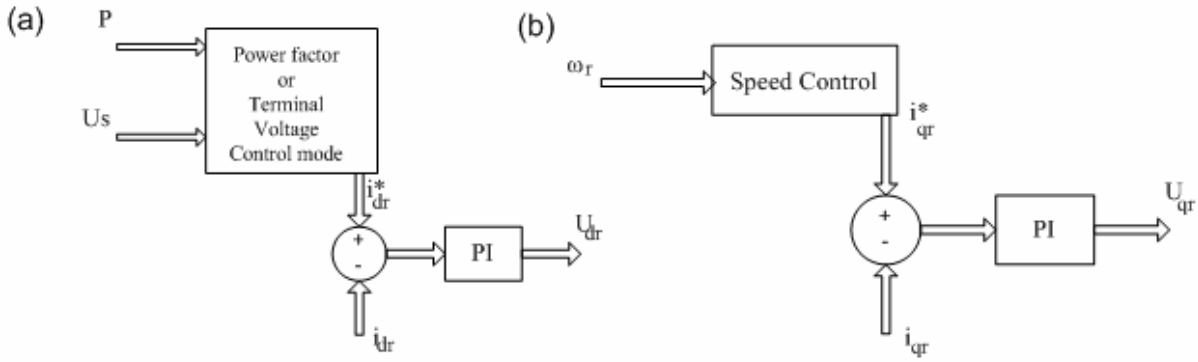

Figure 2-17: Block diagrams of the rotor side converter [30]

(a) Reactive power control block

(b) speed control block [30]

2.4.4 Permanent Magnet Synchronous Generators

The PMSG and conventional synchronous generators differ from the induction generator in that the required magnetization is provided by a Permanent Magnet pole system or a DC excitation on the rotor. Self-excitation allows operation at high power factors and high efficiencies for the PMSG machines. It is worth mentioning again that induction generators are the most common type of generator used in modern wind turbine systems [24, 25]. The main advantage include the low cost of the inverter and filter components. This is due to the low rotor and grid side power conversion ratings (25% - 30%) and the power converter provides the reactive power for magnetisation of the generator [32]. A comparison between the variable speed wind turbine and the constant speed wind turbine shows that variable speed reduces mechanical stresses: gusts of wind can be absorbed dynamically compensate for torque and power pulsations caused by back pressure of the tower. This backpressure causes noticeable torque pulsations at a rate equal to the turbine

rotor speed times the number of rotor blades. The use of a doubly fed induction generator in WECS with the rotor connected to the electric grid through an AC-AC converter offers the following advantages:

- Only the electric power injected by the rotor needs to be handled by the convert implying a less cost AC-AC converter;
- Improved system efficiency and power factor control can be implemented at lower cost as the converter has to provide only excitation energy.

Hence taking advantage of power electronic advances in recent years WECS equipped with doubly fed induction generator systems for variable speed wind turbine are one of the most efficient configurations for wind energy conversion [29].

The advantages of PMSG machines over conventional synchronous generators can be summarized as follows according to literatures: [33]

- Higher efficiency and energy yield;
- No additional power supply for the magnet field excitation;
- Improvement in the thermal characteristics of the PM machine due to the absence of the field losses;
- Higher reliability due to the absence of mechanical components such as slip rings; and
- Lighter and therefore higher power to weight ratio.

However, PM generators have some disadvantages, which can be summarized as follows: [33]

- High cost of permanent magnet material;
- Complicated maintenance such as bearing replacement
- Demagnetization of PM at high temperature.

In the recent years the use of PMSG has been increasing than previously because the performance is improving and the cost is decreasing. The trends make PM machines with a full-scale power converter more attractive for direct-drive wind turbines. In addition to that, the cost of power electronics is also decreasing the variable speed direct-drive PM machines with a full-scale power converter becoming

more and more popular for offshore wind powers. On the other hand, variable speed concepts with a full-scale power converter and a single- or multiple-stage gearbox drive train may be interesting solutions not only in respect to the annual energy yield per cost, but also in respect to the total weight. For example, the market interest of PMSG system with a multiple-stage gearbox or a single-stage gearbox is increasing [33-35].

2.5 Role of synchronous generator and DFIG based wind farm in LVRT.

With respect to this thesis, some papers have shown a comparison analysis between a salient pole synchronous generator based wind power plants to the DFIG based wind farm. Results from [36] state that, during deep voltage sags, the synchronous generator feeds in more reactive current than the DFIG based WF and thus gives a stronger support to the grid voltage. However, for smaller voltage dips resulting from distant faults, the DFIG can feed in higher reactive currents. While in the Synchronous generator, the transient reactive current is determined by the generator parameters, the fast control of the DFIG allows the adjustment of the reactive currents within the current limits of the system during faults. The largest difference between the two systems can be seen during unbalanced faults, where the DFIG has to reduce the positive sequence currents to avoid thermal overloading of the converter.

Synchronous Generators usually operate together, forming a large power system supplying Electrical energy to the loads or consumers. They are built in large units, having their rating ranging from tens to hundreds of Megawatts. Synchronous generators are known to be much more effective in terms of reactive power injection during grid fault and by consequence, the terminal voltage is kept in higher levels as compared to DFIG [36]. As mentioned in section 2.6, most LVRT techniques are based on permanent magnet synchronous generators as compared to the conventional synchronous generators.

In this thesis, the use of STATCOM as a control system on synchronous based wind farm is elaborated and simulated from mathematical model.

DFIG is a popular wind turbine system due to its high efficiency, reduced mechanical stress on the wind turbine, separately controllable active and reactive power and relatively low power rating of the connected converter. But due to the direct connection of the stator to the grid, the DFIG suffers from a great vulnerability to grid faults and requires additional protection of the rotor side power electronic. The Crowbar method of protection is the most useful and convenient way for LVRT.

2.6 Summary

In the light of the above reviews of the LVRT scenarios on wind farms, this research work investigates and compares the LVRT behaviour of a synchronous generator based wind turbine with STATCOM to that of a crowbar controlled DFIG wind turbine. The purpose is to determine how the use of a STATCOM with synchronous generator might improve the LVRT behaviour of a wind farm or whether if there are existing STATCOMs in the system in the vicinity of a synchronous generator wind farm, these devices can be used for helping that wind farm to achieve LVRT if needed instead of replacing them with DFIG based wind generators

Reviews on various components such as STATCOM, synchronous generator, DFIG with crowbar control provide an overview of the work to be presented in this thesis. The synchronous generator based wind farm with STATCOM as the controller for LVRT is simulated and compared to the crowbar method control on a DFIG based wind farm as the latter is the most common and convenient way for LVRT nowadays.

This thesis involves mathematical and empirical research methods. Therefore the investigation is firstly backed up with relevant literature to determine the context of the objectives of this work in relation to what has been done by other researchers. The product of this approach is the literature review presented. Loopholes in the existing knowledge in the area of LVRT are identified from the extensive study of literature. Thus, specific research questions are formulated and pursued in this thesis. Assumptions and propositions are formulated from the research questions, keeping in view the expected outcome. The procedure used is summarised by three stages shown in Figure 2-18 below.

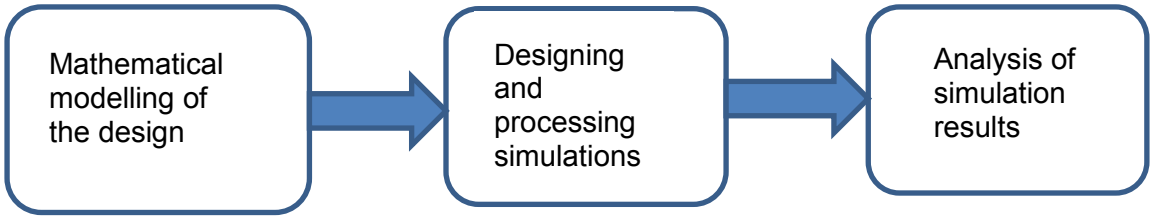

Figure 2-18: Research methodology

3 RESEARCH METHODOLOGY – MODELING AND SIMULATION OF TEST SYSTEM COMPONENTS

3.1 Summary of work

This chapter details the research methodology including modeling and simulation of test networks and the wind farms. In this research, two types of wind generation technology are considered for analysis and comparison of their low voltage ride through capabilities, viz., synchronous generator (with and without STATCOM) and doubly-fed induction generator (DFIG). The research focuses on the low voltage ride through characteristics and efficiency of both the machines under voltage sag caused by faults. In this research, the first case study investigates the LVRT behavior and capability of asynchronous generator based wind farm first without and then with a STATCOM to achieve LVRT during a fault or voltage sag. The second case study investigates the LVRT behavior and capability of a crowbar protected DFIG wind farm under the same fault condition. The modeling and simulations are used to compare the two types of wind farms in terms of their LVRT behavior. The modeling and simulation studies are performed using Matlab Simulink and the mathematical models described in this chapter are in line with this software application.

3.2 Research Plan

The research reported in this thesis is divided into the following tasks as below:

i) Modeling and simulation of the wind resource

ii) Modeling and simulation of the test system, including all components, used for the case studies.

iii) Investigation of LVRT behavior of Synchronous Generator Based Wind Turbine with STATCOM (FACTS devices used for LVRT) – Case 1A

iv) Investigation of LVRT behavior of Synchronous Generator based wind turbine without STATCOM controller (No LVRT capability) – Case 1B

v) Investigation of LVRT behavior of DFIG wind turbine with crowbar controller – Case 2.

vi) The two scenarios are compared to determine which one of the two generators performs better under LVRT and provides stronger grid voltage support under the same fault condition.

3.3 Test System Description for Case Studies 1A, 1B and 2

The test system in Cases 1A and 1B comprises a 10MW wind farm consisting of five 2 MW wind turbines each with a salient pole synchronous generator. The wind farm is connected to a 25kV distribution system that exports power to a 120kV grid through a 25kV feeder 30km in length. The synchronous generators of the wind farms are connected to a diode rectifier, a DC-DC IGBT based PWM boost converter and a DC/AC IGBT based PWM converter modelled by voltages sources. This wind turbine technology allows extracting maximum energy for low wind speeds by optimizing the turbine speed, while minimising mechanical stresses on the turbine during high winds. The control system of the DC-DC converter is used to maintain the speed at 1.0 p.u.

This test system for Case 2 is similar to the one used for Cases 1A and 1B. The only difference is that for Case 2 test system each 2 MW wind farm is equipped with DFIGs with crowbar protection. Figure 3-1 shows the single line diagram of the test system and Figure 3-2 shows the simulation of the same done in Matlab/Simulink.

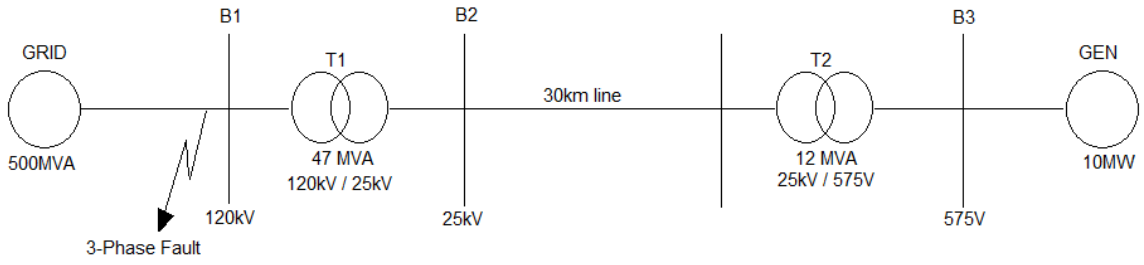

Figure 3-1: Line diagram for Cases 1A, 1B and 2

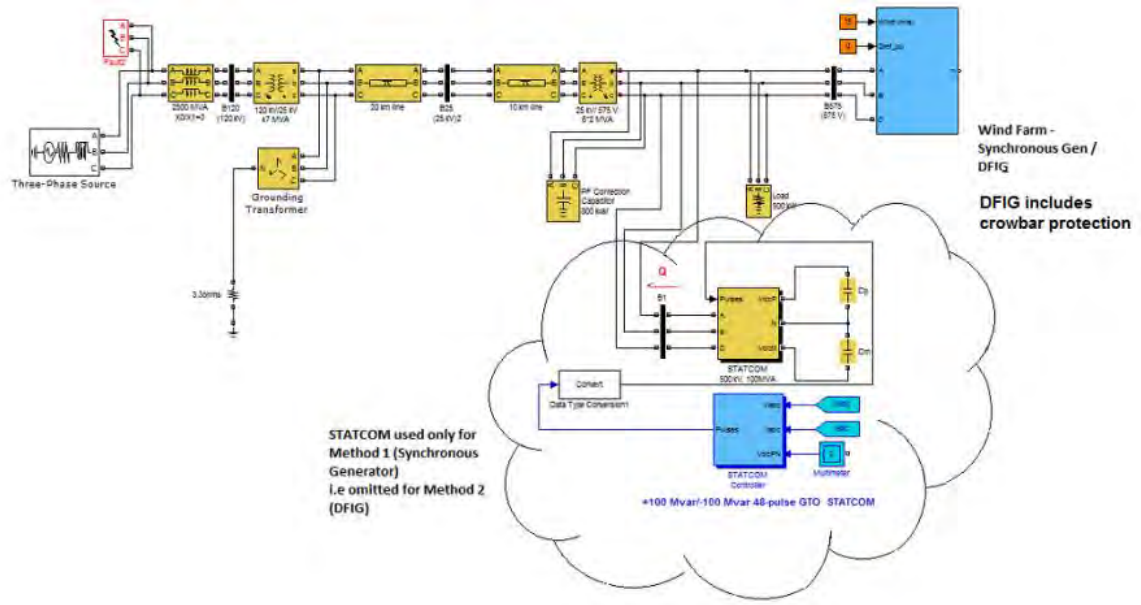

Figure 3-2: Simulated Test system for Case study 1A, 1B & 2

3.3.1 Case Studies

The practicability and effectiveness of the low voltage ride through conditions, the different case studies listed in Table 3-1 are used for each of the case scenarios 1A, 1B and 2:

Table 3-1: Characteristics and parameters of scenarios 1 - 4

Case Scenario	Low voltage clearing time (s)	Voltage drop (p.u.)
1	0.11	0
2	0.5	0.29
3	1	0.4
4	1.8	0.7

The results in chapter 4 are arranged as follows:

a. A comparison between a synchronous generator with and without STATCOM compensation
b. A comparison between synchronous generator with STATCOM compensation and DFIG with crowbar control.

3.4 Choice of Wind Generators and Basis of Comparison of the LVRT Behaviour

The wind generators selected for this study are the salient pole synchronous generator and the doubly fed induction generator. As mentioned in section 2.5 of the

literature review, synchronous generators are described known to provide better compensation characteristics for LVRT as compared to DFIG. According to [27], synchronous generator based wind farms feed in more reactive current than DFIG based wind farms. As a result, the terminal voltage is maintained at higher levels compared to DFIG. DFIG is mostly used in wind farms due to its high efficiency and easy controllability of its active and reactive power. However, as the stator is directly connected to the grid, the DFIG is vulnerable to grid faults and additional protection is required on the rotor side. The additional rotor protection is used to disconnect the converter to protect the DFIG from behaving as a squirrel cage induction machine as the DFIG behaves as a normal SCIG when the power electronic converter is bypassed. The protection unit consisting of power electronics components can short circuit rotor windings when needed and thus can provide an additional path for the rotor current. The crowbar protection for DFIG rotor is the most useful and effective way as discussed in section 2.5 in the literature review.

The parameters used for comparing the LVRT behaviour in the two case studies are as follows:

1. Active power from Generator
2. Reactive power from Generator
3. Comparison of reactive power from generator
4. Voltage profile at bus 2
5. Voltage profile at bus 3
6. Comparison of voltage profiles at bus 2 and 3

Bus 2 and Bus 3, are located in the test system as shown in Figure 3.1 and Figure 3.2. Bus 2 is connected to the 25kV secondary of the 120kV/25kV transformer and marks the starting point of the 25kV feeder as seen from the grid side. Bus 3 is connected at the terminal of the wind generator. Bus 2 and Bus 3 together will provide an overview of the characteristic voltage and current profiles both for grid side and the generator side of the transmission line system w.r.t the test system as depicted in Figure 3.1. Active and reactive powers are measured at the output of the generator so that their variation can be compared for different case studies carried out in this work.

The correctness of mathematical model that forms the basis to this research work, as mentioned in [28], will have a direct impact on the choice and application of the generator. Mathematical modelling of synchronous and asynchronous generators and power networks is an established technique for the evaluation of system dynamic behaviour and control techniques, and it is necessary that the validity of the models used be verified by comparison with real machine behaviour [29]. The mathematical model of the test system as described in this chapter is developed in Matlab /Simulink.

This following sections present modelling and simulation of the wind resource, wind farms components along with controls and protection, STATCOM, external grids, loads and transmission/distribution lines and transformers. This chapter also discusses the selection of Matlab as the software for the study.

3.4.1 Selection of Matlab Software for study

The research uses software modeling for the analysis of the Fault ride through condition on both generators. Modeling on software is chosen as it combines characteristics of different type of modeling. Case studies are used to provide an analysis report with regards to the thesis topic in a timely manner. However, an apparent problem to modeling as compared to real-life system is the accuracy of the system. Therefore, to prevent limitations of the model from affecting the objectives and accuracy of the results, the simulations are supported by theoretical explanations. The validation of a mathematical model however must be performed by comparing the model with the real physical system which is beyond the scope of this thesis.

3.5 Modelling of the Wind Profile and Wind Turbine

This section presents the modelling and simulation of the wind profile and the wind turbine which will be presented as the input to the wind generator models.

3.5.1 Wind Profile Model

The wind model describes the temporal fluctuations in the wind speed which influence the power output, power quality and guide the control requirements of the wind generator. The wind acting on the rotor plane of a wind turbine is very complex and includes various deterministic effects [2]. The wind model used in this research

is developed from the repeating sequence signal block in Matlab/Simulink of very high amplitude values generated randomly as a time series over the simulated period which implements the varying wind gusts conditions as shown in Table 3-2. This is similar to step input signals sampled over a period of time. The input signal is simulated using the repeating sequence block from Matlab/Simulink. The parameters implemented are shown in Table 3-2.

Table 3-2: Characterised output values of Wind Block

Time Values / s	0	0.2	0.4	0.5	0.8	0.9	1.2	1.5	1.6	1.7	1.9	2.0	2.2	2.4	2.5	2.7	2.8	2.9	3.0
Output Values / (m/s)	145	100	90	70	120	150	195	200	45	50	20	65	125	85	195	175	180	160	175

Figure 3-3 demonstrates the wind model developed for this research with a repeating sequence of random but realistic wind speed values.

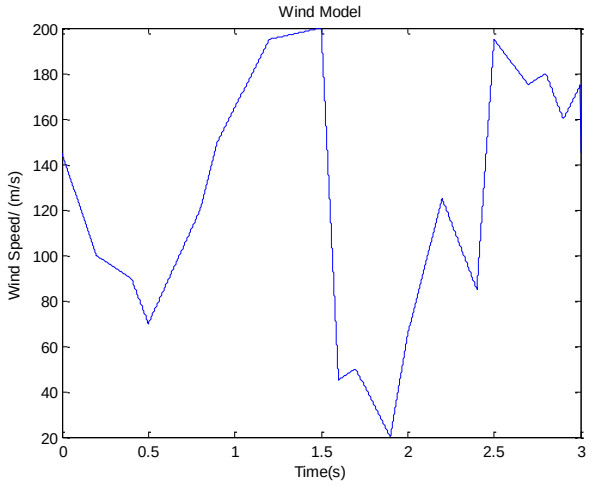

Figure 3-3: Wind Model developed in this research

3.5.2 Implementation of Wind Turbine Model

For this research, the wind turbine has been implemented for the test system by using the standard variable pitch wind turbine Matlab /Simulink model to which the wind profile is directly input. This model is described briefly in this section. In this model, the power coefficient, C_p is obtained by dividing the mechanical power output of the turbine by the wind power and a function of wind speed, rotational speed, and pitch angle. Figure 3-4 shows the power characteristics of this wind turbine model.

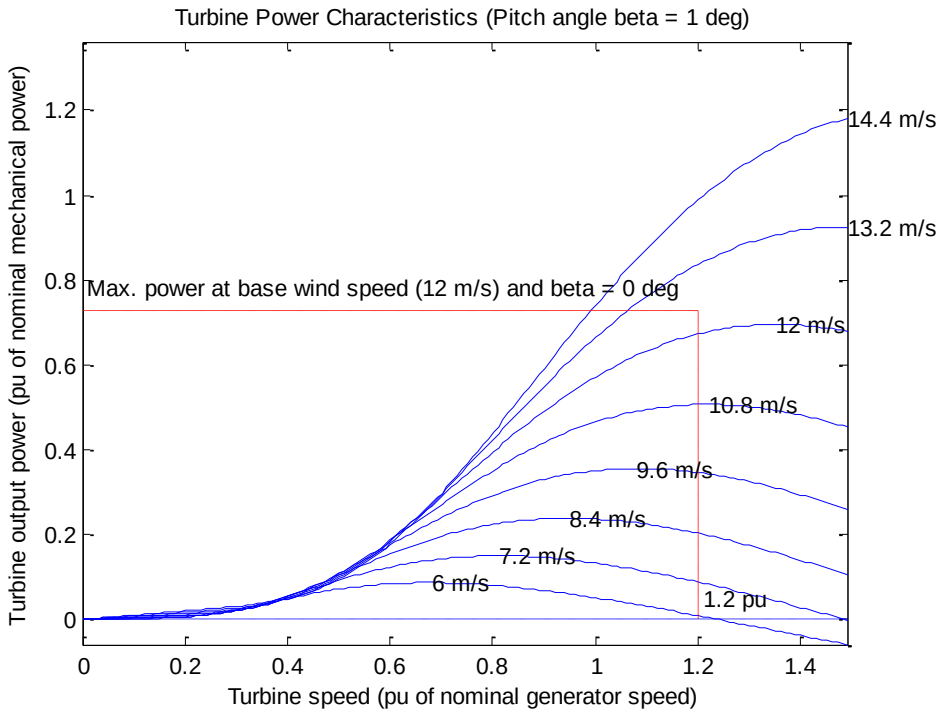

Figure 3-4: Wind turbine characteristic from wind turbine model in Matlab / Simulink [37]

The wind turbine captures the kinetic energy from the wind and converts it to mechanical energy. A horizontal axis wind turbine usually consists of a three-blade rotor. It is commonly fitted with a pitch angle controller mechanism to modify the blade pitch angle and as a consequence, to limit the rotor speed and therefore the generated power at high wind speeds. In the Matlab/Simulink model of the wind turbine used for this study, pitch control mechanism has been assumed. Figure 3-5 shows the schematic diagram of the pitch control mechanism. A detailed discussion of the pitch control mechanism is, however, outside the scope of this thesis.

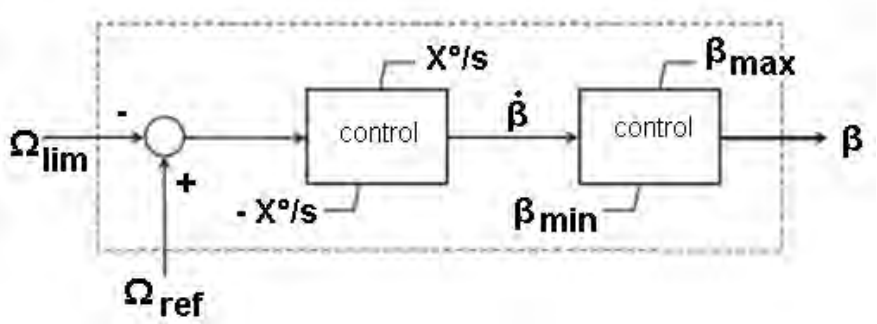

Figure 3-5: Pitch angle controller system model [38]

The aerodynamic torque of the wind turbine is derived from the equation (3.1) [37]:

$$T_{Wt} = \frac{1}{2}\,\pi\,\rho\,R^{2}\frac{V^{3}}{\eta}\,C_p(\lambda,\beta) \qquad (3.1)$$

where:

ρ is the air density (kg/m³)

R is the blade radius (m)

V is the wind speed (m/s)

η is the turbine rotational speed (rpm)

C_p is the power coefficient

β is the blade pitch angle (rad)

λ is the tip speed ratio

In the above model, C_p is dependent on the pitch angle β. The control involves the gain, k, and the limits of the pitch angle controller, β_{max} and β_{min}. Ω_{lim} is the limit value of the rotational speed [37,39].

Moreover, the torque output also depends on the power coefficient C_p look-up table from manufacturer's datasheet. Manufacturers usually give an experimental relationship between C_p and λ parameter, for several values of the blade pitch angle, β. The C_p coefficient is evaluated by using interpolation functions to approximate this experimental relationship, within each range of instantaneous values of λ. Equation (3.2) is used for calculating C_p [37,39]:

$$C_p(\lambda,\beta) = C_p(max)\left[1 - \left(\frac{(\lambda - \lambda_{\max}(\beta))}{\lambda_0(\beta) - \lambda_{max}(\beta)}\right]^{2}\right. \qquad (3.2)$$

for $\lambda_{max}(\beta) < \lambda < \lambda_0(\beta)$

where for each β,

$C_{p\,max}(\beta)$ is the maximum value of C_p,

$\lambda_{max}(\beta)$ is the λ value for $C_{p\,max}$,

$\lambda_0(\beta)$ is the λ limit value above which C_p is null.

A typical relationship between C_p and TSR (λ) is given in Figure 3-6 and the power curve is shown in Figure 3-7. It can be seen that the turbine will operate at its maximum efficiency at only one unique Tip Speed Ratio (TSR). Since the radius of the blades is constant, the ratio between the rotor speed and the wind speed will determine the operating point of the turbine. The maximum power curve is determined by using the typical output power curves for different wind speeds as shown in Figure 3-7. The cubic curve intercepts the maximum point of each power curve. Operation on this curve allows maximum power capture and therefore maximum efficiency. These curves are usually provided by the manufacturer of the wind turbine to allow the user to predict the performance of the wind turbine [37,39].

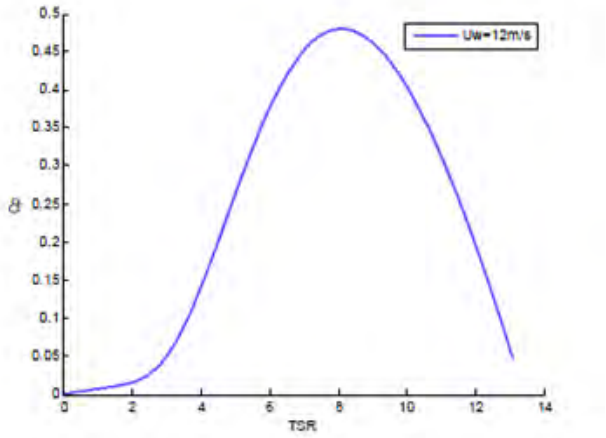

Figure 3-6: Cp versus TSR curve for a typical wind turbine [39,40]

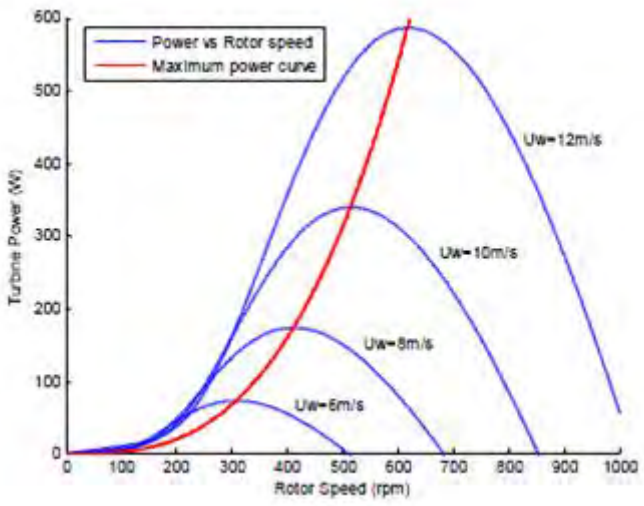

Figure 3-7: Power Curve for a typical wind turbine [39,40]

The wind turbine model implemented in the test system is based on the steady state power characteristics of the turbine. The stiffness of the drive train is infinite and the friction factor and the inertia of the turbine must be combined with those of the generator coupled to the turbine. The output power of the turbine is given by the following equation (3.3): [39, 40]

$$\boldsymbol{P_m = C_p(\lambda, \beta)\frac{\rho A}{2}v^3_{wind}} \quad (3.3)$$

where

P_m - Mechanical output power of the turbine (W)

C_p - Performance coefficient of the turbine

ρ is the air density (kg/m³)

A - Turbine swept area (m2)

v_{wind} - Wind speed (m/s)

ρ is the air density (kg/m³)

λ is the tip speed ratio of the rotor blade tip speed to wind speed

β - Blade pitch angle (deg)

A generic equation is used to model $C_p\ (\lambda, \beta)$ as shown by equation (3.4) below [39]:

$$C_P(\lambda, \beta) = c_1(\frac{c_2}{\lambda_i} - c_3\beta - c_4\beta^x - c_5)e^{\frac{c_6(\lambda,\beta)}{\lambda_i}} \quad (3.4)$$

with

$$\frac{1}{\lambda_i} = \frac{1}{\lambda + 0.08\beta} - \frac{0.035}{\beta^3 + 1} \quad (3.5)$$

C_{1-6} = empirical power coefficient parameters

From reference [41], values of coefficients c_1 to c_6 can be derived as the empirical power coefficient parameters. These are defined values and are as follows: [40, 41]

c_1 = 0.5176,

c_2 = 116

c_3 = 0.4

c_4 = 5

c_5 = 21

c_6 = 0.0068.

The $C_P - \lambda$ characteristics, for different values of the pitch angle β, are illustrated below:

The maximum value of C_p($C_{p\,max}$= 0.48) is achieved for β = 0 degree and for λ =8.1. This particular value of λ is defined as the nominal value (λ_{nom}).

3.6 Modeling and Simulation of Synchronous Generator based Wind Farm with STATCOM

3.6.1 The Synchronous Generator Model

The choice of a salient pole generator is based on the fact that the salient pole rotor structure is preferred for low speed and small to medium sized power applications such as hydro-electric power plants and wind power plants. On the contrary, non-salient pole or wound rotor synchronous generators are used for high speed, high power applications such as The generator has three identical armature windings symmetrically distributed around the air-gap, and one field winding. There are two types of rotor structures in synchronous generators: round (non-salient pole) rotor and salient pole rotor. Usually, the non-salient pole rotor structure is used for high speed and large power synchronous mechanisms, such as steam turbine generators and nuclear power plants, while the salient pole structure is preferred for low speed and small to mid-size power applications such as hydro-electric and wind turbine applications. It is also cheaper to use a salient pole design in wind

generators than a round rotor. This model assumes that there is one damper winding on each axis of the machine. Armature windings are placed on the stator and field and damper windings are on the rotor [42].

In Case 1A and 1B, the synchronous generator for the wind turbine is implemented using the standard synchronous generator model of Matlab and the mathematical basis of the model and parameter selection are discussed in the following sections.

Assumptions for Synchronous Generator Model Development

To be able to simplify the model development of the synchronous generator model in Matlab/Simulink, the following assumptions have been made [42]:

1. It is assumed that every winding present in the machine produces a sinusoidal MMF along the air gap, which for phase *a*, can be expressed by equation (3.6) [42]:

   $$\theta_a = \theta_a \sin(\frac{p}{2} \gamma_s) \quad (3.6)$$

   where:

   p : machine's number of poles

   γ : stator's angular coordinate

2. Iron permeability in the machine is assumed to be infinite. All effects due to magnetic saturation and flux fringing are neglected [42].

3. In other reviews, rotor construction is assumed to be the only factor contributing to magnetic asymmetry in the machine. However, if effects of the stator or rotor slots are taken into account, this assumption results in approximating the magnetic conductivity function as equation (3.7) [42]:

   $$\lambda = \lambda_0 - \lambda_2 \cos(p, \gamma_s) \quad (3.7)$$

   λ_0 and λ_2 are dependent on the geometry of the air gap.

4. Local value of magnetic flux density is obtained by multiplying local values of MMF and magnetic conductivity. The third harmonic of the magnetic flux density resulting from this multiplication is neglected [42].

Model reference system

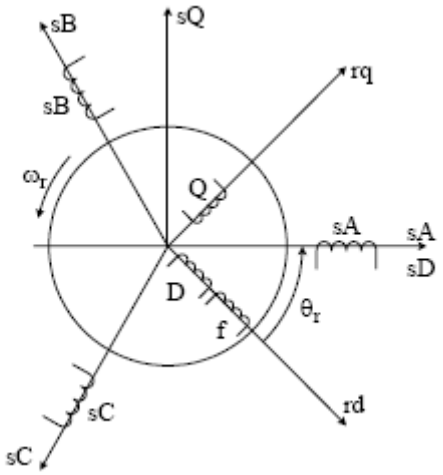

Figure 3-8: dq reference of three - phase synchronous generator [42]

A synchronous machine in generator mode can be described by a system of *n+1* equation, *n* of which are electrical and one of which is mechanical. The number of electrical equations, *n*, is equal to the number of independent electrical variables necessary to describe the generator [42]. These variables can be either currents or flux linkages. In this research, currents are chosen to be the independent variable [42].

Kirchhoff's voltage law is applied to every winding and corresponding electrical equations are obtained. This is achieved by equating the voltage at the winding's terminal to the sum of resistive and inductive voltage drops across the winding. The damper windings are always short circuited [42]. As a result, the terminal voltage of the damper windings is zero.

Total magnetic flux linked with the winding need to be evaluated to be able to have a correct value of the inductive voltage drop across a winding [42]. That is achieved by means of an inductance matrix, which relates all windings' flux linkages to all windings' currents [42]. For a salient pole synchronous machine, the inductance matrix is dependent on the rotor position. This is because of the magnetic asymmetry of the rotor in the machine generator. As a result, there is a preferable magnetic direction which coincides with the direction of the flux produced by the field

winding and is defined as the machine's d-axis [42]. The q-axis of the machine is placed at 90 degrees (in a clockwise direction) with respect to the generator's d-axis [42]. Thus, an angle θ exists between the magnetic axis of the armature phase, *a*, and the rotor's q-axis [42]. The d- and q-axes of the generator is shown in Figure 3-8. The stator voltages in the d and q axes are denoted by *sD* and *sQ* respectively, whereas the rotor voltages are denoted by *rd* and *rq*.

The reference system of the synchronous generator, in which the machine's electrical and magnetic variables are expressed, is changed to simplify the modelling of the machine. Thus, the stationary reference frame known as the *abc* reference frame, is transformed to a *dq* reference frame, in which all the variables are expressed in relation to an observer placed on the rotor. The transformation from the *abc* to the *dq* reference frame is carried out by the following transformation matrix as shown in equations (3.8) and (3.9) [42]:

$$M = \sqrt{\frac{2}{3}} \begin{bmatrix} \sin\theta & \sin(\theta - \frac{2\pi}{3}) & \sin(\theta + \frac{2\pi}{3}) \\ \cos\theta & \cos(\theta - \frac{2\pi}{3}) & \cos(\theta + \frac{2\pi}{3}) \end{bmatrix} \quad (3.8)$$

Inverse transform from dq to abc reference frame) is:

$$M_{INV} = \sqrt{\frac{2}{3}} \begin{bmatrix} sin\theta & cos\theta \\ \sin\left(\theta - \frac{2\pi}{3}\right) & \cos\left(\theta - \frac{2\pi}{3}\right) \\ \sin\left(\theta + \frac{2\pi}{3}\right) & \cos\left(\theta + \frac{2\pi}{3}\right) \end{bmatrix} \quad (3.9)$$

where *θ* can be calculated using the following equation (3.10): [42]

$$\theta(t) = \int_0^t \omega(t)dt + \theta o \quad (3.10)$$

Therefore, any set of three-phase variables: X_a, X_b, X_c such as voltage and current, expressed in the *abc* reference frame can be transformed into the dq reference frame variables , X_d , X_q, by multiplying by transform matrix M which involves the combination of Park and Clarke transform where the total system power is

preserved. The abc-to-dq transformation and dq-to-abc inverse transformation are expressed by the following equations (3.11) and (3.12) respectively:[42]

$$\begin{bmatrix} X_d \\ X_q \end{bmatrix} = M \begin{bmatrix} X_a \\ X_b \\ X_c \end{bmatrix} \tag{3.11}$$

and

$$\begin{bmatrix} X_a \\ X_b \\ X_c \end{bmatrix} = M_{INV} \begin{bmatrix} X_d \\ X_q \end{bmatrix} \tag{3.12}$$

Modelling equations and equivalent circuit of a synchronous generator

The synchronous generator's equivalent circuit in the rotor reference frame for d-axis and q-axis are shown in Figures 3-9 and 3-10 respectively. Electrical description of the generator is given by the set of equations (3.13) to (3.19) which are listed below and categorised as armature equations, field equations and damper winding equations [43]:

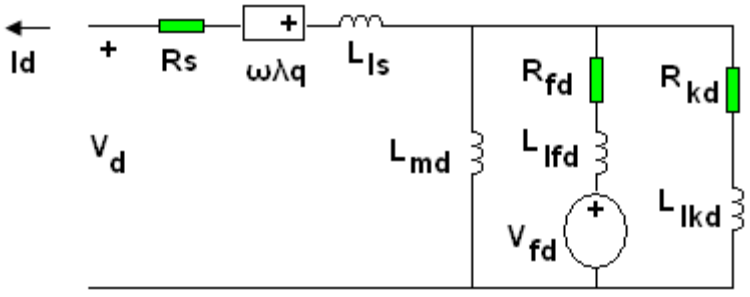

Figure 3-9: Synchronous generator equivalent circuit in rotor reference frame d-axis[43]

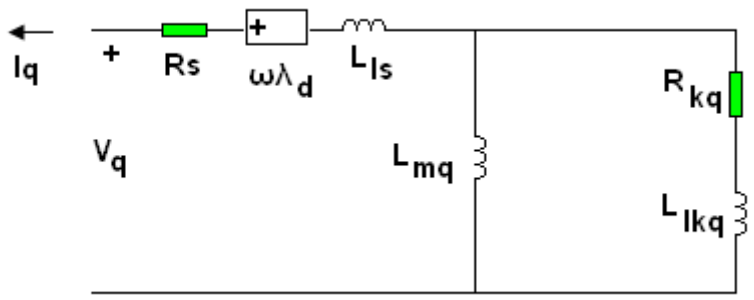

Figure 3-10: Synchronous generator equivalent circuit in rotor reference frame q-axis [43]

a) Armature equations [42,43]

$$V_d = -R_s i_d - \omega\lambda_q - (L_{ls} + L_{md})\frac{di_d}{dt} + L_{md}.\frac{di_{fd}}{dt} + L_{md}.\frac{di_{kd}}{dt} \quad (3.13)$$

$$V_q = -R_s i_q + \omega\lambda_d - (L_{ls} + L_{md})\frac{di_q}{dt} + L_{mq}.\frac{di_{kq}}{dt} \quad (3.14)$$

where:

$$\lambda_d = -(L_{ls} + L_{md})i_d + L_{md}(i_{fd} + i_{kd}) \quad (3.15)$$

$$\lambda_q = -(L_{ls} + L_{mq})i_q + L_{mq}i_{kq} \quad (3.16)$$

b) Field equation [42,43]:

$$V_{fd} = R_{fd}i_{fd} - L_{md}\frac{di_d}{dt} + (L_{lfd} + L_{md})\frac{di_{fd}}{dt} + L_{md}.\frac{di_{kd}}{dt} \quad (3.17)$$

c) Damper winding equations [42,43]:

$$0 = R_{kd}i_{kd} - L_{md}.\frac{di_d}{dt} + L_{md}.\frac{di_{fd}}{dt} + (L_{lkd} + L_{md}).\frac{di_{kd}}{dt} \quad (3.18)$$

$$0 = R_{kq}\,i_{kq} - L_{mq}.\frac{di_q}{dt} + (L_{lkq} + L_{mq})\frac{di_{kq}}{dt} \quad (3.19)$$

The representation for the parameters and variables used in the above equations are as follows [42,43]:

- ω : rotor speed (rad/s)
- V_d: armature d axis terminal voltage (V)
- V_q : armature q axis terminal voltage (V)
- i_d : armature d axis terminal current (A)
- i_q : armature q axis terminal current (A)
- V_{fd}: field winding terminal voltage (reflected to the stator) (V)
- I_{fd}: field winding terminal current (reflected to the stator) (A)
- I_{kd} : d axis damper winding current (reflected to the stator) (A)
- I_{kq} : q axis damper winding current (reflected to the stator) (A)
- λ_d : total armature flux in d axis (Wb)
- λ_q : total armature flux in q axis (Wb)
- R_s : armature phase resistance (Ω)
- L_{ls} : armature phase leakage inductance (H)
- L_{md} : d axis coupling inductance (H)
- R_{fd} : field winding resistance (reflected to the stator) (Ω)
- L_{lfd} : field winding leakage inductance (reflected to the stator) (H)
- R_{kd} : d axis damper winding resistance (reflected to the stator) (Ω)
- L_{lkd} : d axis damper winding leakage inductance (reflected to the stator) (H)
- L_{mq} : q axis coupling inductance (H)
- R_{kq} : q axis damper winding resistance (reflected to the stator) (Ω)
- L_{lkq} : q axis damper winding leakage inductance (reflected to the stator) (H)

Selection of Parameters for Implementation of the model

In the view of the mathematical modelling described in section 3.6.1.3, the section now discusses the modelling of the stator and rotor parameters of synchronous generator model, which is represented by a sixth-order state-space model. The model takes into account the dynamics of the stator, rotor and damper windings. The equivalent circuit of the model is represented in the rotor reference frame (dq frame). All rotor parameters and electrical quantities are examined from the stator.

The model assumes currents flowing into the stator windings. Per unit values are computed to set paramaters for this synchronous generator model [42].

Stator and rotor parameters

The base input values are calculated for stator windings using the following equations (3.20) to (3.28) [40]:

Base stator voltage (V):

$$V_{s\_base} = \frac{V_{ll}\sqrt{2}}{\sqrt{3}} \quad (3.20)$$

where, the base stator voltage is also known as the peak nominal line–to-neutral voltage(V).

Base stator current (A):

$$I_{s\_base} = \frac{P_{nom}\sqrt{2}}{V_{ll}\sqrt{3}} \quad (3.21)$$

Base stator impedance (Ω):

$$Z_{s\_base} = \frac{V_{stator\_base}}{I_{stator\_base}} = \frac{{V_{ll}}^2}{P_{nom}} \quad (3.22)$$

Base angular frequency (rad/s):

$$\omega_{ang\_base} = 2\pi\, f_{nom} \quad (3.23)$$

Base stator inductance (H):

$$L_{s\_base} = \frac{Z_{s\_base}}{\omega_{ang\_base}} \quad (3.24)$$

where,

P_{nom} = Three-phase nominal power (VA)

V_{ll} = Nominal line-to-line voltage (Vrms)

f_{nom}= Nominal frequency (Hz)

i_{f_nom} = Nominal field winding current producing nominal stator voltage at no load(A)

The stator resistance and inductance parameters for the model are calculated as follows using equations (3.25) to (3.28):[27]

Base stator resistance per phase (p.u.):

$$R_{s\_pu} = \frac{R_s}{Z_{s\_base}} \quad (3.25)$$

Base stator leakage inductance (p.u.):

$$L_{ls\_pu} = \frac{L_{ls}}{L_{s\_base}} \quad (3.26)$$

Direct axis magnetising inductance (p.u.):

$$L_{md\_pu} = \frac{L_{md}}{L_{s\_base}} \quad (3.27)$$

Quadrature-axis magnetising inductance (p.u.):

$$L_{mq\_pu} = \frac{L_{mq}}{L_{s\_base}} \quad (3.28)$$

Rotor values reflected to stator values

The rotor windings reflected to the stator input base values are derived from the stator to rotor transformation ratio and are computed using the following equations (3.29) to (3.34); [40,42,43]

Base rotor winding terminal current (reflected to the stator) (A):

$$I_{f\_base} = i_{f\_nom} L_{md\_pu} \quad (3.29)$$

Base rotor winding voltage (reflected to the stator) (V):

$$V_{f\_base} = \frac{P_{nom}}{I_{f\_base}} \quad (3.30)$$

Base rotor winding impedance (reflected to the stator) (Ω):

$$Z_{f\_base} = \frac{V_{f\_base}}{I_{f\_base}} \quad (3.31)$$

Base rotor windinginductance (reflected to the stator) (H):

$$L_{f\_base} = \frac{Z_{f\_base}}{\omega_{base}} \quad (3.32)$$

Thus,

Base rotor winding resistance (reflected to the stator) (p.u.):

$$R_{f\_pu} = \frac{R_f}{Z_{fbase}} \quad (3.33)$$

Base rotor winding leakage inductance (p.u.):

$$L_{lfd\_pu} = \frac{L_{lfd}}{L_{fbase}} \quad (3.34)$$

Values of Parameters for the synchronous generator model

The aforesaid parameters of the synchronous generator model are calculated from values of synchronous generator preset model from Matlab/Simulink. The values of the preset model are $P_{nom}, V_{ll}, f_{nom}, R_s$ as shown in Table 3-3.

Table 3-3: Parameters of the synchronous generator

Parameters of the synchronous generator model		
Parameter	**Value**	**Unit**
Nominal Power (P_{nom})	2	MW
Nominal line to line voltage (V_{ll})	575	V
Frequency (f_{nom})	50	Hz
Stator Resistance (R_s)	0.006	Ω
Inertia constant (H)	0.062	s
Number of pole pairs (p)	3	-
Rotor field winding resistance (R_f)	5.79E-4	Ω
Rotor field winding leakage inductance (L_{lfd_pu})	0.114	H

Base stator voltage (V_{stator_base})	469.5	p.u.
Base stator current (I_{stator_base})	2231.3	p.u.
Base stator impedance (Z_{stator_base})	0.14878	p.u.
Base angular frequency (ω_{ang_base})	314.2	p.u.
Base stator inductance: (L_{stator_base})	4.736e-4	p.u.
Base stator resistance per phase (R_{s_pu})	0.01916	p.u.
Base Stator leakage inductance (L_{ls_pu})	295.6	p.u.
Base direct axis magnetising inductance (L_{md_pu})	6.427e-4	p.u.
Base quadrature-axis magnetising inductance (L_{mq_pu})	1.218e-3	p.u.
Base rotor field winding terminal current (I_{f_base})	0.6986	p.u.
Base field winding voltage (V_{f_base})	3.181e6	p.u.
Base field winding impedance (Z_{f_base})	4.553e6	p.u.
Base field winding inductance (L_{f_base})	14.492e3	p.u.
Base rotor field winding resistance (R_{f_pu})	1.272e-10	p.u.
Base rotor field winding leakage inductance (L_{lfd_pu})	7.866e-6	p.u.

Modelling of the Controller Components for Synchronous Generator

Power electronic controllers and regulators have been used to regulate the output voltage and current waveform at the load terminals of the generator in order to ensure proper power quality. This can be realized by coupling a pulse-width modulation (PWM) rectifier and a PWM inverter to the DC-link. The DC-link consists of a capacitor C for the voltage DC-link or an inductor L for the current DC-link. The PWM rectifier is controlled in a way that a sinusoidal AC line current is drawn, which is in phase or anti-phase (for energy feedback) with the corresponding AC line phase voltage [44].

Due to the DC-link storage element, there is the advantage that both converter stages are to a large extent decoupled for control purposes. Furthermore, a constant, AC line independent input quantity exists for the PWM inverter stage, which results in high utilization of the converter's power capability. The diode acts as a rectifier to the output voltage from the generator. The models and parameters

of the components of the power electronic controller, such as, diode rectifier, DC link, inverter and PWM control are presented in the following sub sections.

Diode Rectifier

A simple diode three-bridge arms component is used to rectify to output voltage from the generator. The values of diode rectifier parameters are listed in Table 3-4.

Table 3-4: Parameters of diode rectifier for synchronous generator model

Snubber resistance (Ω)	100 Ω
Ron (Ω)	1 mΩ
Lon(H)	0 H
Forward Voltage (V)	0 V

DC Link and inverter with PWM control

The DC link is modelled with an inductor and a capacitor of values 1mH and 1μF respectively. It is used between the grid and the generator. The DC link model is shown in Figure 3-11.

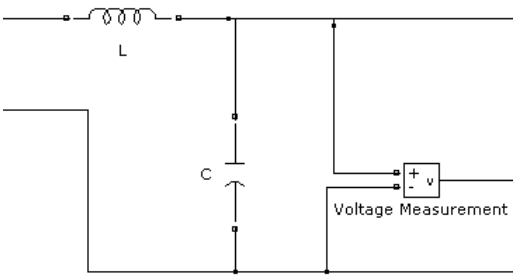

Figure 3-11: DC Link Model as implemented in MATLAB [40]

Inverter

The inverter model used consists of the IGBT / DIODE devices. The maximum power tracking of the wind energy conversion system is monitored through the PWM control which is an input to the inverter control system as shown in Figure 3-12.

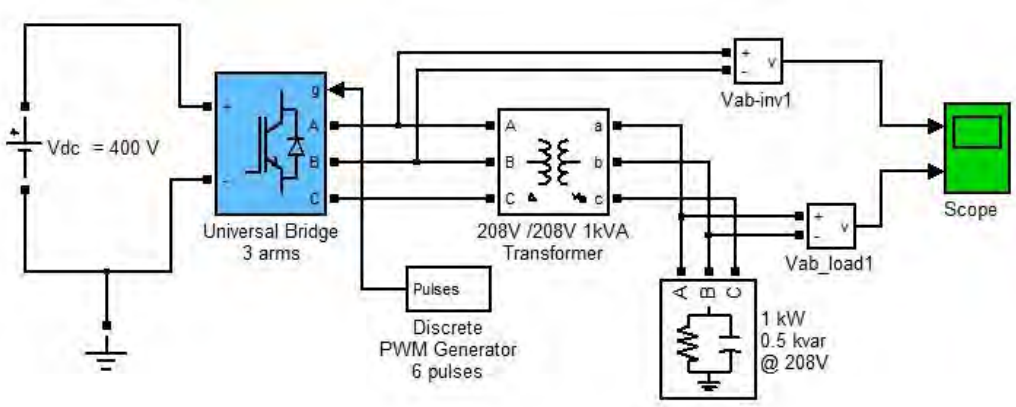

Figure 3-12: DC/DC booster control to implement PWM signal [40]

The connection of the controllers, as mentioned above, to the synchronous generator model is shown in Figure 3-13.

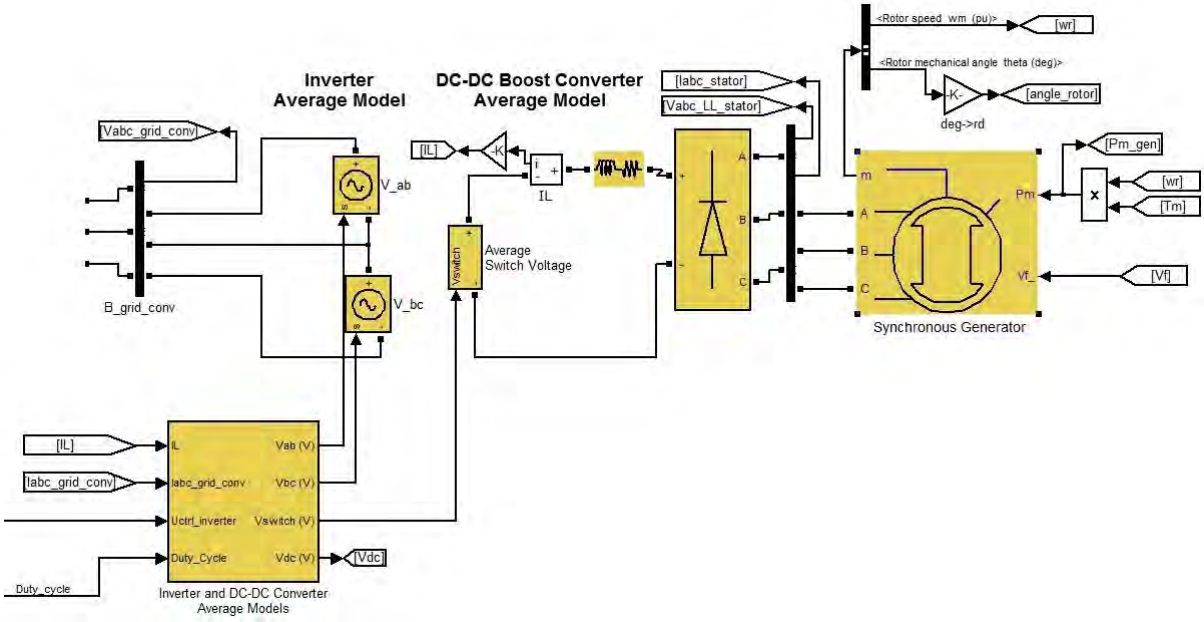

Figure 3-13: Synchronous generator with connection controllers [40, 42]

3.6.2 The STATCOM Model

This section details the modelling of the 575V/100MVA STATCOM model used in Case 1B. The STATCOM provides reactive power compensation during periods of low voltage on the synchronous generator based wind turbine and is connected at the PCC between the bus B575 and the wind generator as shown in Figure 3-14a. The 48-pulse STATCOM uses a Voltage-Sourced Converter (VSC) built of four 12-pulse three-level GTO inverters. The four sets of three-phase voltages obtained at

the output of the four three-level inverters are applied to the secondary windings of four phase-shifting transformers [44, 45].

The STATCOM model operates as follows: during steady-state operation, the STATCOM control system keeps the fundamental component of the VSC voltage in phase with the system voltage. If the voltage generated by the VSC is higher (or lower) than the system voltage, the STATCOM generates (or absorbs) reactive power. The amount of reactive power depends on the VSC voltage magnitude and on the transformer leakage reactance. The fundamental component of VSC voltage is controlled by varying the DC bus voltage. In order to vary the DC voltage, thus the reactive power, the VSC voltage angle (α) which is normally kept close to zero is temporarily phase shifted. This VSC voltage lag or lead produces a temporary flow of active power which results in an increase or decrease of capacitor voltages [45].

The principle of operation of the STATCOM is explained in Figure 3-14, showing the active and reactive power transfer between a source V_1 and a source V_2. In Figure 3-15, V_1 represents the system voltage to be controlled and V_2 is the voltage generated by the VSC [45].

In steady state operation, the voltage V_2 generated by the VSC is in phase with V_1 (δ=0), so that only reactive power is flowing (P=0). If V_2 is lower than V_1, Q is flowing from V_1 to V_2 (STATCOM is absorbing reactive power). On the contrary, if V_2 is higher than V_1, Q is flowing from V_2 to V_1 (STATCOM is generating reactive power). The amount of reactive power is given by the following equations (3.35) and (3.36): [44, 45]

$$P = \frac{V_1 V_2 \sin\delta}{X} \tag{3.35}$$

$$Q = \frac{V_1 (V_1 - V_2 \cos\delta)}{X} \tag{3.36}$$

where:

P is the active power

Q is the reactive power

V_1 is line to line voltage of the power system

V_2 is the line to line voltage of the VSC

δ is the angle of V_1 with respect to V_2

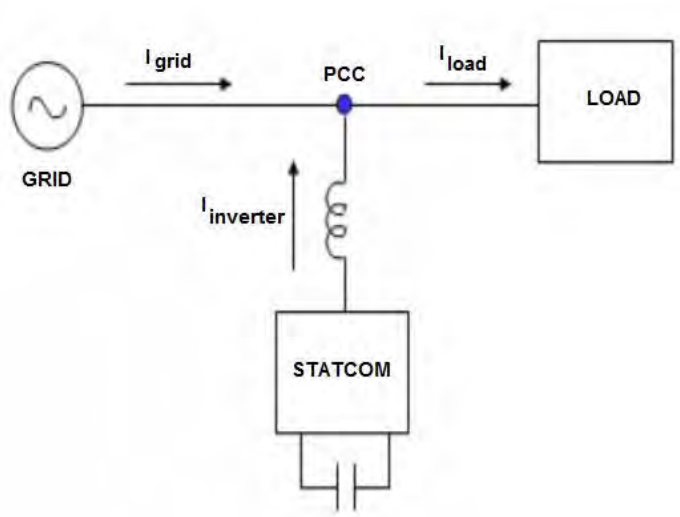

Figure 3-14: Typical circuit diagram for STATCOM[45]

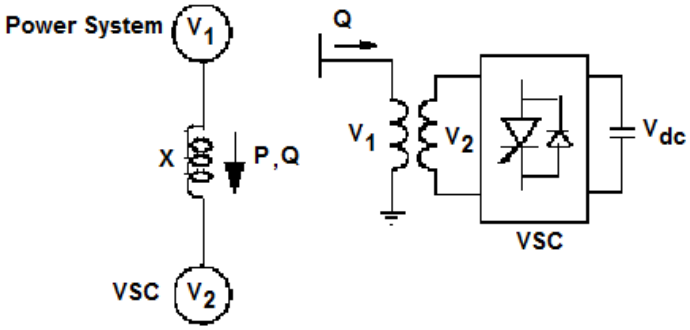

Figure 3-15: Operating principle of STATCOM[45]

In Case 1B, a 100-MVAr STATCOM is used between the bus B3 and the wind generator as shown in Figure 3.1 to regulate voltage on a 10km transmission line and a 575V system bus. The STATCOM model implementation is shown in Figure 3-16 and the model parameters are listed in Table 3-5.

Table 3-5: Parameters of the STATCOM Controller

Parameters of the STATCOM controller		
Operation Mode	**Voltage regulation**	
Parameter	**Value**	**Unit**
Line to line voltage power system (V1)	575	V
Line to line voltage VSC (V2)	25e3	V
Phase shift (δ)	+7.5	deg

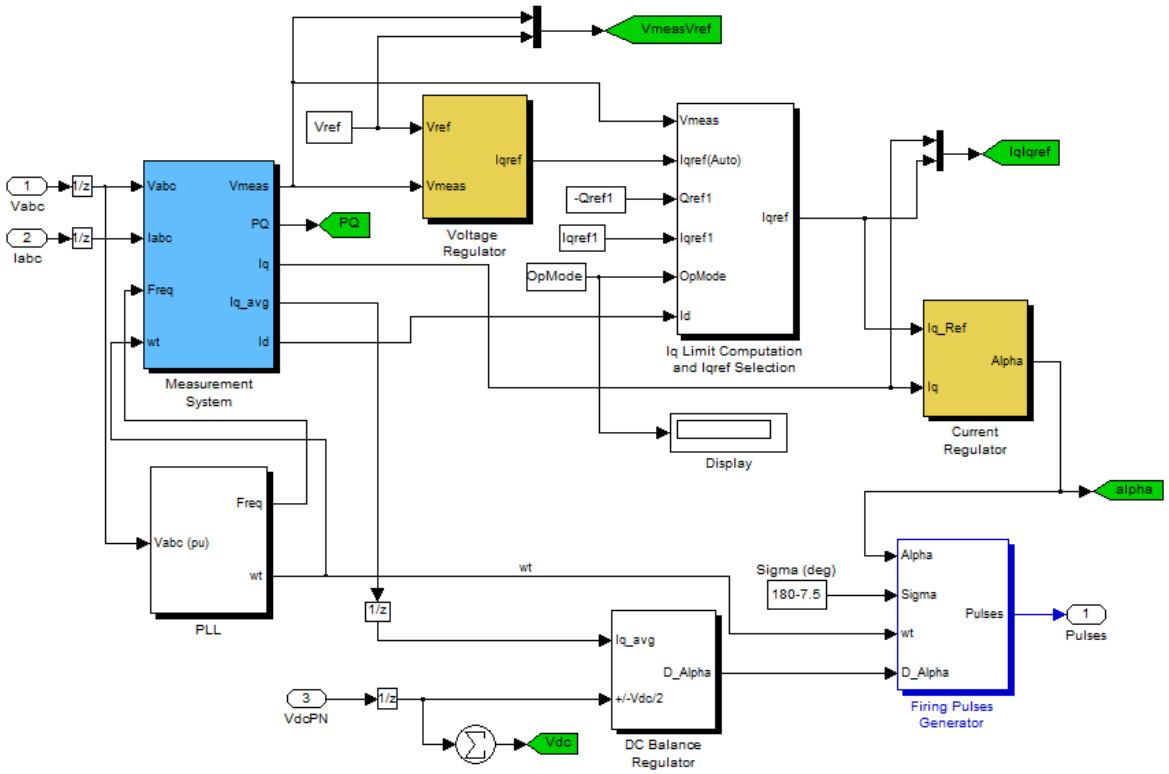

Figure 3-16: STATCOM model in MATLAB/SIMULINK® [40]

3.7 Modelling of the Doubly Fed Induction Generator with Crowbar protection

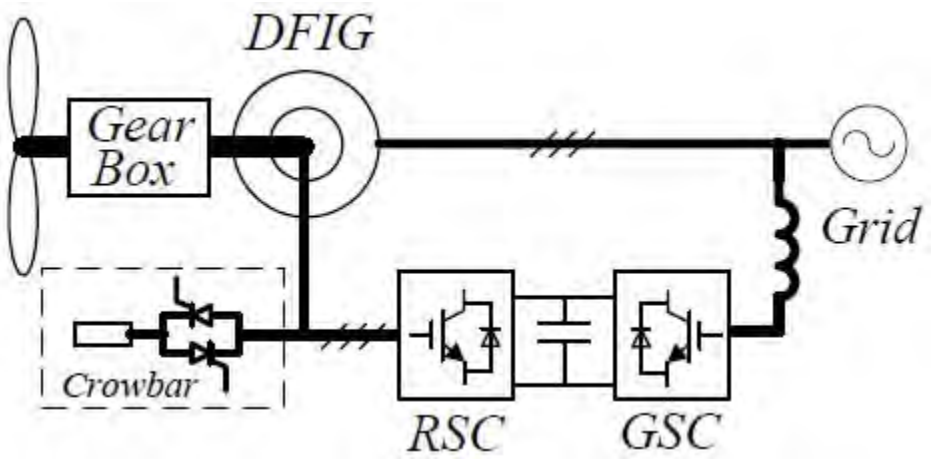

Figure 3-17: Block diagram of grid connected DFIG [46,47]

A typical block diagram of a grid connected DFIG is shown in Figure 3-17. The grid is connected to the grid side converter of the control system and the rotor side converter is connected to the rotor of the DFIG. Furthermore the voltage functions of the DFIG can be defined from the equivalent circuit of the DFIG as depicted in Figures 3-18 and 3-19.

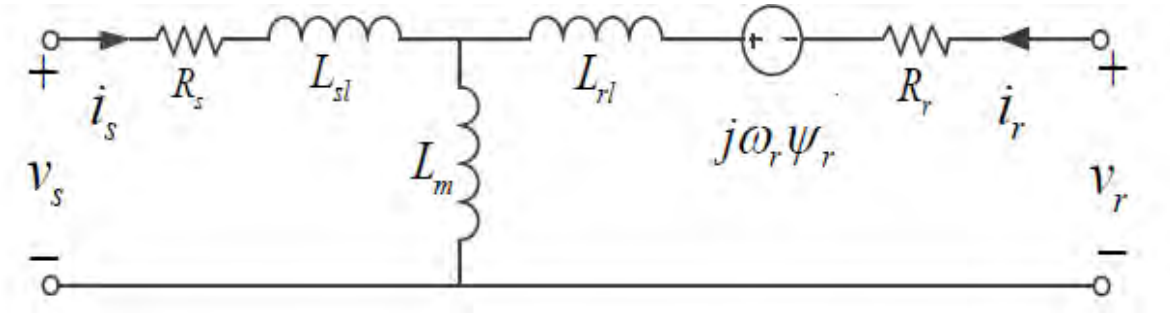

Figure 3-18: Equivalent circuit of DFIG for transient analysis – stator oriented reference frame [47]

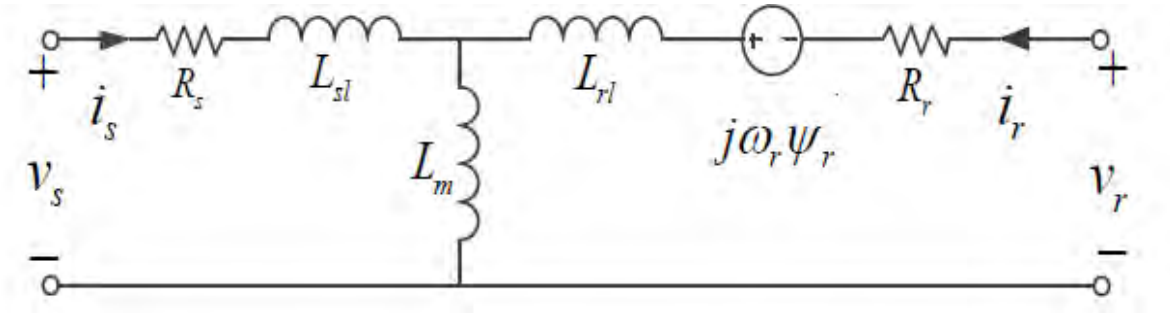

Figure 3-19: Equivalent circuit of DFIG for transient analysis – rotor oriented reference frame [47]

The study of the transient response characteristics of the DFIG to grid fault is based mainly on the following mathematical model. In the Synchronous rotating reference frame, the DFIG voltage equations on the stator and rotor, (3.37) and (3.38) are as follows:[23, 47]

$$V_s = R_s I_s + p\,\Psi_s - j\omega_s \Psi_s \tag{3.37}$$

$$V_r = R_r I_r + p\,\Psi_r - j\omega_{sl} \Psi_r \tag{3.38}$$

The flux equation can be described using equations (3.39) to (3.41) as follows:

$$\Psi_s = L_s I_s + L_m I_r \tag{3.39}$$

$$\Psi_r = L_m I_s + L_r I_r \tag{3.40}$$

where:

$$L_m = \frac{3}{2} L_{aA}, \tag{3.41}$$

where,

V_s , V_r, Ψ_s, Ψ_r I_s, I_r are the voltage, flux and current vectors of the stator and rotor respectively.

L_s, L_r are the stator and rotor self inductances

L_m is the magnetising inductance

$R_s$and R_r are the stator and rotor self resistance

ω_s and ω_{sl} are the stator and slip angular frequency respectively

p is the differential operator

All parameters are referred to the stator.

L_{aA} is the peak value of the induction between stator and rotor.

Thus, from equations (3.37) to (3.41), the following equations (3.42) and (3.43) can be obtained for I_s and I_r: [47]

$$I_s = (L_r\psi_s - L_m\psi_r) / (L_sL_r - L^2{}_m) \quad (3.42)$$

$$I_r = (L_s\psi_r - L_m\psi_s) / (L_sL_r - L^2{}_m) \quad (3.43)$$

In this thesis, the DFIG is assumed to include a crowbar protection for LVRT purpose during low voltage conditions caused by faults. The next section details the modelling of the crowbar protection on the DFIG as per Matlab/Simulink model, which is used in Case 2. The DFIG model implementation is shown in Figure 3-20 and the Parameters of the preset model in Matlab are listed in Table 3-6.

Table 3-6: Parameters of the DFIG Model

Parameters of the DFIG model		
Parameter	**Value**	**Unit**
Nominal Power (P_{nom})	2	MW
Nominal line to line voltage (V_{ll})	575	V
Frequency (f_{nom})	50	Hz
Stator Resistance (R_s)	0.006	Ω
Inertia constant (H)	0.062	s
Number of pole pairs (p)	3	-
stator voltage (V_s)	469.5	p.u.
stator current (I_s)	2231.3	p.u.
Base angular frequency (ω_s)	314.2	p.u.
Base stator resistance per phase (R_s)	0.01916	p.u.
Base Stator leakage inductance (L_s)	4.736e-4	p.u.
Base rotor voltage (V_r)	3.181e6	p.u.
Base rotor terminal current (I_r)	0.6986	p.u.
Base rotor resistance per phase (R_r)	0.007	p.u.
Base rotor inductance (L_r)	0.156	p.u.
Base magnetising inductance (L_m)	1.218e-3	p.u.
Stator flux (Ψ_s)	4.553e6	p.u.
Rotor flux (Ψ_r)	14.492e3	p.u.

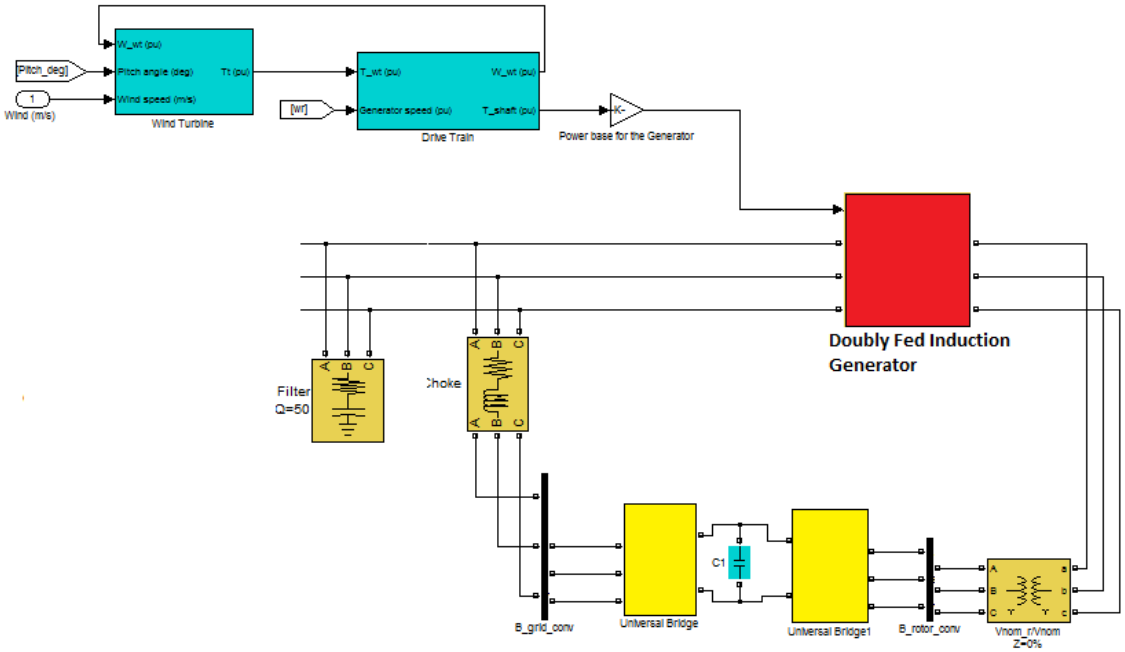

Figure 3-20: Test model for DFIG [23, 40, 47]

3.7.1 Crowbar Protection

The crowbar protection mechanism can provide low voltage ride through condition for the DFIG. It does not allow current to pass through, when the wind generator is operating under normal condition. The crowbar operates while the DC Link voltage is increasing, when short circuit fault occurs at the grid, so that no current is supplied to the converter of the rotor side and that of the grid. Thus, the transient flux causing the overcurrent on the rotor decreases. Subsequently, if the current at the DC link decreases below the limit which is characterised by equation (3.44), the limit characterises the current level at which the crowbar will be cut off from operation and when the DFIG enters into normal mode of operation [48].

$$I_{Smax} \approx I_{rmax} \approx \frac{\omega_r}{\omega_s} \frac{V_s}{\sqrt{(\omega_r L_\sigma)^2 + R^2 cr}} \quad (3.44)$$

When short circuit fault occurs at the grid side, the crowbar circuit provides a current discharge path to the DFIG rotor windings and RSC. This helps in preventing damage to the devices due to overcurrent. Therefore, it is very important to select the right value for crowbar resistance. When the crowbar resistance is small, the DFIG short circuit characteristics are similar to an asynchronous induction generator with a small resistance in its rotor windings. The rotor current is too large which is unfavourable to RSC. Therefore, crowbar resistance value is basically at a high level, not less than 30 times the DFIG rotor resistance. When short circuit fault occurs, the crowbar protection is activated. It obstructs the trigger pulses of the RSC, which has not been disconnected from the system. If the crowbar resistance is too large, then the voltage on the crowbar resistance may be higher than the DC bus voltage. The freewheeling diodes on the controller are turned on, leading to the connection of the rotor windings and the DC side capacitor. The crowbar connection to the DFIG is shown in Figure 3-21 below [47, 48].

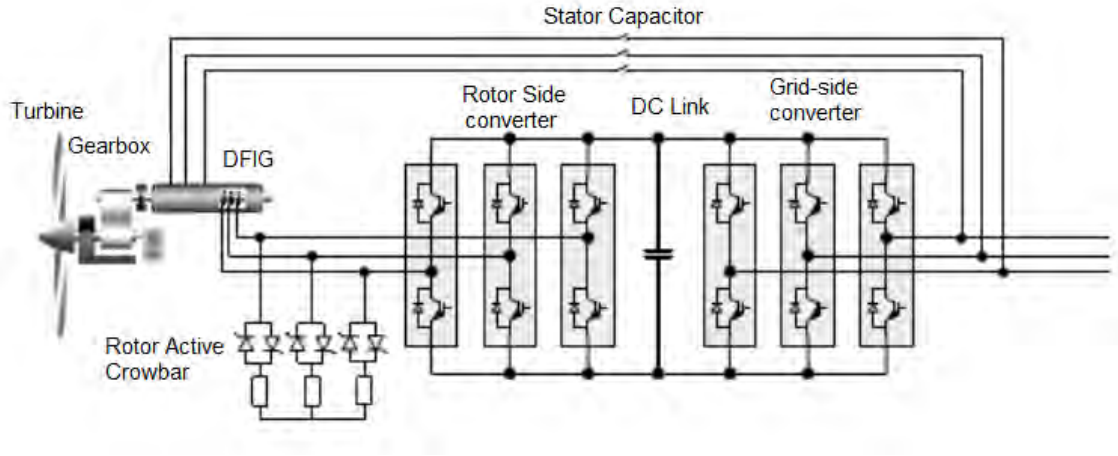

Figure 3-21: Schematic diagram of crowbar connected to DFIG [47]

In case of a grid voltage dip, RSC must shut down and the thyristors of rotor active crowbar are then turn on [35]. The rotor overvoltage is restrained and overcurrent is bypassed from RSC to the crowbar power resistors, R_{crow}. RSC shuts down followed by the three phase power resistors, R_{crow} short the rotor circuits. The DFIG operates as an induction machine with high rotor resistors. When the crowbar resistors short the rotor, the total rotor resistance increases to Rrc, where the value of Rrc is determined through equation (3.45) [48].

$$Rrc = Rr + Rcrow \tag{3.45}$$

where, R_{crow} is the crowbar resistor (referred to the stator side)

The time constants for the damping of the DC components in stator and rotor during crowbar protection are as given by equations (3.46) and (3.47) below: [50].

$$\tau_s = \frac{L_s L_r - L_m^2}{R_s L_r'} \tag{3.46}$$

$$\tau_r = \frac{L_s L_r' - L_m^2}{R'_{rc} L_s} \tag{3.47}$$

When the crowbar is deactivated, the time constant for the damping of the DC components in stator becomes longer than τ_s. Because of the open circuit of rotor, this time constant τ_{s0} can be expressed as equation (3.48) below: [48]

$$\tau_{s0} = \frac{L_s}{R_s} \quad (3.48)$$

The choice of the of three-phase power resistor values is very important to design the crowbar protection. System simulation indicates that smaller R_{crow} induces lower rotor overvoltage but higher electromagnetic torque and overcurrent; in contrast, larger value of R_{crow} induces lower electromagnetic torque and overcurrent but higher rotor overvoltage. The high rotor overvoltage results in excessive energy flow into DC-link capacitors. For the design without DC-link chopper, the DC-link voltage deviation is very dangerous to the DC capacitors and makes vulnerable the power semiconductor devices in the converter. Thus crowbar must perform at least two functions: firstly restraining the overcurrent, $Irmax$ below an acceptable multiple of rotor normal current, l_{rn}, and secondly ensuring that the rotor rectifying line-to-line voltage, $\sqrt{2}\,Urm$ is below the normal running DC-link voltage, U_{dc0} when the crowbar resistors are connected into the rotor circuit. The recommended value of one of three-phase crowbar resistors $Rcrow$ is given as follows by equation (3.49): [48, 49]

$$R_{crow} = \frac{U_{dc0}}{\sqrt{6} I_{rmax}} = \frac{U_{dc0}}{\sqrt{6} h I_{rn}} \quad (3.49)$$

where *h* is the acceptable multiple of the rotor normal current.

During the occurrence of a terminal voltage dip, the stator flux cannot immediately follow the stator voltage fluctuations, and thus result in the appearance of DC component in the transient flux in the stator side. Hence large fault currents are generated in the stator and rotor windings due to constant flux linkage. Generally, the largest fault current will appear right at the terminal of the DFIG when a short circuit occurs. Under the assumption that the voltage dip to zero at $t_0 = 0$, the transient stator and rotor flux vectors can be expressed by equations (3.50) and (3.51): [48,49]

$$\psi_s(t) = \frac{U_s(t_0)}{j\omega_s} e^{\frac{-t}{T_s}} + \frac{U_s(t_0)}{j\omega_s} e^{j\omega_s t} \quad (3.50)$$

$$\psi_r(t) = \psi_{rdc0} e^{j\omega_r t} e^{\frac{-t}{T_r}} + \psi_{rf_0} e^{j\omega_s t} \quad (3.51)$$

where;

ω_r is the rotor angular frequency

ω_s is the base angular frequency

ψ_{rf0} is forced rotor flux component

ψ_{rdc0} is the DC component of the rotor flux at the occurring instant of the dip

The single phase T-equivalent circuit of DFIG with crowbar fired for sinusoidal steady state analysis is shown in Figure 3-22 and 3-23. R_r includes the rotor resistance and the crowbar resistance [47].

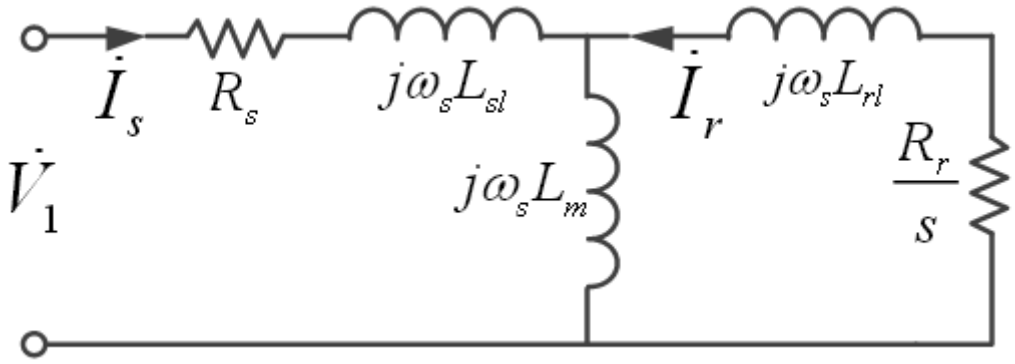

Figure 3-22: Positive sequence equivalent circuit of DFIG with crowbar [47]

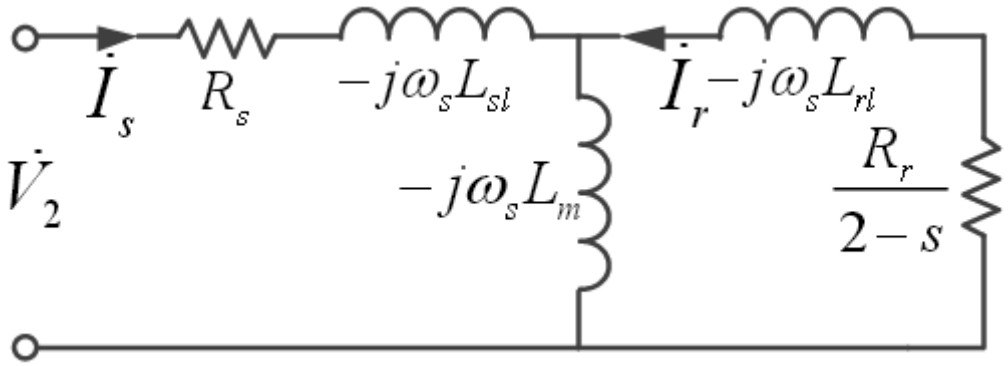

Figure 3-23: Negative sequence equivalent circuit of DFIG with crowbar [48]

Taking into consideration, equations (3.50) and (3.51), the faulty stator current of three-phase short circuit is obtained in the synchronously rotating reference frame with reference to the stator are as equations (3.52) and (3.53) as follows: [47,49]

$$I_s = \frac{-\omega_s L_r + j\frac{R_r}{s}}{-\omega_s L_s \frac{R_r}{s} + j{\omega_s}^2\left({L_m}^2 - L_s L_r\right)} V_1 e^{j\omega_s t} + \frac{\omega_s L_s + j\frac{R_r}{2-s}}{\omega_s L_s \frac{R_r}{2-s} + j{\omega_s}^2\left({L_m}^2 - L_s L_r\right)} V_1 e^{j\omega_s t}$$
$$+ \frac{-\omega_s L_r + j\frac{R_r}{s-1}\frac{L_s(L_m - L_r)}{{L_m}^2 - L_s L_r}}{-\omega_s L_s \frac{R_r}{s-1} + j{\omega_s}^2\left({L_m}^2 - L_s L_r\right)} [V_{s-}(V_1 - V_2)e^{\frac{-t}{\tau_s}} + L_m A e^{\frac{t}{\tau_s}} e^{j\omega_s t}$$

(3.52)

$$I_r = \frac{\omega_s L_m}{-\omega_s L_s \frac{R_r}{s} + j{\omega_s}^2\left({L_m}^2 - L_s L_r\right)} V_1 e^{j\omega_s t} + \frac{-\omega_s L_m}{\omega_s L_s \frac{R_r}{2-s} + j{\omega_s}^2\left({L_m}^2 - L_s L_r\right)} V_2 e^{-j\omega_s t}$$
$$+ \frac{\omega_s L_m + j\frac{R_r}{s-1}\frac{L_s(L_m - L_s)}{{L_m}^2 - L_s L_r}}{-\omega_s L_s \frac{R_r}{s-1} + j{\omega_s}^2\left({L_m}^2 - L_s L_r\right)} [V_{s-}(V_1 - V_2)e^{\frac{t}{\tau_s}} - L_s A e^{\frac{t}{\tau_s}} e^{j\omega_r t}$$

(3.53)

where;

β is the angle between ψ_r and d-axis

L_σ is the sum of stator and rotor leakage inductances

ψ_{s0} = $\frac{U_s(t_0)}{j\omega_s}$ is the initial value of the stator flux after the dip occurs

$T_r = \frac{L_\sigma}{R_s}$ is the rotor transient time constants

$T_s = \frac{L_\sigma}{R_r}$ is the stator transient time constants

As the crowbar relates to the DFIG for operation, the parameters of the DFIG applied to the crowbar model as per the preset model unit in Matlab are shown in Table 3-7.

Table 3-7: Parameters of the crowbar model

Parameters of the crowbar model		
Parameter	**Value**	**Unit**
Crowbar resistance (R_{crow})	0.15	p.u.
Time constant (τ_{s0})	0.02469	s
Stator transient time constant (τ_s)	0.02419	s
Rotor transient time constant (τ_r)	4.6349e-4	s

The Matlab/Simulink model is shown in Figure 3-24.

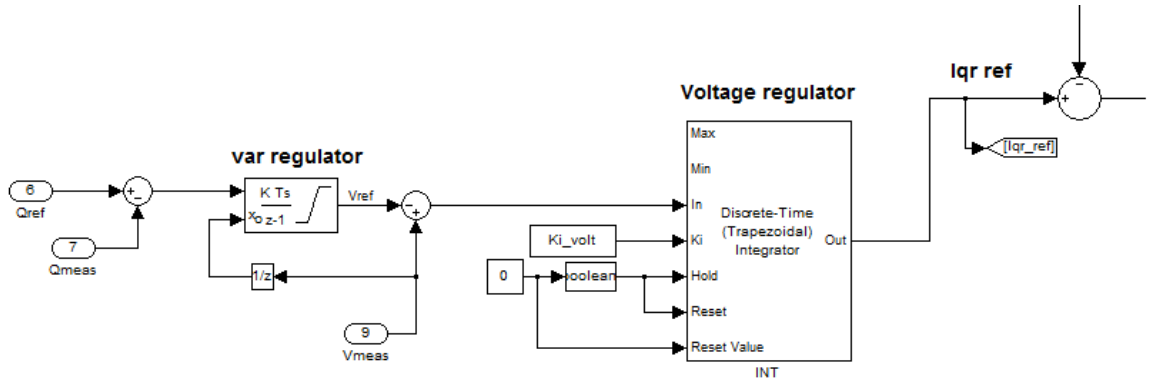

Figure 3-24: Test system for crowbar control [40, 49]

3.7.2 The External Grid Model

The external grid system is modelled using a controllable three-phase symmetrical voltage source including an inductance and resistance. The phase voltages are defined by using standard balanced three-phase voltage equations (3.54), (3.55) and (3.56): [50]

$$V_{a=} E_m . \cos(w.t) \tag{3.54}$$

$$V_b = E_m . \cos(w.t - \frac{2\pi}{3}) \tag{3.55}$$

$$V_c = E_m . \cos(w.t - \frac{4\pi}{3}) \tag{3.56}$$

where

w = angular frequency

E_m = Phase voltage amplitude

The three-phase line-line voltages are defined as equations (3.57), (3.58) and (3.59):

$$V_{ab} = V_a - V_b \quad (3.57)$$

$$V_{bc} = V_b - V_c \quad (3.58)$$

$$V_{ca} = V_c - V_a \quad (3.59)$$

According to [37], the grid affected by a voltage dip can be modelled by an impedance and a three-phase voltage source as shown in Figure 3-25 [50].

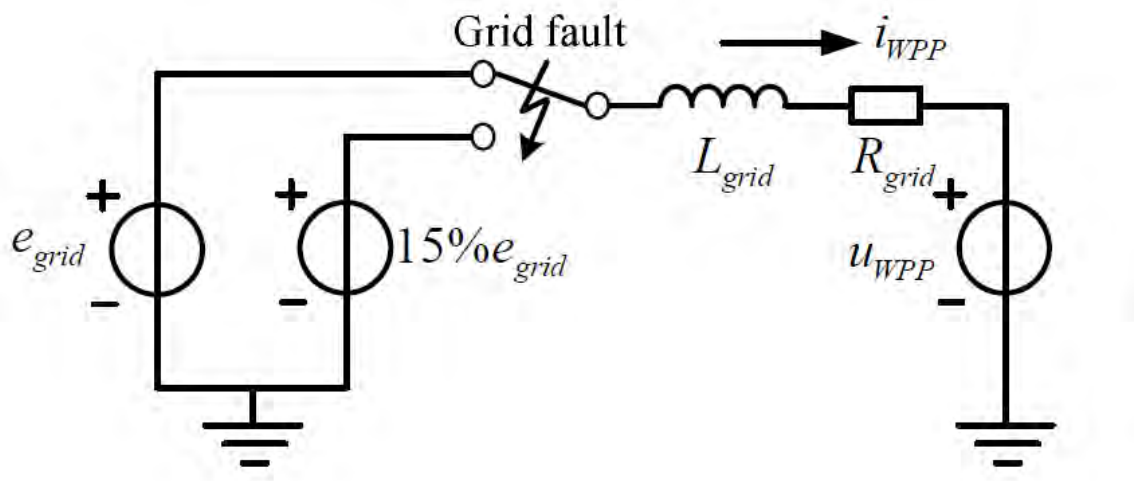

Figure 3-25: Grid model of voltage dip [27, 50]

The mathematical equation of the grid model used in this research is defined by equation (3.60):

$$e_{grid} = u_{wpp} + R_{grid} i_{WPP} + L_{grid} \frac{di_{WPP}}{dt} \quad (3.60)$$

where;

e_{grid} is the grid voltage,

u_{wpp} is the connection point voltage of the wind power plant,

R_{grid} and L_{grid} are the resistance and inductance of equivalent series impedance.

The parameters used in the model are as per Table 3-8.

Table 3-8: Parameters of the external grid model

Parameters of the external grid model		
Parameter	**Value**	**Unit**
Grid voltage (e_{grid})	120	kV
Voltage of wind power plant($Uwpp$)	575	V
Grid Resistance (R_{grid})	0.003	p.u
Grid Inductance (L_{grid})	0.3	p.u

3.8 Modeling of the test system

The test systems pictured are for case 1A, case 1B and case 2. The cases are implemented using Matlab/Simulink models described in this chapter 3 as shown in figures 3-26, 3-27 and 3-28 respectively. The simulation section is presented in chapter 4 where result graphs are portrayed and discussed as depicted in Table 3-9:

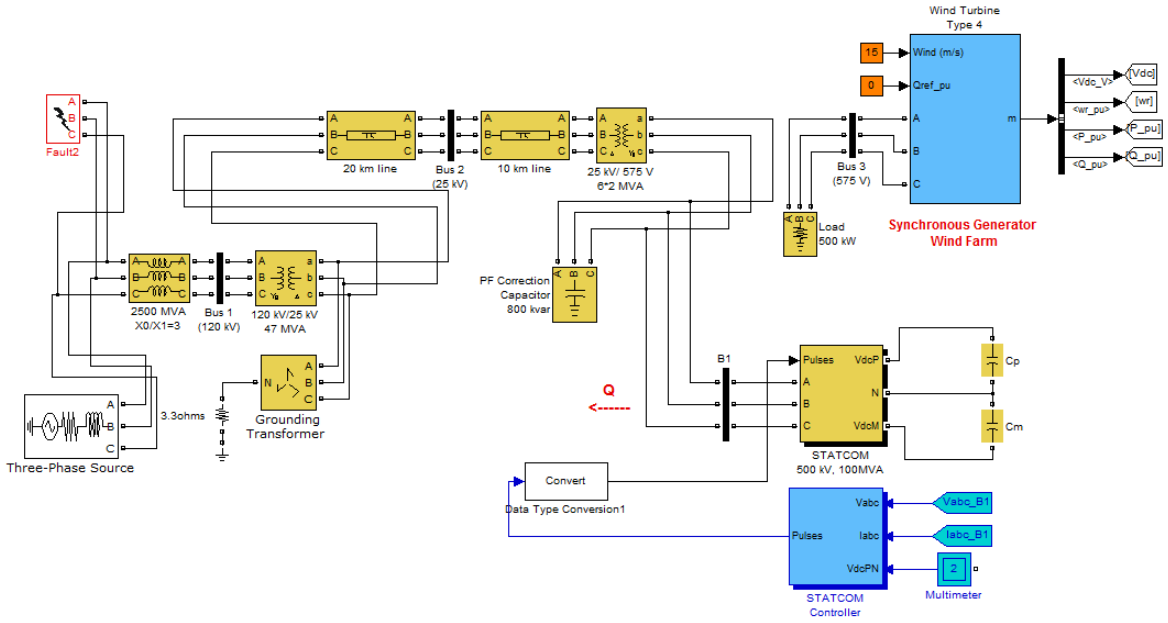

Figure 3-26: Test system of case study 1A in Matlab/Simulink

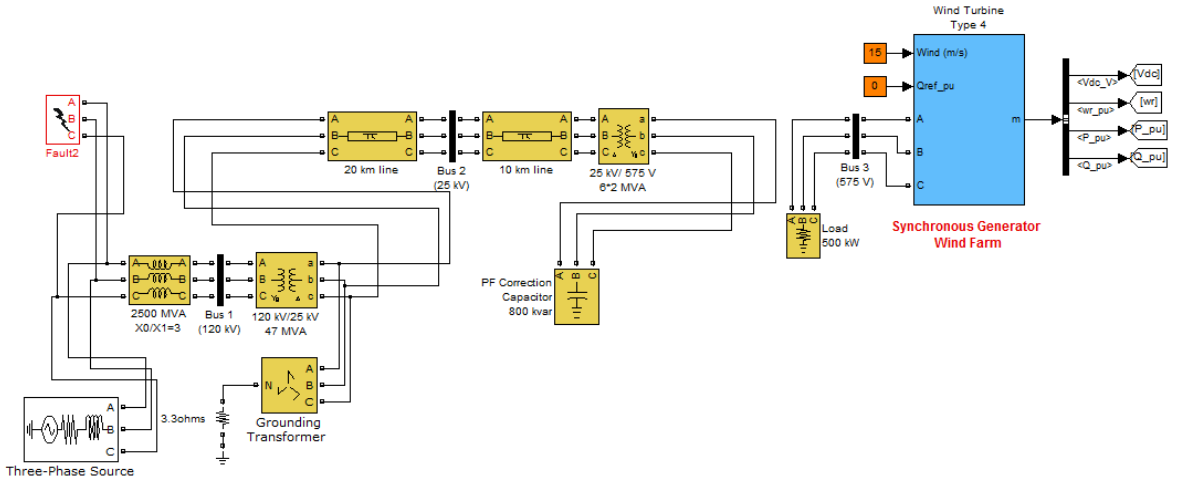

Figure 3-27; Test system of case study 1B in Matlab/Simulink

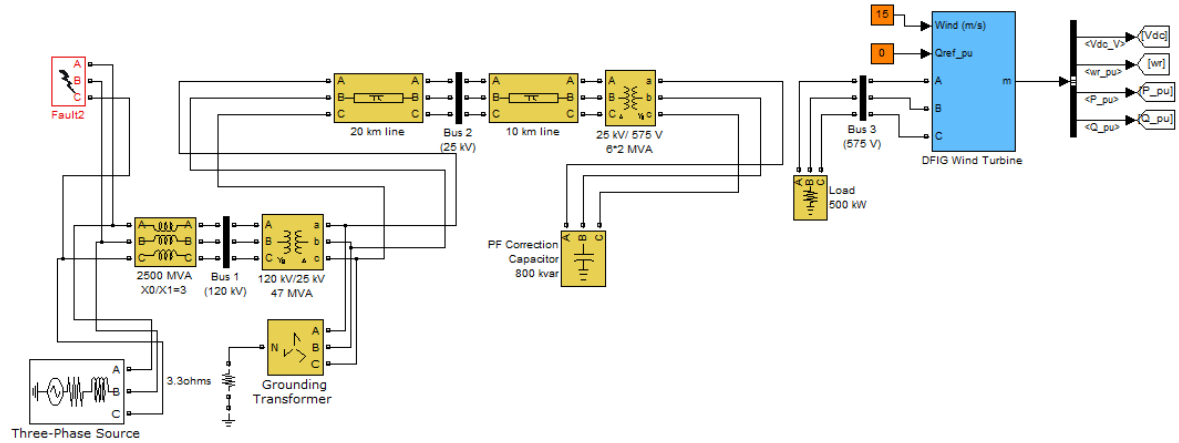

Figure 3-28: Test system of case study 2 in Matlab/Simulink

Chapter 3 described the research methodology and modelling of the system used in Matlab/Simulink. The modelling simulation scenarios are used to compare the behaviour of the two types of wind farms. The mathematical modelling are described as per the model used in Matlab/Simulink. The following chapter – chapter 4 presents the simulation results of the test system of the three case studies. The results will be presented as follows:

- The voltage profile at bus1 (120kV), indicating the voltage drop at the grid due to low voltage condition

- The voltage profiles at bus2 (25kV) and bus3 (575V) of the case studies. The profiles are used to show the voltage characteristics (p.u.) at the transmission line..
- The active and reactive power measured at the output from the generator; synchronous in cases 1A and 1B and DFIG in case 2, to show the variation in the power generated from the generator.
- The reactive power output profile from the STATCOM showing the reactive power compensation from the STATCOM.

Table 3-9: Description of the result graphs to be portrayed for scenarios 1 to 4

Case Scenario	Low voltage clearing time (s)	Time interval (s) as in the simulation	Voltage drop (p.u.)
1	*0.11*	*1.50 - 1.61*	*0*
Simulation cases	Case 1A		
	Case 1B		
	Case 2		
2	*0.5*	*1.50 - 2.00*	*0.29*
Simulation cases	Case 1A		
	Case 1B		
	Case 2		
3	*1*	*1.50 - 2.50*	*0.4*
Simulation cases	Case 1A		
	Case 1B		
	Case 2		
4	*1.8*	*1.50 - 3.30*	*0.7*
Simulation cases	Case 1A		
	Case 1B		
	Case 2		

The results are then discussed to show the ability of the synchronous generator with STATCOM compensation to ride through low voltage condition and the practicability / effectiveness of the synchronous generator with STATCOM control (case1A) over the DFIG (case 2).

4 RESULTS FROM SIMULATIONS

The Methodology presented in chapter 3 is followed by the simulation section whereby the results are presented from the simulated test system in MATLAB® Simulink version 7.14. This chapter involves graph description of the two proposed scenarios described in the previous chapter to investigate and compare the LVRT performance. The two scenarios consist of synchronous generator-based wind farm with STATCOM and DFIG-based wind farm with crowbar protection under a three phase short circuit fault.

4.1 Section 1 – Description of Scenario 1

The proposed method; wind energy conversion system based synchronous generator using STATCOM as controller, has been applied to reduce the peak of the voltage drop during low voltage period. The scenario is portrayed as case 1A. The results are presented in this chapter to demonstrate the effectiveness of the method during faults in terms of low voltage. Different output waveforms in the form of graphs are illustrated to show the performance output from the generator in relation to the function of the STATCOM.

The results are then compared to those from case 1B and case 2 scenario, which portray a wind energy conversion system based synchronous generator without any controller and a DFIG wind energy conversion system with crowbar control respectively. WECS based DFIG is the most commonly used wind energy systems due to the simplicity of the design. The linear waveform of the R.M.S output of the voltage and current are also included to provide a clear interpretation of the output. The simulation is carried out over a period of two seconds (2s) and the circuits used are as shown in Figure 4-1:

The test system, as also described earlier, comprises 10 MW wind farm consisting of five 2 MW wind turbines based on synchronous generator is connected to a 25 kV distribution system, exports power to a 120 kV grid through a 30 km, 25 kV feeder.

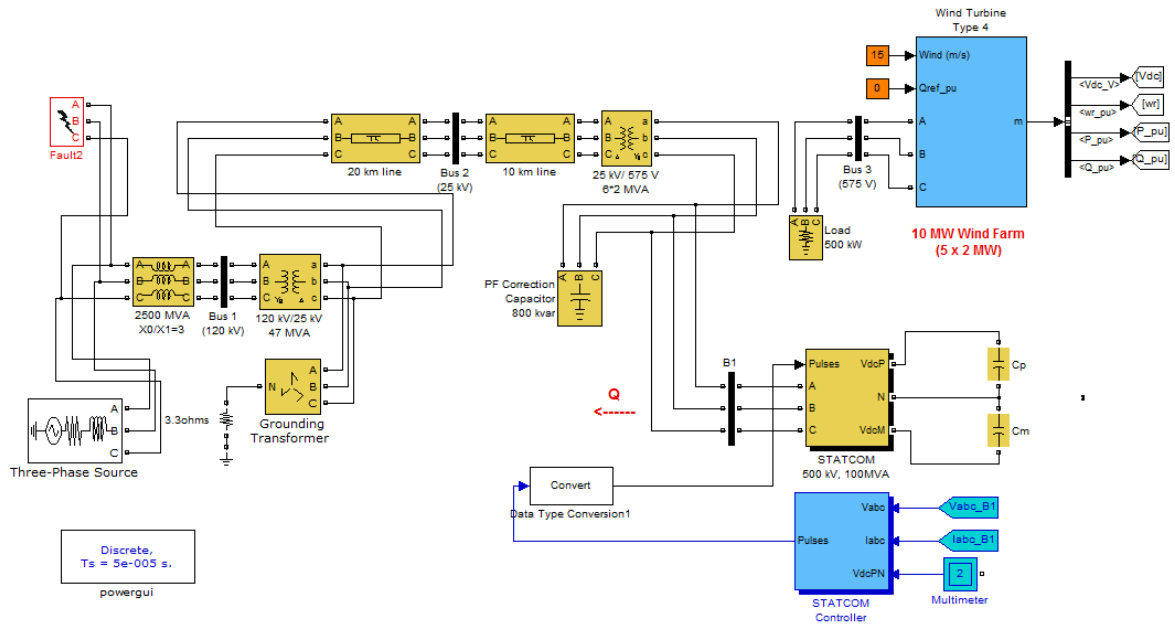

Figure 4-1: Wind energy conversion system based on synchronous generator with STATCOM for reactive compensation - Case study 1A

The parameters used for performance analysis are:

- The voltage dip at bus 2 (25kV)
- The voltage dip at bus 3 (575V)
- Active power output from synchronous generator
- Reactive power output from synchronous generator
- Reactive power output from STATCOM

The voltage dip and current profile provide an overview of effect of the fault on the wind farm and how they affect the performance of the wind farm, whereas the active and reactive power output outline the generated power from the synchronous generator.

The voltage dip and current profile are measured at bus 2 and bus 3, whereas the reactive and active power from the generator is measured at the output of the synchronous generator.

4.2 Three-phase fault inception

A balanced three phase fault is applied at the grid to represent the abnormal condition of fault inception. Balance three phase faults, although rarely occurs in practice is used in this thesis since these are the easiest to analyse as compared to other unbalanced faults which are more common as mentioned in section 2.8 in Chapter 3. Taking into consideration that this study strictly involves the performance analysis of the protection scenario on synchronous generator based wind farm with STATCOM and a DFIG wind farm with

crowbar protection, the balanced three-phase fault is initiated to simplify the analysis. The three phase fault induced at the grid causes a low voltage drop amplitude at the grid whereby, the voltage amplitudes depict a low voltage condition on a specific phase in the grid. The voltage amplitudes values are selected based on the low voltage ride through characteristic setup from authorities, Figure 2.1 in chapter 2. The voltage values are as listed in Table 4-1:

Table 4-1: Presenting the voltage drop amplitude

Case Scenario	Voltage drop (p.u.)
1	***0***
2	***0.29***
3	***0.4***
4	***0.7***

4.3 Low voltage clearing time and voltage drop

The low voltage clearing times selected are 0.11s, 0.5s, 1s and 1.8s according to the low voltage ride through characteristic shown in Figure 2.1 in chapter 2 with voltage v/s time graph showing the minimum required protection of the wind farm. The Low voltage values; voltage drop, 0p.u., 0.29p.u., 0.4p.u., 0.7p.u are selected as per the acceptable voltage drop from Figure 2.1 in chapter 2. The selected time intervals are as presented in Table 4-2.

Table 4-2: Presenting the case scenarios

Case Scenario	Low voltage clearing time (s)	Time interval (s) as in the simulation
1	***0.11***	***1.50 - 1.61***
2	***0.5***	***1.50 - 2.00***
3	***1***	***1.50 - 2.50***
4	***1.8***	***1.50 - 3.30***

4.4 Case studies

Based on the values listed in Table 4-1 and Table 4-2, the scenarios – 1 to 4 will be investigated with the following low voltage clearing times for different voltage drop amplitudes as shown in Table 4-3:

Table 4-3: Description of the scenarios 1 to 4

Case Scenario	Low voltage clearing time (s)	Time interval (s) as in the simulation	Voltage drop (p.u.)
1	*0.11*	*1.50 - 1.61*	*0*
	Case 1A		
	Case 1B		
	Case 2		
2	*0.5*	*1.50 - 2.00*	*0.29*
	Case 1A		
	Case 1B		
	Case 2		
3	*1*	*1.50 - 2.50*	*0.4*
	Case 1A		
	Case 1B		
	Case 2		
4	*1.8*	*1.50 - 3.30*	*0.7*
	Case 1A		
	Case 1B		
	Case 2		

In this thesis, in order to show the practicability and effectiveness of the STATCOM compensation for LVRT, the following steps are followed:

c. A comparison is done between a synchronous generator with and without STATCOM compensation (between Case 1A and Case 1B)
d. A comparison is done between synchronous generator with STATCOM compensation and DFIG with crowbar control (between Case 1A and 2)

For each case study mentioned in Table 4.3, the results, including the comparisons are presented graphically as follows:

- The voltage profile at bus1 (120kV), which indicates the voltage drop at the grid.
- The voltage profiles at bus2 (25kV) and bus3 (575V). The profiles are used to show the voltage characteristics (p.u.) at the transmission line and the synchronous generator in case 1A and 1B; DFIG in case 2, respectively.

- The active and reactive power measured at the output from the generator; synchronous in cases 1A and 1B and DFIG in case 2, to show the variation in the power generated from the generator.
- The reactive power output profile from the STATCOM showing the reactive power compensation from the STATCOM.

4.4.1 Scenario 1: Low voltage clearing time = 0.11s; for voltage drop amplitude (minimum value) = 0.0 p.u. at Bus 1 (120kV)

Table 4.4 lists the figures that are used to present the graphical results for the results graphs for scenario 1.

Table 4-4: List of Figure for scenario 1 results

Figure No	***Description***
4.2	Voltage drop profile for scenario 1
4.3	Active power generated from synchronous generator with STATCOM compensation (Case 1A)
4.4	Reactive power generated from synchronous generator with STATCOM compensation (Case 1A)
4.5	Reactive power generated from STATCOM
4.6	Active power generated from synchronous generator without STATCOM compensation (Case 1B)
4.7	Active power generated from DFIG (Case 2)
4.8	Reactive power generated from DFIG (Case 2)
4.9	Reactive power comparison generated from synchronous generator with STATCOM and DFIG
4.1	Voltage profile at Bus 2 for synchronous generator with STATCOM compensation (Case 1A)
4.11	Voltage profile at Bus 3 for synchronous generator with STATCOM compensation (Case 1A)
4.12	Voltage profile at Bus 2 for synchronous generator without STATCOM compensation (Case 1B)
4.13	Voltage profile at Bus 3 for synchronous generator without STATCOM compensation (Case 1B)
4.14	Voltage profile at Bus 2 for DFIG (Case 2)
4.15	Voltage profile at Bus 3 for DFIG (Case 2)
4.16	Voltage profile comparison at Bus 3 for synchronous generator with STATCOM compensation and DFIG
4.17	Voltage profile comparison at Bus 2 for synchronous generator with STATCOM compensation and DFIG

Figure 4-2 shows that the voltage at bus 1 is almost 0.0 p.u. during the low voltage condition continuing for 0.11s at the grid. This low voltage condition is simulated by inception of a balanced three-phase balanced at 1.5s from the start of simulation and cleared at 1.61s.

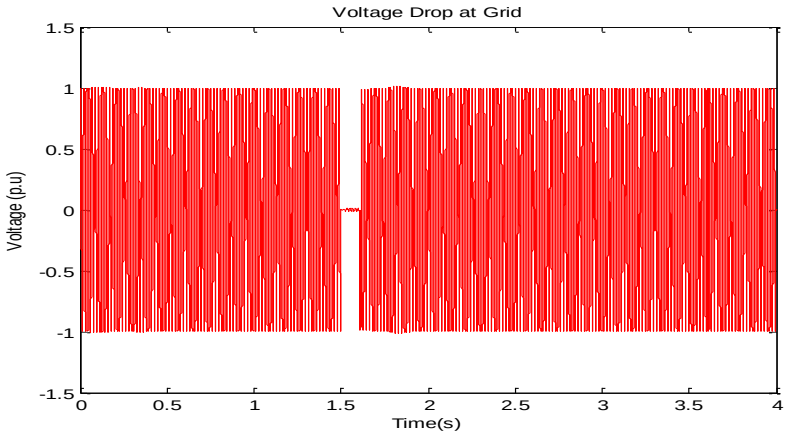

Figure 4-2; Active power output from synchronous generator with STATCOM compensation (Case 1A)

The simulation assumes that under normal operating condition, all the wind farms are delivering rated power to the loads. Figure 4-3 shows the profile of active power output of the synchronous generator. And Table 4-5 shows that prefault, during-fault and post fault value of the synchronous generator with STATCOM compensation. The instantaneous transient active power seen at start up is due to the relative impedances of the generator. In general, generator has to recover rated power utmost by few cycles. Small deviation from the rated value can be seen due to variation in the reference of the reactive power of the generator (ref value = 0) as depicted in Figure 4-4. Also the reactive power from the STATCOM, shown in Figure 4-5 is injecting partial reactive power to the PCC of the transmission system at the bus, causing the fluctuations in the active power during the low voltage condition.

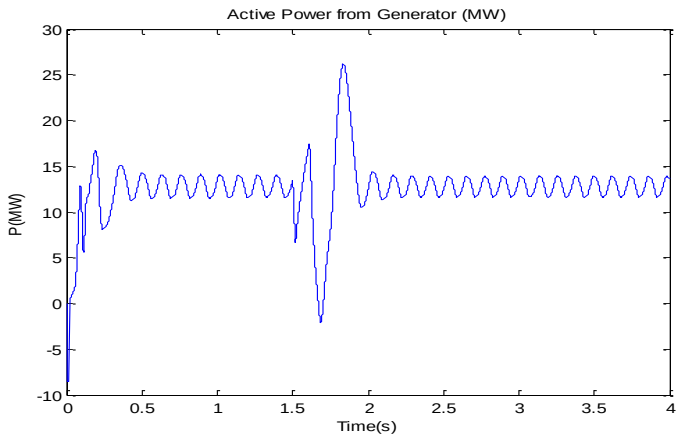

Figure 4-3: Active power output from synchronous generator with STATCOM compensation (Case 1A)

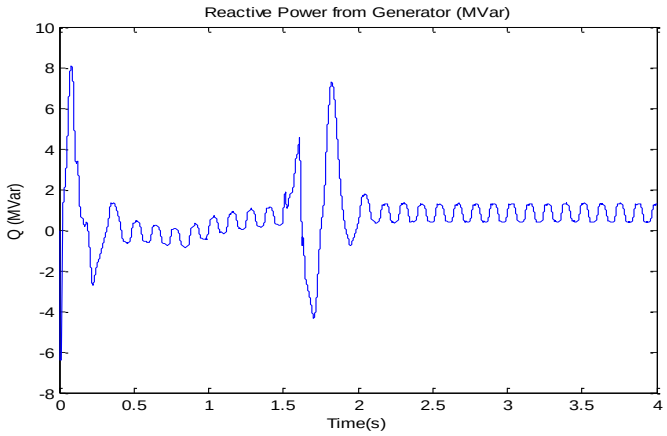

Figure 4-4: Reactive power output from synchronous generator with STATCOM compensation (Case 1A)

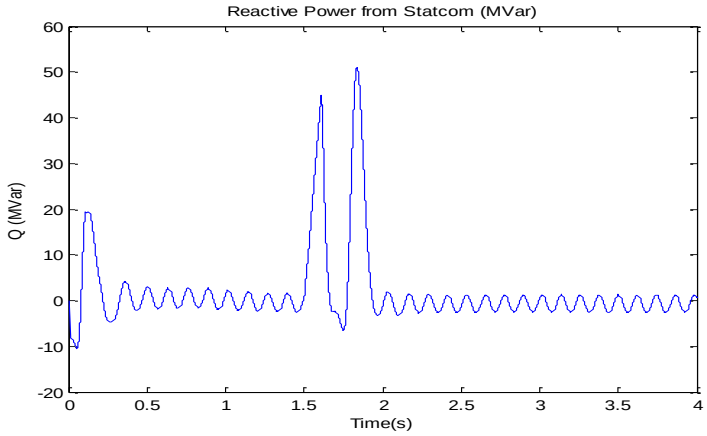

Figure 4-5: Reactive power output from STATCOM

Table 4-5: Active power values for synchronous generator with STATCOM (case 1A)

	Pre-fault (Maximum value in MW)	During-fault (Maximum value in MW)	Post-fault (Maximum value in MW)
Active power from synchronous generator with STATCOM compensation	14	0	14

From Figure 4-6, it can be seen that there is no reactive power compensation for SG without STATCOM (Case 1B). The active power output profile is steady up to 1.5s, when the low voltage condition occurs. During low voltage condition, the synchronous generator can no longer produce reactive power, and as no reactive power compensation is injected into the system, the system becomes highly unstable from which does not recover even after fault clearance at 1.61s. However, the synchronous generator is unable to sustain the unstable

condition for more than 0.5s. This results in an unfavourable rise of the active power generated, which can be very detrimental to the transmission system if the generator is allowed to continue in operation.

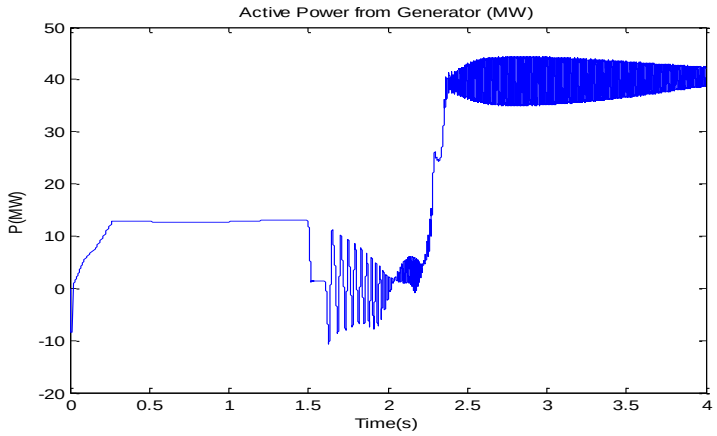

Figure 4-6: Active power output from synchronous generator without STATCOM compensation (Case 1B)

For the most commonly used LVRT system, i.e. in case of DFIG with crowbar control, Figures 4-7 and 4-8 show the active and reactive power outputs respectively of the DFIG. The reactive power compensation for DFIG occurs adequately in the event of low voltage condition. The system recovers after fault clearing. However, the rated active power is lower for DFIG (active power = 9MW) than the synchronous generator with STATCOM (active power = 14MW), which shows an advantage for the synchronous generator. From literature [36], the ohmic losses in the DFIG windings due to excitation power can reduce the power output of the generator.

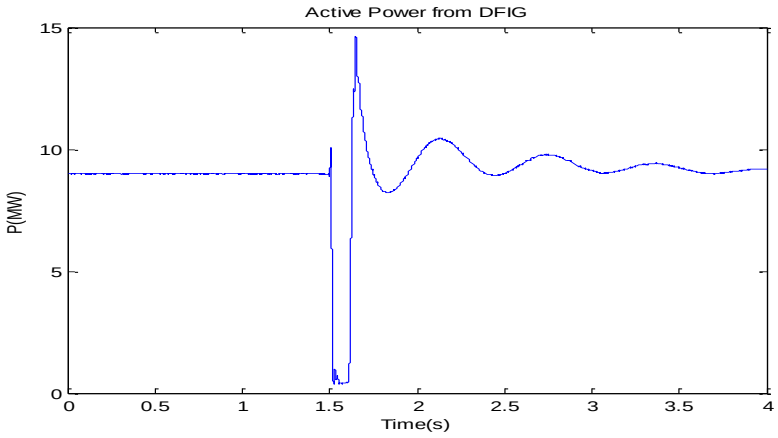

Figure 4-7: Active power output from DFIG for case study 1 (Case 2)

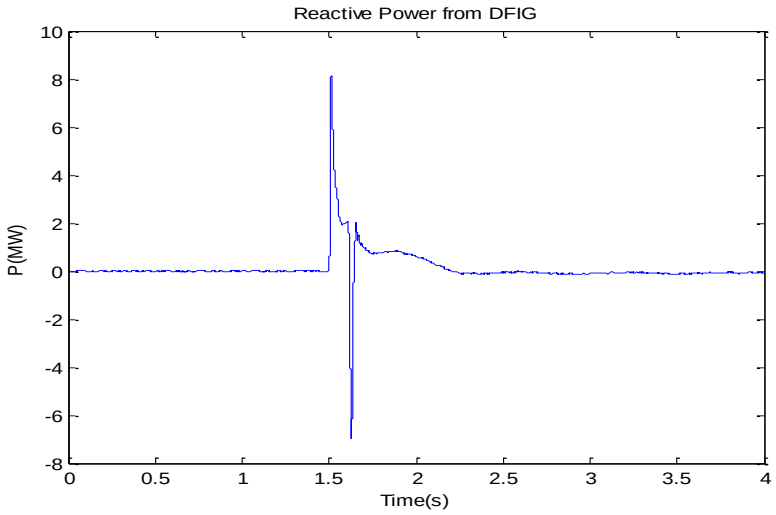

Figure 4-8: Reactive power output from DFIG (Case 2)

A comparison of the reactive power outputs between the synchronous generator with STATCOM control (Case 1B) and DFIG with crowbar control (Case 2) is shown in Figure 4-9. Figure 4.9 shows the reactive power from the two generators; the synchronous generator and the DFIG. The reactive power compensation for the wind system with DFIG comes from the generator itself, whereas the synchronous generator can generate small amount of reactive power only. However the reactive power generated from the synchronous generator is not sufficient for LVRT. STATCOM control is added to the system with synchronous generator to provide reactive power compensation during low voltage conditions. The voltages at bus 2 and bus 3 are also affected. The voltage change is discussed in figures 4-10 to 4-17.

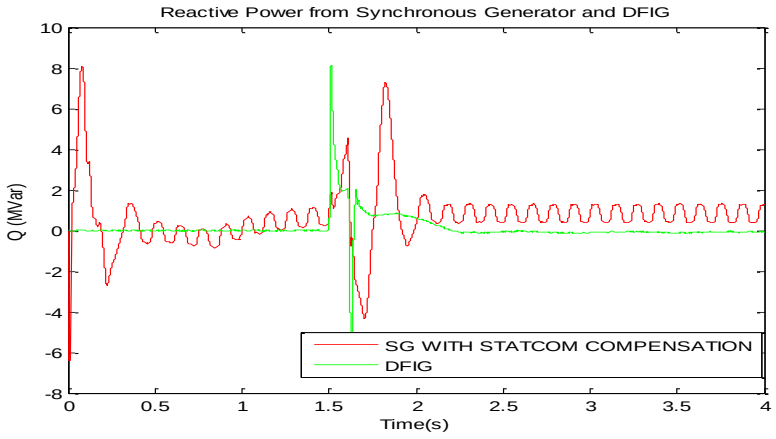

Figure 4-9: Comparison of reactive power output from synchronous generator with STATCOM and DFIG (Case 1A and 2)

Looking at the voltage profiles for synchronous generator with STATCOM compensation at buses 2 and 3 shown in Figure 4-10 and 4-11 respectively, it relates to the active power graphs. The injection and absorption of reactive power at the PCC of the transmission system; of the inverter control at bus 3, affect the magnitude of the voltages at the buses on the transmission line. In graphs 4-11, an increase and decrease of the voltage of +/- 40% at low voltage clearance can be seen at bus 3. The voltage is recovered at low voltage clearance.

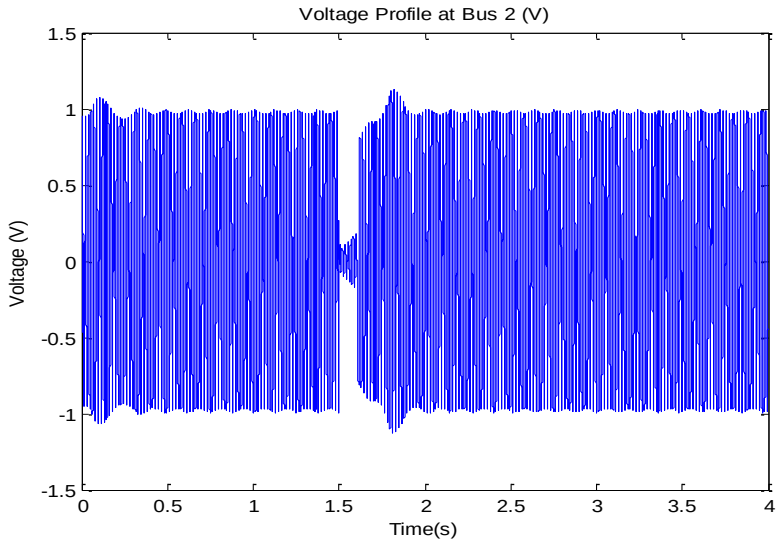

Figure 4-10: Voltage profile at Bus 2 for synchronous generator with STATCOM compensation (Case 1A)

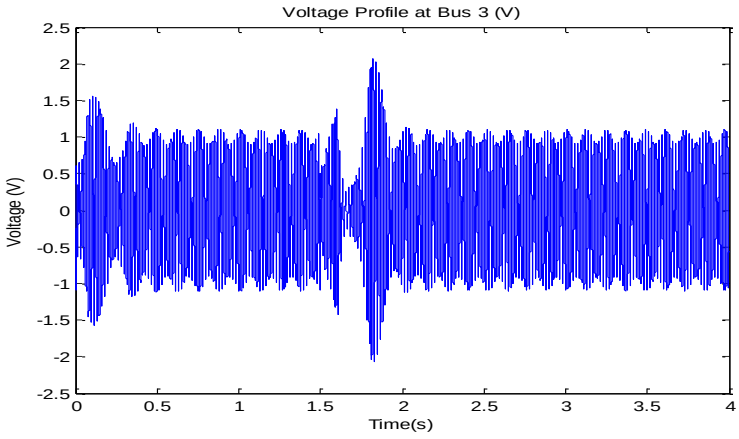

Figure 4-11: : Voltage profile at Bus 3 for synchronous generator with STATCOM compensation (Case 1A)

Conversely, considering the synchronous generator without STATCOM compensation gives a different result. The results are shown in figures 4-12 and 4-13 for voltage profiles at bus 2 and bus 3 respectively. The voltage profile is at unity until the low voltage condition whereby the system is unable to sustain the low voltage condition. This results in high instability of the voltage profile along the transmission line. As seen in Figure 4.4, an unfavourable and dangerous rise of the active power generated can be detrimental as a high rise in voltage profile can be expected, which can be very harmful to the transmission system if the latter is not setup to trip and allowed to continue in operation.

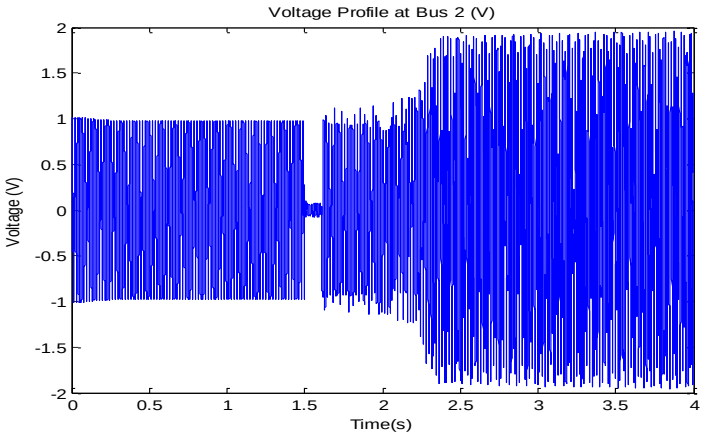

Figure 4-12: Voltage profile at Bus 2 for synchronous generator without STATCOM compensation (Case 1B)

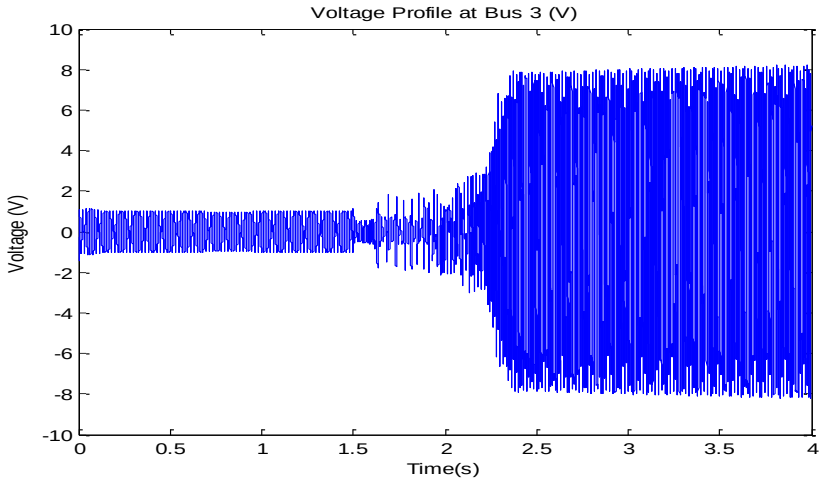

Figure 4-13: Voltage profile at Bus 3 for synchronous generator without STATCOM compensation (Case 1B)

Voltage profiles at bus 2 and 3 for the DFIG operation are shown in Figure 4.14 and 4.15 respectively. the graphs 4-14 and 4-15 show the ability of the generator to sustain the Low voltage condition and the system. The system recovers after the low voltage condition due to the reactive power compensation from the crowbar control at the point of common coupling of the wind turbine system.

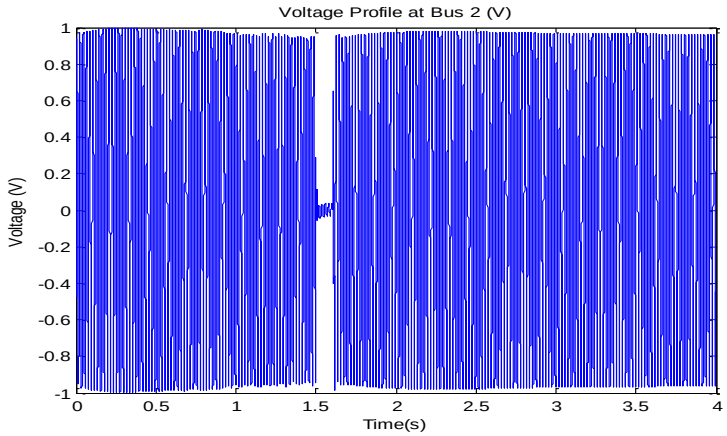

Figure 4-14: Voltage profile at Bus 2 for DFIG (Case 2)

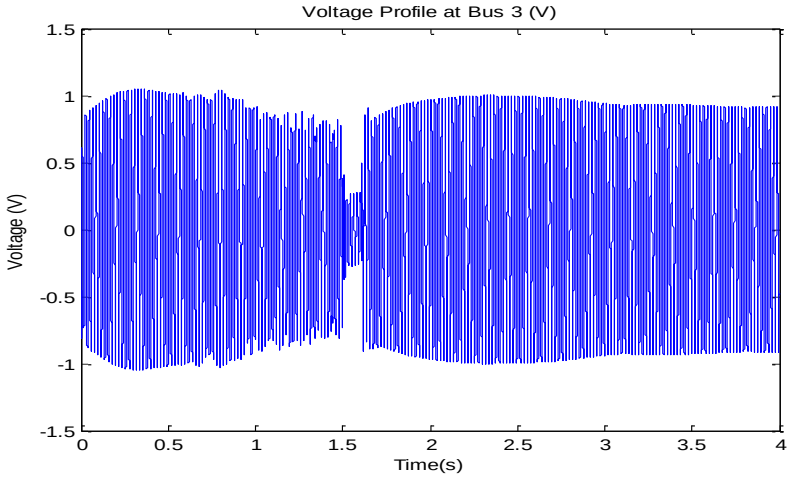

Figure 4-15: Voltage profile at Bus 3 for DFIG (Case 2)

Now considering a comparison between the synchronous generator with STATCOM control and the DFIG, the two voltage profiles at bus 2 and 3; for synchronous generator with STATCOM compensation and DFIG are analysed as per figures 4-16 and 4-17 respectively. It can be noted that the lowest voltage obtained for synchronous generator with STATCOM

compensation is higher than the lowest voltage amplitude for DFIG. From the comparison graphs, 4-9, 4-16 and 4-17. The values noted are shown in Table 4-6.

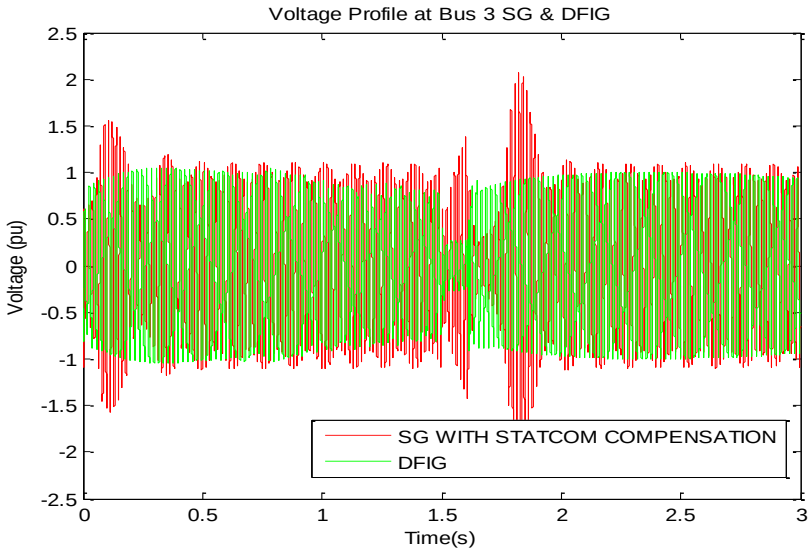

Figure 4-16: Voltage profile comparison at Bus 3 for synchronous generator with STATCOM compensation and DFIG (Cases 1A and 2)

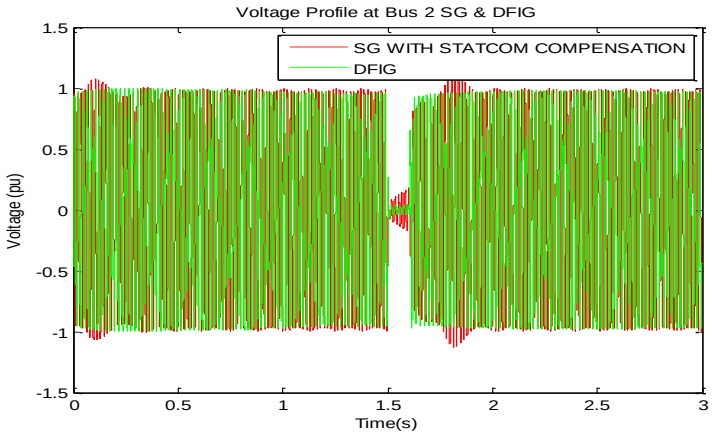

Figure 4-17: Voltage profile comparison at Bus 2 for synchronous generator with STATCOM compensation and DFIG (Case 1A and 2)

From this scenario, the graphs 4-3 and 4-6 show the ability of the STATCOM control to provide low voltage ride through capability to the synchronous generator. Looking at the comparison between the synchronous generator with STATCOM control and DFIG with crowbar control as shown in 4-9, 4-16 and 4-17, the effectiveness of using the synchronous generator over the DFIG can be seen.

Table 4-6: Comparison values for Case 1A, 1B and 2

		Pre-fault value	During-fault value	Post-fault value
Active power (MW)	*Synchronous generator with STATCOM compensation (Case 1A)*	12 - 14	0	12 - 14
	Synchronous generator without STATCOM compensation *(Case 1B)*	12	unstable	35 - 42
	DFIG with crowbar control *(Case 2)*	11 - 14	0	17
Reactive power (Mar)	*Synchronous generator with STATCOM compensation (Case 1A)*	0.5	8	0.5
	Synchronous generator without STATCOM compensation *(Case 1B)*	0	unstable	Unstable / high value
	DFIG with crowbar control *(Case 2)*	0	4	0
Voltage at bus 3 (p.u.)	*Synchronous generator with STATCOM compensation (Case 1A)*	0.95 - 1.05	0.3	0.95 - 1.05
	Synchronous generator without STATCOM compensation*(Case 1B)*	1.0	Unstable	High value / Unstable
	DFIG with crowbar control *(Case 2)*	0.95	0.23	0.95
Voltage at bus 2 (p.u.)	*Synchronous generator with STATCOM compensation (Case 1A)*	0.99	0.15	0.99
	Synchronous generator without STATCOM compensation *(Case 1B)*	1.0	Unstable	Unstable / High value
	DFIG with crowbar control *(Case 2)*	0.99	0.03	0.99

The difference in voltage drop values between case 1A and 2 is due to the design of the DFIG. A 30% improvement can be seen as per the voltage profile at bus 3 for the synchronous generator with STATCOM control over the DFIG system. The higher voltage drop during low voltage condition for the synchronous generator with STATCOM compensation can be explained; the rotor side converter of the DFIG is blocked during the complete low voltage time and the rotor windings are connected to the crowbar system.

Only the Grid Side Converter is capable of injecting reactive power into the grid, thus limiting the effectiveness of the voltage control. Reactive power is injected into the synchronous generator during the complete low voltage period, thus enabling higher voltage at the buses.

In the following subsections, scenarios 2 – 4 depict the ability of the designed synchronous generator with STATCOM control system to recover after a low voltage condition as per the grid code setup mentioned in Figure 2.1 in chapter 2. The results graphs are compared to the DFIG with crowbar simulated system graphs.

4.4.2 Scenario 2: Low voltage clearing time = 0.5s; for voltage drop amplitude (minimum value) =0.29 p.u. at Bus 1 (120kV)

Table 4.7 presents the results graphs

Table 4-7: List of figures for scenario 2 results for case study 2

Figure No	***Description***
4.18	Voltage drop profile for scenario 2
4.19	Active power generated from synchronous generator with STATCOM compensation (Case 1B)
4.20	Reactive power generated from synchronous generator with STATCOM compensation (Case 1B)
4.21	Reactive power generated from STATCOM
4.22	Active power output from SG without STATCOM compensation(Case 1B)
4.23	Active power generated from DFIG (Case 2)
4.24	Reactive power generated from DFIG (Case 2)
4.25	Reactive power comparison generated from synchronous generator with STATCOM and DFIG
4.26	Voltage profile at Bus 2 for synchronous generator with STATCOM compensation (Case 1B)
4.27	Voltage profile at Bus 3 for synchronous generator with STATCOM compensation (Case 1B)
4.28	Voltage profile at Bus 2 for DFIG (Case 2)
4.29	Voltage profile at Bus 3 for DFIG (Case 2)
4.30	Voltage profile comparison at Bus 2 for synchronous generator with STATCOM compensation and DFIG
4.31	Voltage profile comparison at Bus 3 for synchronous generator with STATCOM compensation and DFIG

Figure 4-18 shows that the voltage at bus 1 is almost 0.29 p.u. during the low voltage condition continuing for 0.5s at the grid. An inception of a balanced three-phase fault is simulated at 1.5s from the beginning of the simulation and cleared at 2.0s to simulate the low voltage condition.

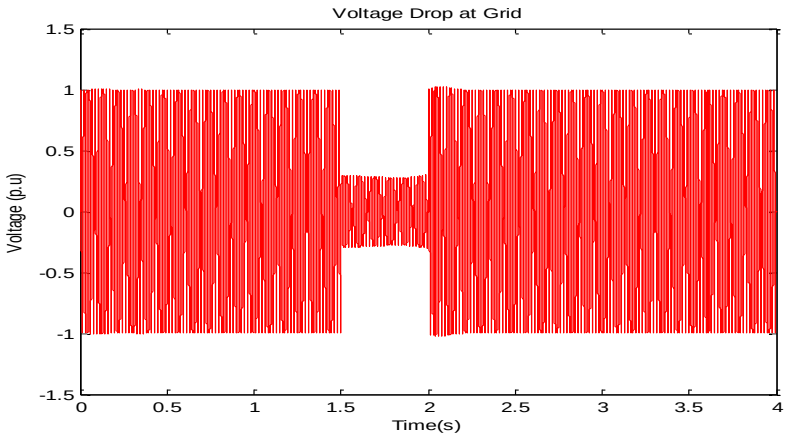

Figure 4-18: Voltage drop at Bus 1 during fault inception

Figures 4-19 and 4-20 show the active and reactive power output from the generator. It is noted from the mentioned graphs that the synchronous generator with STATCOM control has a drop in active and reactive power at the time of low voltage condition – 1.5s – 2.0s. From Figure 4-21, the STATCOM compensation can be clearly seen. However a high transient rise just after the low voltage drop clearance can be noted during the time 2.0s to 2.3s in Figure 4-21 due to the control stability in the FACT device. This is impacted on the active power output of the generator. The active power stabilises after 2.3s to the rated power output value of 14MW. Figure 4-19 also shows the low voltage ride through of the synchronous generator with STATCOM compensation as compared to Figure 4-22. Figure 4-22 shows the synchronous generator without STATCOM compensation; active power drops to 0MW during low voltage condition (1.5s to 2.0s). The transient rise can still be noted due to excitation control start up of the synchronous generator.

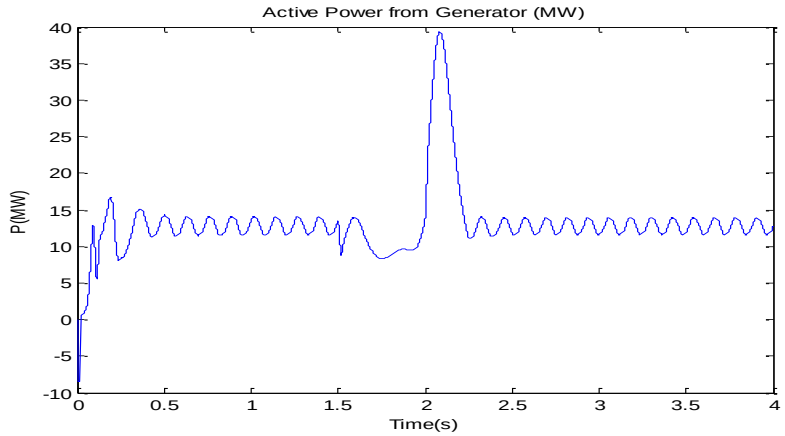

Figure 4-19: Active power output from synchronous generator with STATCOM compensation (Case 1A)

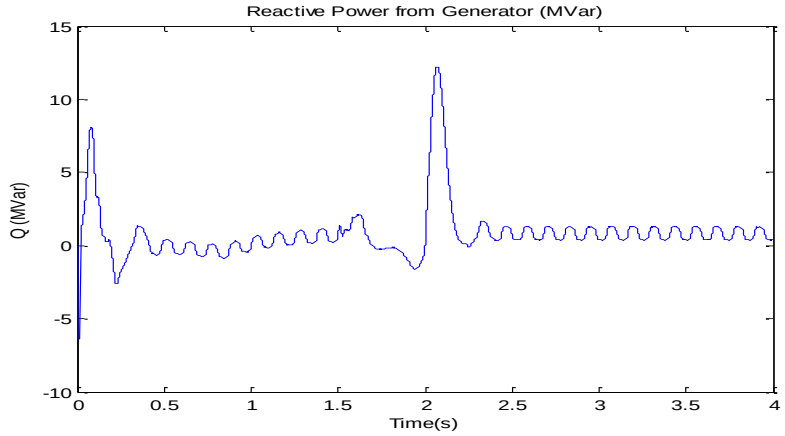

Figure 4-20: Reactive power outout from synchronous generator with STATCOM compensation (Case 1A)

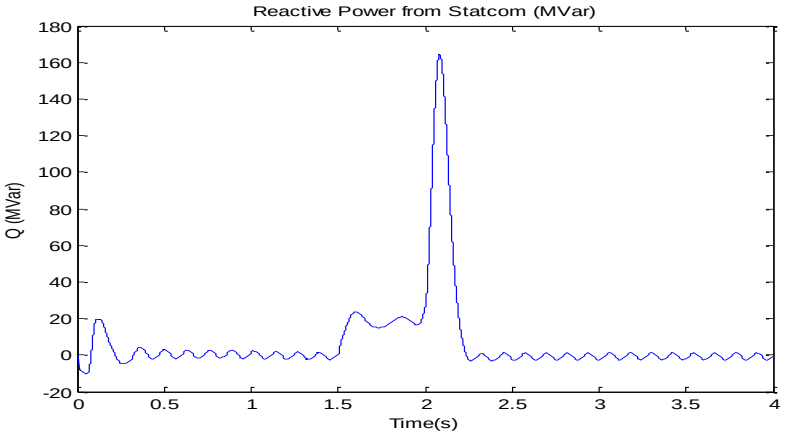

Figure 4-21: Reactive power output from STATCOM (Case 1A)

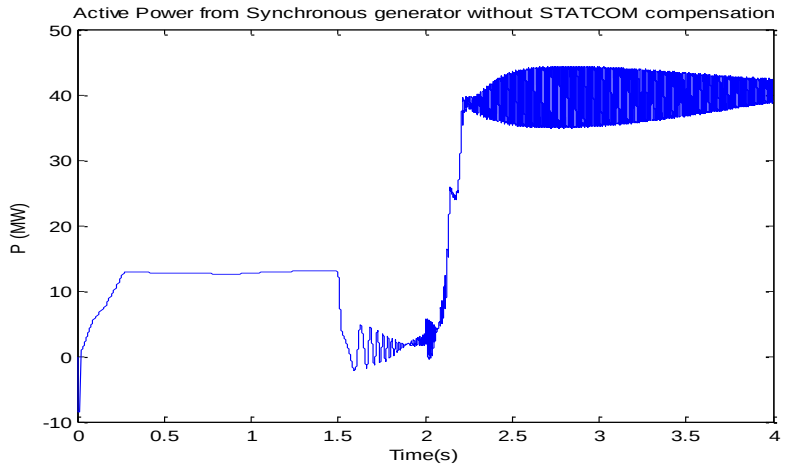

Figure 4-22: Active power output from SG without STATCOM compensation(Case 1B)

With regards to the DFIG as compared to the synchronous generator with STATCOM control, it can be noted from Figure 4.23 and 4.24, that the built-in crowbar control in the DFIG helps the generator to overcome the low voltage condition during 1.5s to 2.0s by reactive power compensation. The DFIG recovers to the rated power of 9MW.

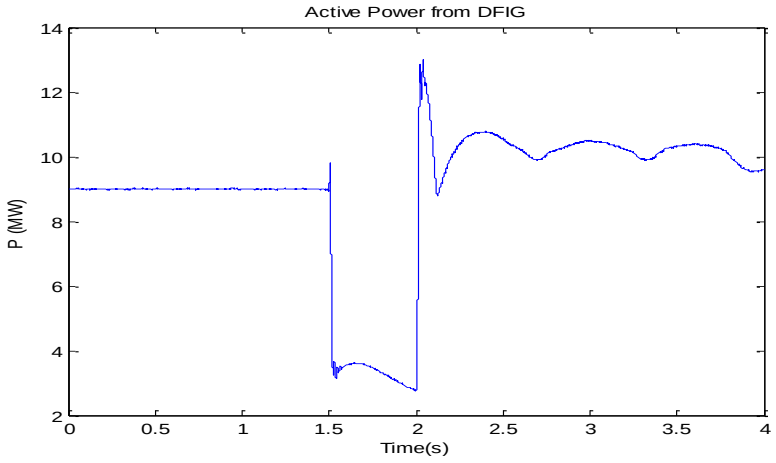

Figure 4-23: Active power output from DFIG (Case 2)

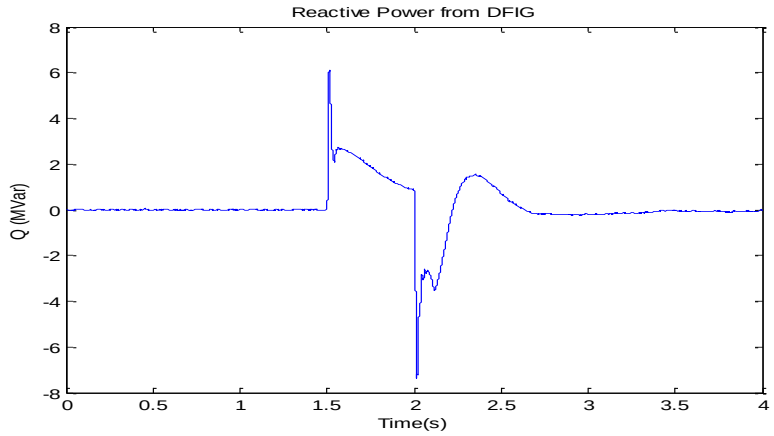

Figure 4-24: Reactive power output from DFIG (Case 2)

Figure 4-25 depicts the comparison between the synchronous generator with STATCOM control and the DFIG. The DFIG shows the compensation from the reactive power output at 1.5s to 2.0s. As shown in the reactive power profile from the STATCOM, Figure 4-21 shows small deviation from the reference reactive power (0p.u) of the reactive power profile of the STATCOM. This is impacted on the reactive power profile of the synchronous generator; a small deviation of +/-10% of the rated power is noted.

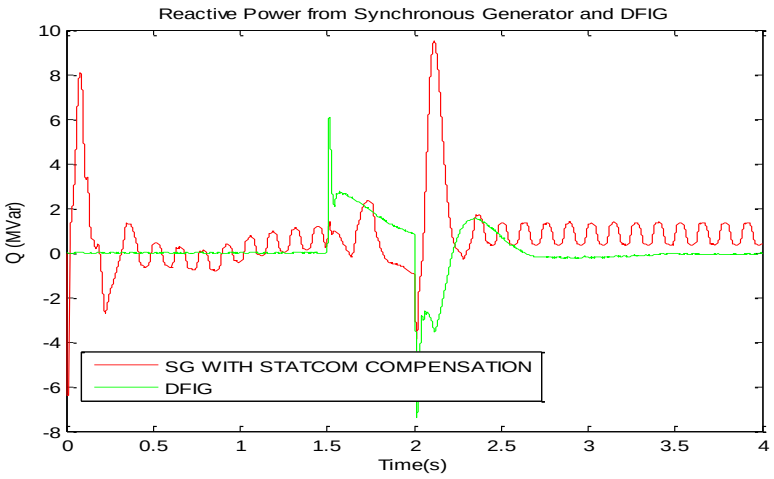

Figure 4-25: Comparison of reactive power output from synchronous generator with STATCOM and DFIG (Case 1A and 2)

Figure 4-26 and 4-27 depict the voltage profile at bus 2 and bus 3 respectively for the synchronous generator with STATCOM control along the transmission line. The values during the low voltage drop are 0.65p.u at bus 2 and 0.2p.u at bus 3. However, a high rise in voltage occurs at the time of voltage clearance due to the sudden change in reactive power from the STATCOM at the point of common coupling.

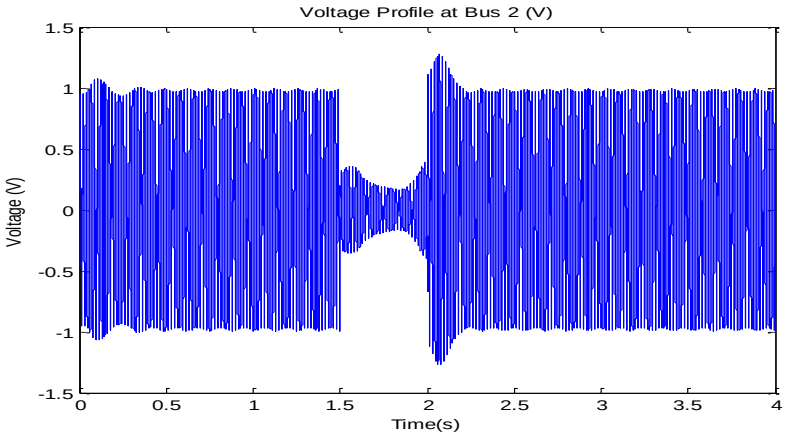

Figure 4-26: Voltage profile at Bus 2 for synchronous generator with STATCOM compensation (Case 1A)

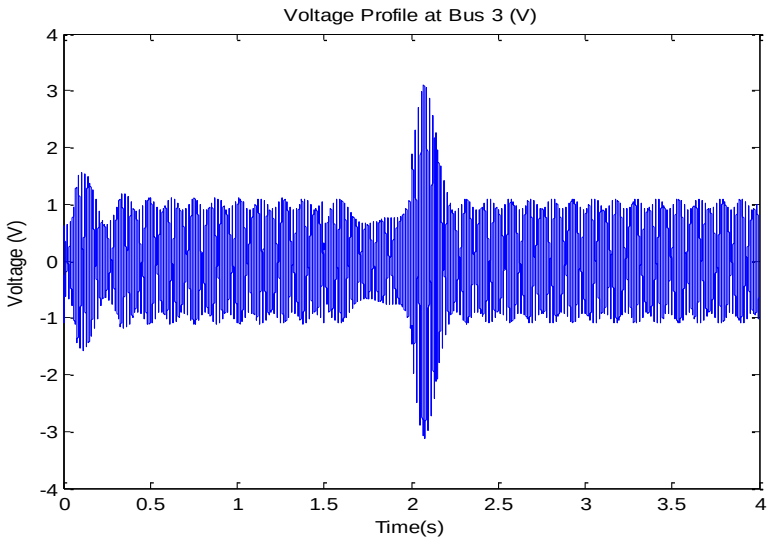

Figure 4-27: Voltage profile at Bus 3 for synchronous generator with STATCOM compensation (Case 1A)

In case 2, DFIG, the voltage drops to 0.28p.u at bus 2 and 0.29 p.u. at bus 3 along the transmission line. The voltage profiles for the DFIG at bus 2 and 3 are shown in Figure 4-28 and 4-29 respectively. The profiles show the recovery to rated voltage after fault clearance at bus 2. However, at bus 3 the DFIG encounters a transient increase and decrease of 40% in voltage for 0.5s. The voltage profile recovers to rated value at 2.5s.

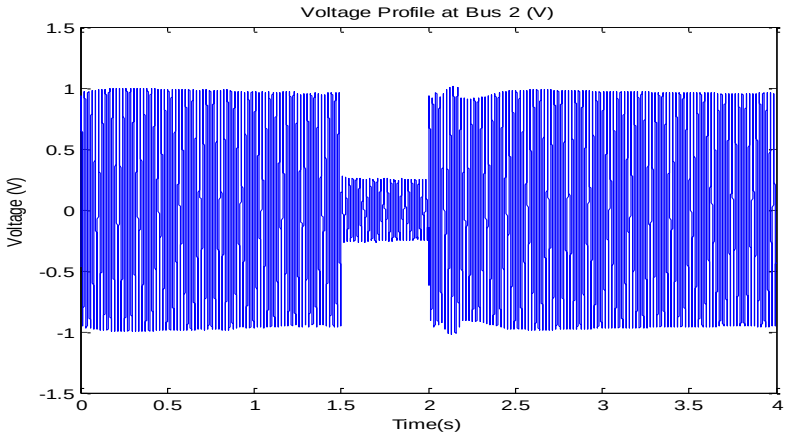

Figure 4-28: Voltage profile at Bus 2 for DFIG (Case 2)

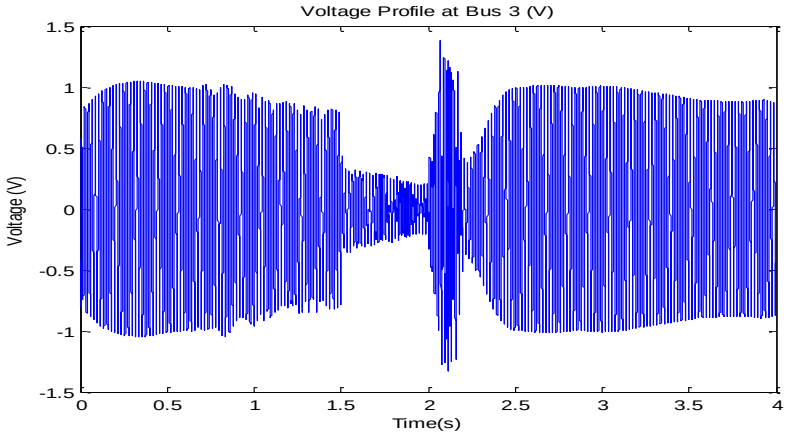

Figure 4-29: Voltage profile at Bus 3 for DFIG (Case 2)

The voltage profiles for the two generators (case 1A and case 2) are compared as shown in figures 4-30 and 4-31 and the values are shown in Table 4-8.

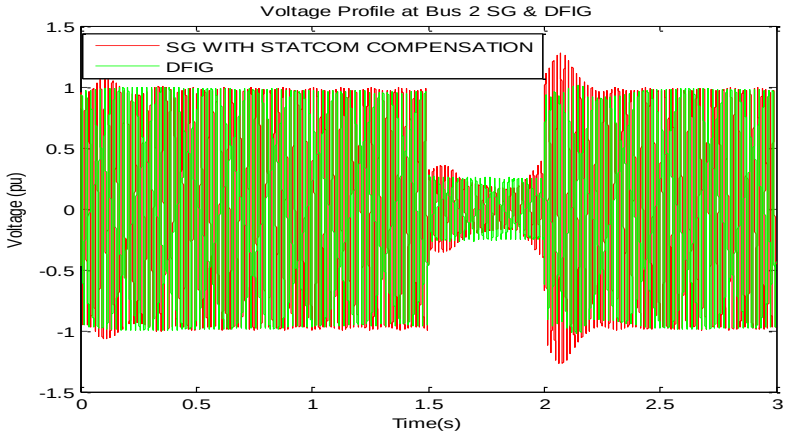

Figure 4-30: Voltage profile comparison at Bus 2 for synchronous generator with STATCOM compensation and DFIG (Case 1A and 2)

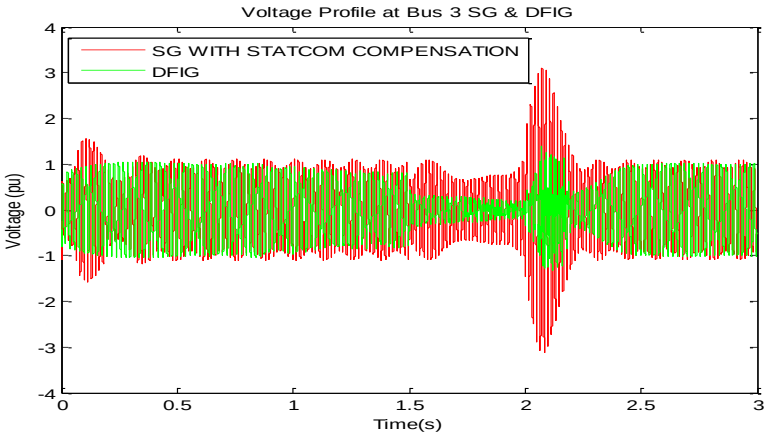

Figure 4-31: Voltage profile comparison at Bus 3 for synchronous generator with STATCOM compensation and DFIG (Cases 1A and 2)

Table 4-8: Comparison values for Case 1A, 1B and 2

		Pre-fault value	During-fault value	Post-fault value
Active power (MW)	*Synchronous generator with STATCOM compensation (Case 1A)*	11.5-14	0-15	High rise to 32MW, then stabilises to 11.5 - 14
	DFIG with crowbar control	9	0	stabilises to 9
Reactive power (Mar)	*Synchronous generator with STATCOM compensation (Case 1A)*	0 - 1	2	0.5 - 1.5
	DFIG with crowbar control	0	1 - 6	stabilises to 0
Voltage at bus 3 (p.u.)	*Synchronous generator with STATCOM compensation (Case 1A)*	0.9 - 1.1	0.65	high rise to 2.5p.u. Then drop to 0.9 - 1.1
	DFIG with crowbar control	1.1	0.29	1.1
Voltage at bus 2 (p.u.)	*Synchronous generator with STATCOM compensation (Case 1A)*	0.97 - 0.99	0.2 – 0.3	0.97 - 0.99
	DFIG with crowbar control	1.1	0.28	1.1

The results demonstrate that the synchronous generator can ride through low voltage condition with the help of STATCOM compensation only. Ripples can be seen in the power output of the generator as shown in figure 4.19, 4.20, 4.21. This is due to the control system more precisely harmonics generated from the STATCOM device causing small

overshoots. As STATCOM is a harmonic voltage source, network voltage distortion occurs as a result of voltage division between the STATCOM phase impedance and the network impedance. The harmonic distortion is very low as harmonic filters are included in the STATCOM device. It can be noted from Table 4.8, the synchronous generator with STATCOM compensation provides an improved LVRT than the DFIG. This due to the difference in design of the DFIG as explained in section 4.4.2. Only the Grid Side Converter is capable of injecting reactive power into the grid, while the rotor side convertor is blocked and the rotor windings are connected to the crowbar control system. However, in case 1A, synchronous generator with STATCOM control, the reactive power is injected into the synchronous generator during the complete low voltage period, thus enabling higher voltage at the buses.

4.4.3 Scenario 3: Low voltage clearing time = 1.0s; for voltage drop amplitude (minimum value) = 0.4 p.u. at Bus 1 (120kV)

Table 4-9 presents the results graphs for case study 3

Table 4-9: List of figures for scenario 3 results

Figure No	***Description***
4.32	Voltage drop profile for scenario 3
4.33	Active power generated from synchronous generator with STATCOM compensation (Case 1A)
4.34	Reactive power generated from synchronous generator with STATCOM compensation (Case 1A)
4.35	Reactive power generated from STATCOM
4.36	Active power output from SG without STATCOM compensation(Case 1B)
4.37	Active power generated from DFIG (Case 2)
4.38	Reactive power generated from DFIG (Case 2)
4.39	Reactive power comparison generated from synchronous generator with STATCOM and DFIG
4.40	Voltage profile at Bus 2 for synchronous generator with STATCOM compensation (Case 1A)
4.41	Voltage profile at Bus 2 for DFIG (Case 2)
4.42	Voltage profile comparison at Bus 2 for synchronous generator with STATCOM compensation and DFIG
4.43	Voltage profile at Bus 3 for synchronous generator with STATCOM compensation (Case 1A)
4.44	Voltage profile at Bus 3 for DFIG (Case 2)
4.45	Voltage profile comparison at Bus 3 for synchronous generator with STATCOM compensation and DFIG

The voltage drop at bus 1 to 0.4p.u. is shown in Figure 4-32 during the low voltage condition continuing for 1s at the grid. The low voltage condition is simulated by having an inception of a balanced three-phase fault simulated at 1.5s from the start of the simulation and cleared at 2.5s

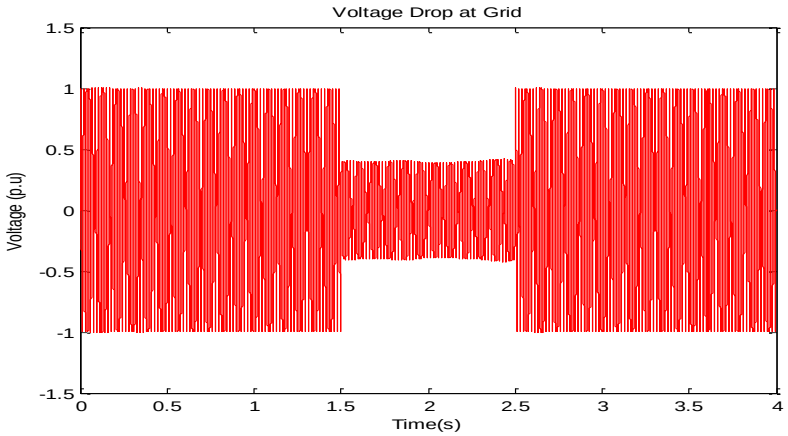

Figure 4-32: Voltage drop at Bus 1 during fault inception

Similar to previous scenarios, the active and reactive power generated from the synchronous generator is analysed and the power profile of each generator is shown in figures 4-33 to 4-36 for synchronous generator with and without STATCOM and DFIG. The active power profile of the synchronous generator shows a drop in value of about 70% the rated power output. However, the profile restores to rated power at 2.6s from the beginning of the simulation. The synchronous generator with STATCOM control can clearly ride through low voltage condition when the power profile of Figure 4-33 is compared to Figure 4-36. Figure 4-36 shows the active power profile from the synchronous generator without STATCOM control and the system does not recover after low voltage clearance at 2.5s. The synchronous generator without STATCOM control should be tripped during Low voltage as the high voltage can be harmful for transmission. However, from figures 4-33, 4-34 and 4-35 the high rise is still noted after the clearance of the voltage drop due to the control stability of the FACT device during a time period of 2.5s to 2.6s. The transient rise at the beginning of the start up is as per the excitation control at start up of the synchronous generator. The active power of the synchronous generator stabilises to 13MW after the system recovers from the low voltage condition at 2.7s from the start of the simulation.

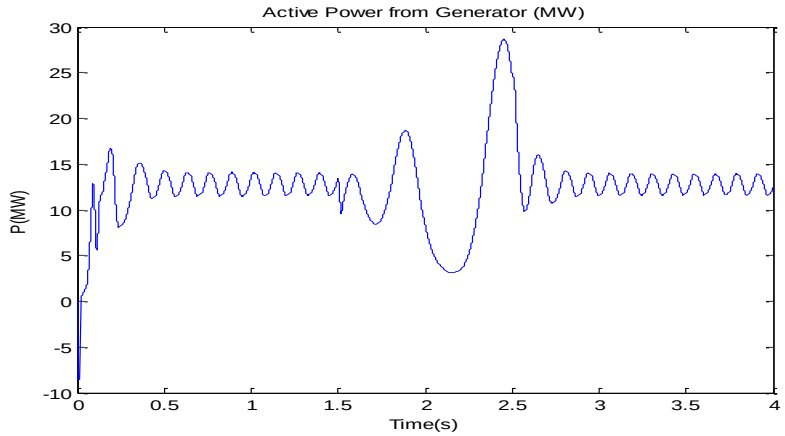

Figure 4-33: Active power output from synchronous generator with STATCOM compensation (Case 1A)

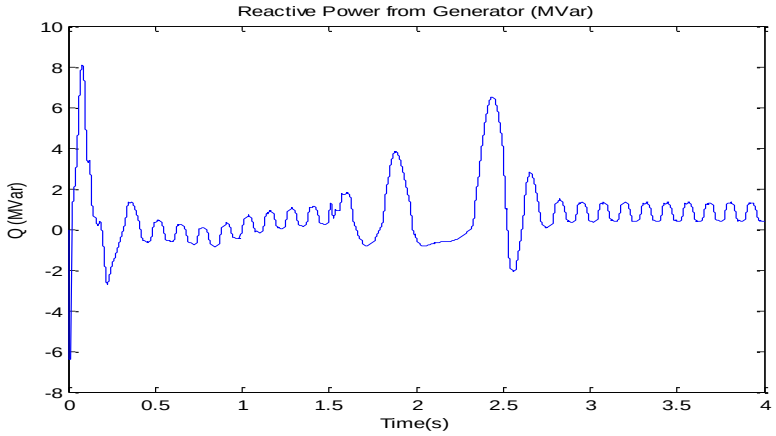

Figure 4-34: Reactive power outout from synchronous generator with STATCOM compensation (Case 1A)

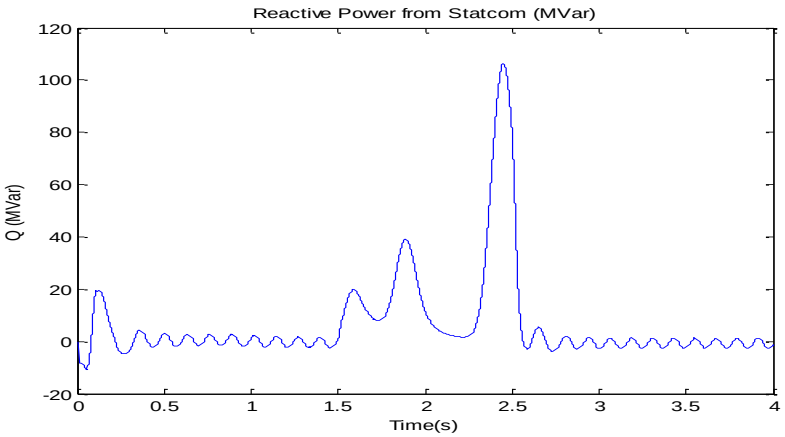

Figure 4-35; Reactive power output from STATCOM

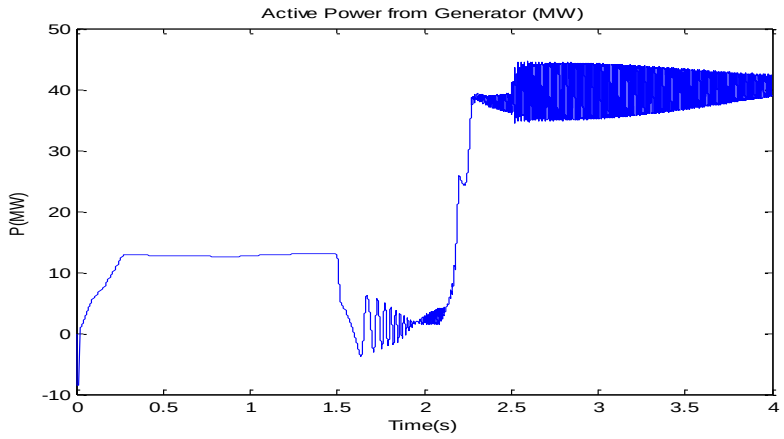

Figure 4-36: Active power output from synchronous generator without STATCOM compensation (Case 1B)

The DFIG with crowbar control similar to scenario 1 and 2 is simulated with a voltage drop of 0.4p.u during the time 1.5s to 2.5s from the beginning of the simulation. Figure 4-37 and 4-38 show the active and reactive power output profile of the system. The DFIG recovers from the low voltage condition at 2.8s to the rated power of about 10MW. the crowbar control provides the reactive power compensation for the DFIG to ride through the low voltage condition.

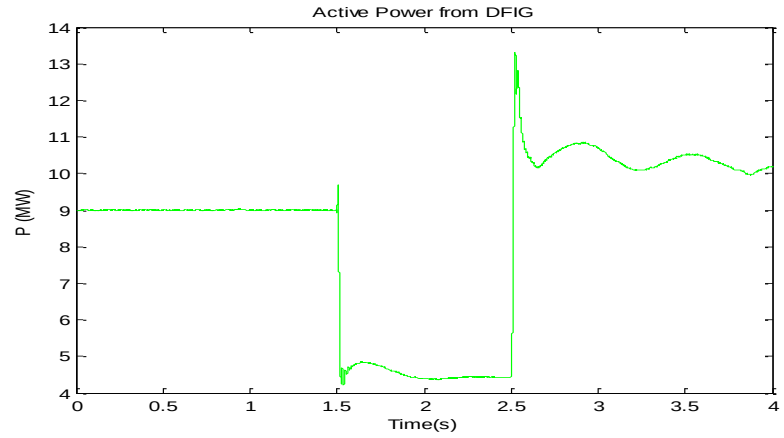

Figure 4-37: Active power output from DFIG (Case 2)

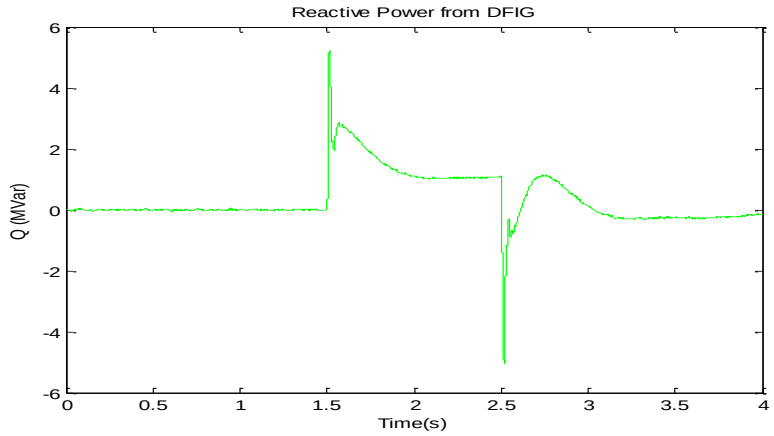

Figure 4-38: Reactive power output from DFIG (Case 2)

Figure 4-39 shows the reactive power profile of the synchronous generator with STATCOM control compared with the DFIG reactive power profile. The reactive power of the synchronous generator is due to the STATCOM control connected to the PCC at bus 3 of the transmission line, whereas the reactive power from the DFIG is from the crowbar control included in the generator itself.

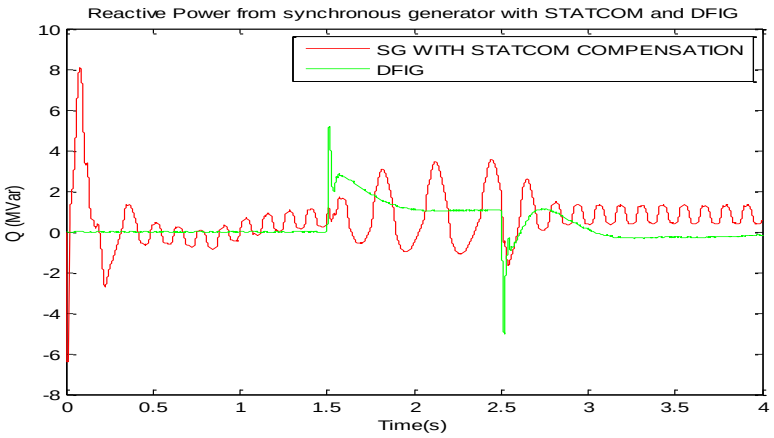

Figure 4-39: Comparison of reactive power output from synchronous generator with STATCOM and DFIG (Case 1A and 2)

Figure 4-40 and 4-41 depict the voltage profile at bus 2 for the synchronous generator with STATCOM control and the DFIG respectively. The values during the low voltage drop at bus 2 range from 0.6 p.u to 0.65p.u for the synchronous generator with STATCOM and 0.45p.u for DFIG. The comparison of the voltage profiles at bus 2 for the two generators are compared and it can be seen that the synchronous generator with STATCOM control provide a higher voltage at bus 2 than DFIG. As mentioned in the previous scenarios, the

difference in voltage and performance of the two generators are due to the different designs. The DFIG injects reactive power at the PCC only by the grid side convertor of the system, whereas the STATCOM connected can inject reactive power during the complete low voltage condition.

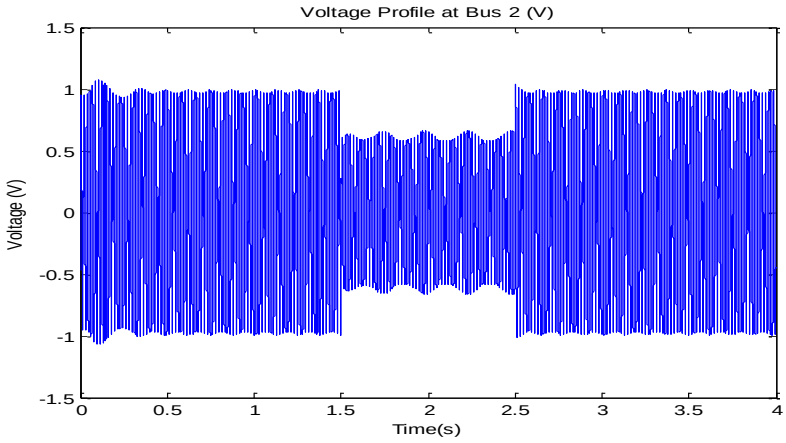

Figure 4-40: Voltage profile at Bus 2 for synchronous generator with STATCOM compensation (Case 1A)

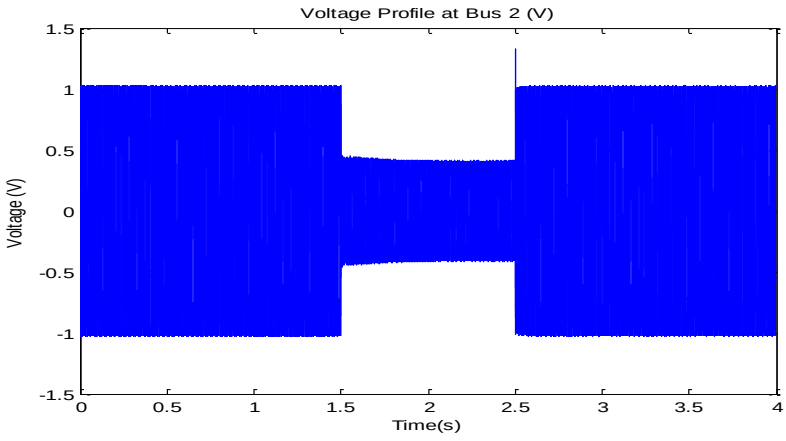

Figure 4-41: Voltage profile at Bus 2 for DFIG (Case 2)

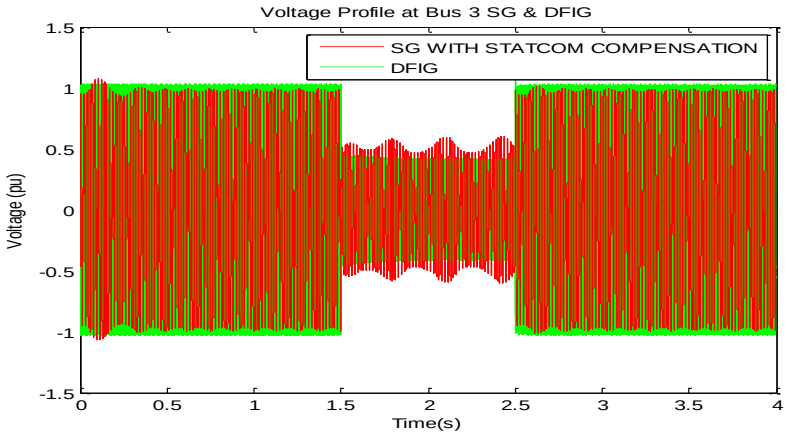

Figure 4-42: Voltage profile comparison at Bus 2 for synchronous generator with STATCOM compensation and DFIG (Case 1A and 2)

The voltage profile at bus 3 for synchronous generator with STATCOM control and DFIG is illustrated in Figure 4-43 and 4-44 respectively. Similar to bus 2 behaviour, the voltage at bus 3 for the synchronous generator with STATCOM control (case 1A) is higher than the voltage of the DFIG (case 2). The voltage at bus 3 for case 1A ranges from 0.73p.u. to 1.2 whereas the voltage for the DFIG is at 0.5p.u. Figure 4-45 depicts the voltage comparison for the two generators at bus 3.

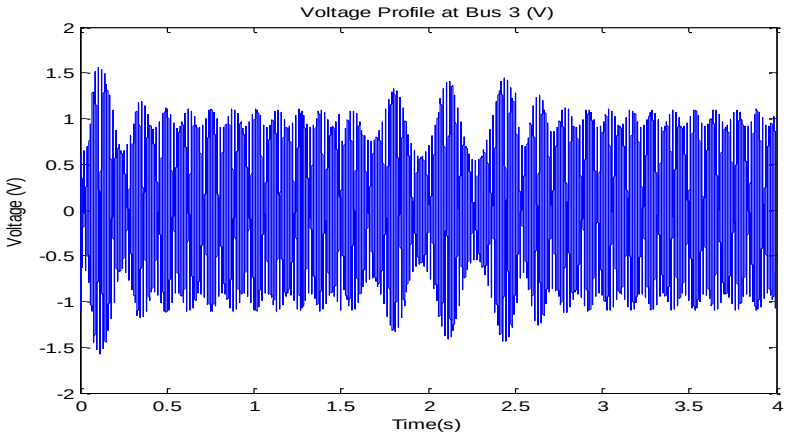

Figure 4-43: Voltage profile at Bus 3 for synchronous generator with STATCOM compensation (Case 1A)

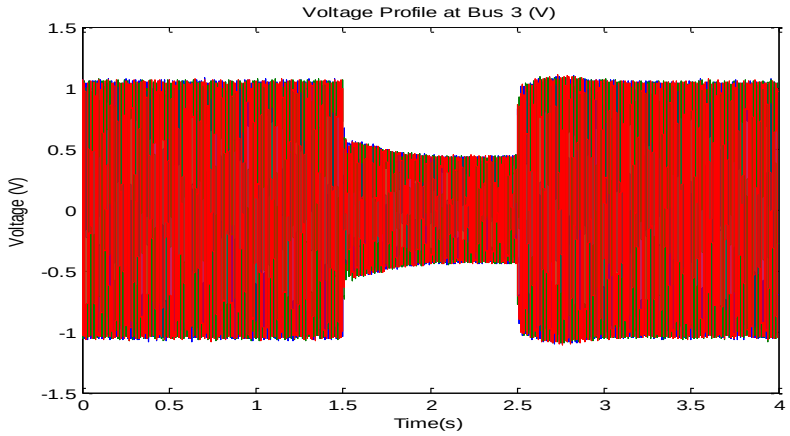

Figure 4-44: Voltage profile at Bus 3 for DFIG (Case 2)

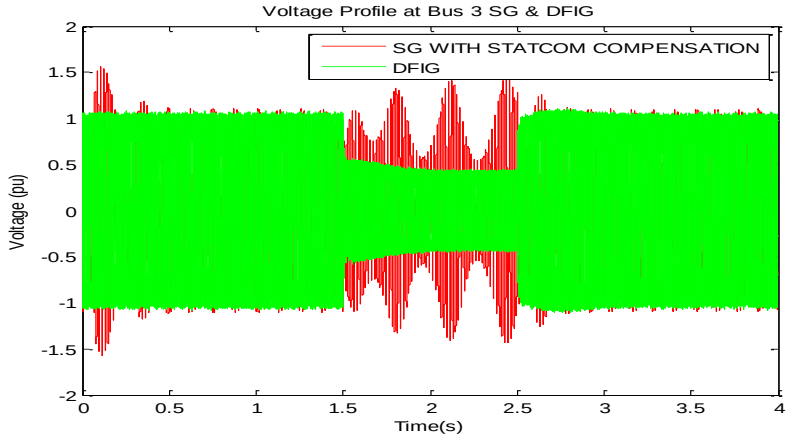

Figure 4-45: Voltage profile comparison at Bus 3 for synchronous generator with STATCOM compensation and DFIG (Cases 1A and 2)

The results shown in Table 4-10 demonstrate and confirms the previous scenario results. The synchronous generator can ride through low voltage condition with the help of STATCOM compensation only and can provide a better LVRT than the DFIG. As discussed earlier in scenario 1 & 2, this due to the difference in design of the DFIG as explained in section 4.4.2. Only the Grid Side Converter is capable of injecting reactive power into the grid, while the rotor side convertor is blocked and the rotor windings are connected to the crowbar control system. However, the reactive power is injected into the grid at the PCC during the complete low voltage period in case 1A, synchronous generator with STATCOM control, thus enabling higher voltage at the buses. The comparison values are shown in Table 4-10 for scenario 3.

Table 4-10: Comparison values for Case 1A, 1B and 2

		Pre-fault value	During-fault value	Post-fault value
Active power (MW)	*Synchronous generator with STATCOM compensation (Case 1A)*	12 - 13	Drops to 3 then just before Low Voltage clearance rises to 28	12 - 13
	Synchronous generator without STATCOM compensation	13	unstable	unstable
	DFIG with crowbar control	9	4.4	stabilises to 10
Reactive power (Mar)	*Synchronous generator with STATCOM compensation (Case 1A)*	0	6.4	0
	DFIG with crowbar control	0	1-2.5	0
Voltage at bus 3 (p.u.)	*Synchronous generator with STATCOM compensation (Case 1A)*	0.98-1.2	drops to 0.73	0.98 - 1.2
	DFIG with crowbar control	1.0	0.5	1.0
Voltage at bus 2 (p.u.)	*Synchronous generator with STATCOM compensation (Case 1A)*	1	0.6 - 0.65	1
	DFIG with crowbar control	1	0.4	1

4.4.4 Scenario 4: Low voltage clearing time = 1.8s; for voltage drop amplitude(minimum value)= 0.7 p.u. at Bus 1 (120kV)

An inception of a balanced three-phase fault is simulated at 1.5s from the start of the simulation and the fault is cleared at 3.3s to simulate a low voltage situation for scenario 4 at bus 1. The voltage is at 0.7p.u for the period of 1.8s at the grid. The voltage drop at bus 1 during low voltage is shown in Figure 4-46.

Table 4-11 presents the results graphs for case scenario.

Table 4-11: List of figures for scenario 4 results

Figure No	***Description***
4.46	Voltage drop profile for scenario 4
4.47	Active power generated from synchronous generator with STATCOM compensation (Case 1A)
4.48	Active power generated from DFIG (Case 2)
4.49	Reactive power generated from synchronous generator with STATCOM compensation (Case 1A)
4.50	Reactive power generated from STATCOM
4.51	Reactive power generated from DFIG (Case 2)
4.52	Reactive power comparison generated from synchronous generator with STATCOM and DFIG
4.53	Voltage profile at Bus 2 for synchronous generator with STATCOM compensation (Case 1A)
4.54	Voltage profile at Bus 2 for DFIG (Case 2)
4.55	Voltage profile comparison at Bus 2 for synchronous generator with STATCOM compensation and DFIG
4.56	Voltage profile at Bus 3 for synchronous generator with STATCOM compensation (Case 1A)
4.57	Voltage profile at Bus 3 for DFIG (Case 2)
4.58	Voltage profile comparison at Bus 3 for synchronous generator with STATCOM compensation and DFIG

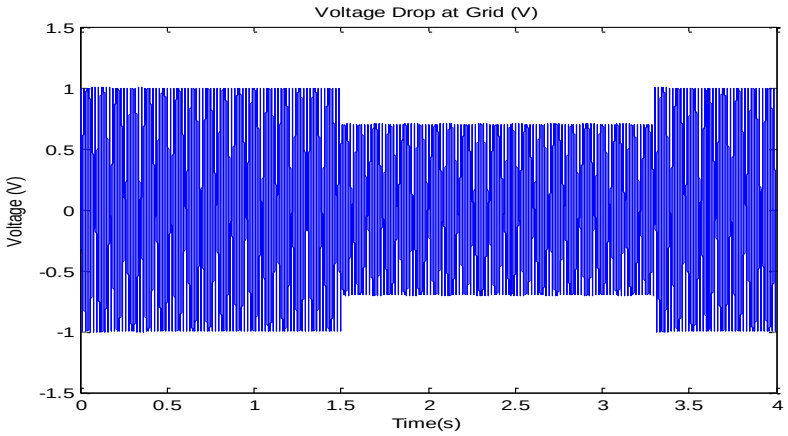

Figure 4-46: Voltage drop at Bus 1 during fault inception

This scenario also confirms the low voltage ride through of the synchronous generator with STATCOM control. Figures 4-47 and 4-48 show the active power from the synchronous generator with STATCOM control (case 1A) and DFIG (case 2) respectively. Case 1A involves small deviations from the rated power of 13MW due to the reactive power

compensation from the STATCOM as shown in Figure 4-50. The deviations also impact the reactive power generated for case 1A depicted in Figure 4-49. The reactive power control of the DFIG shown in Figure 4-51 comes from the generator itself through the integrated crowbar control. The Comparison of the reactive power output from synchronous generator with STATCOM and DFIG (Case 1A and 2) is shown in Figure 4-52.

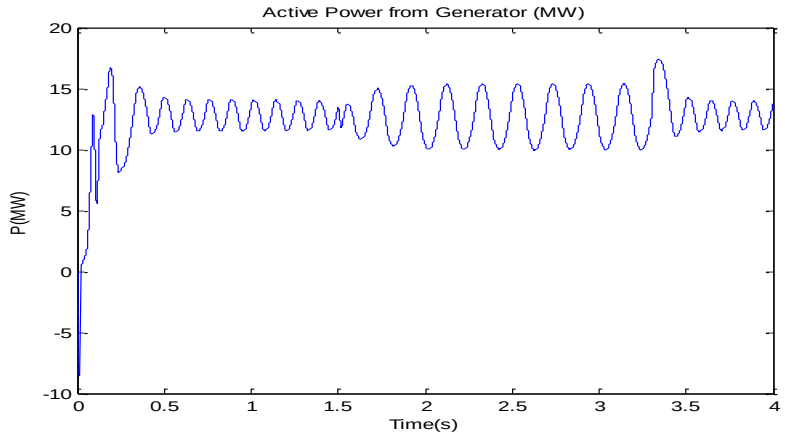

Figure 4-47: Active power output from synchronous generator with STATCOM compensation (Case 1A)

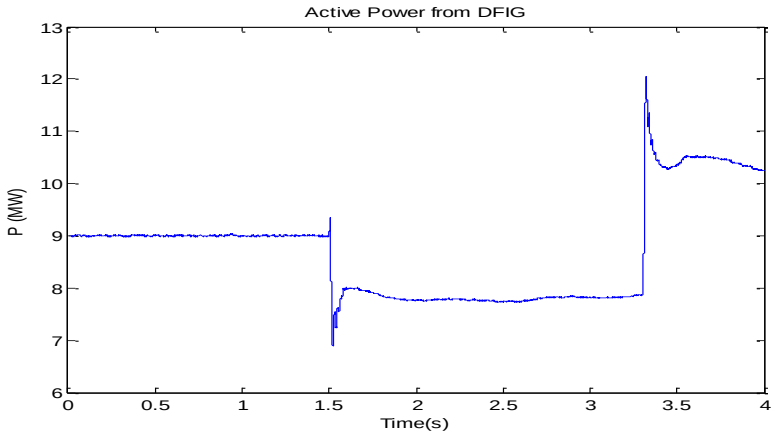

Figure 4-48: Active power output from DFIG (Case 2)

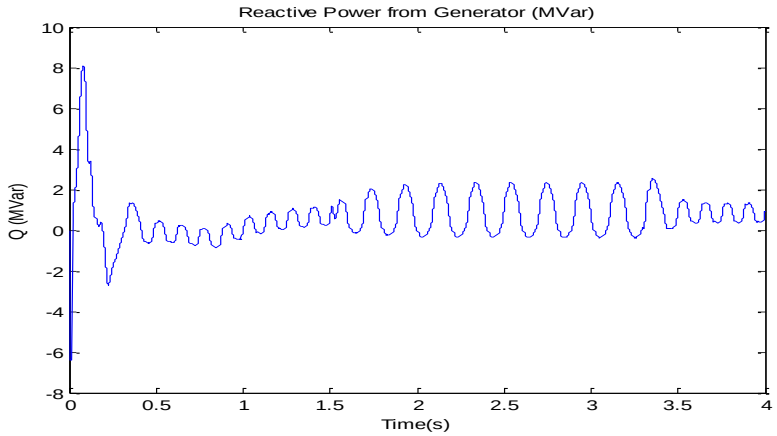

Figure 4-49: Reactive power outout from synchronous generator with STATCOM compensation (Case 1A)

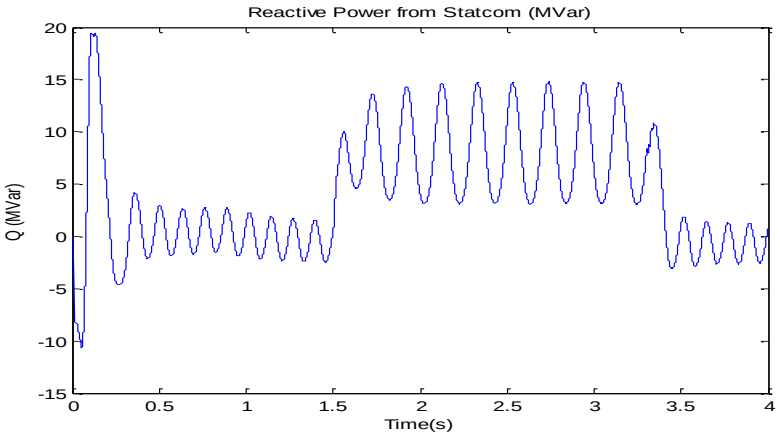

Figure 4-50: Reactive power output from STATCOM

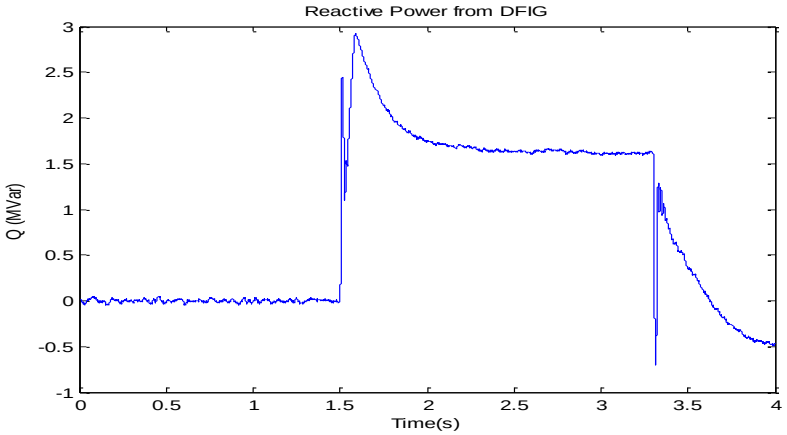

Figure 4-51: Reactive power output from DFIG (Case 2)

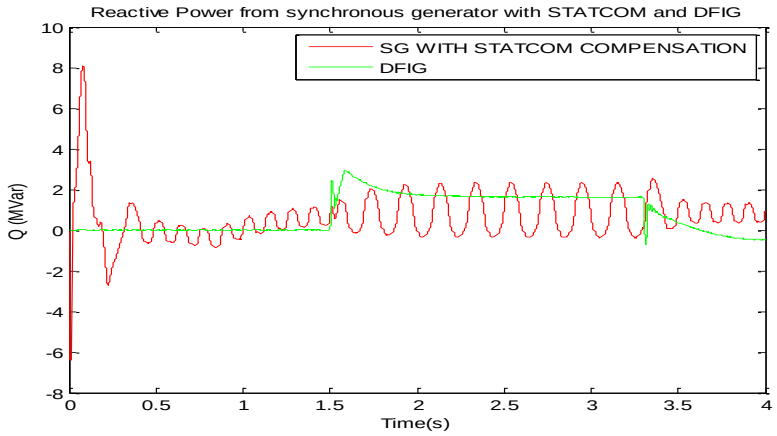

Figure 4-52: Comparison of reactive power output from synchronous generator with STATCOM and DFIG (Case 1A and 2)

Figure 4-53 and 4-54 show the voltage profiles at bus 2 for case 1A and case 2 respectively. The figures confirm the ability of the synchronous generator with STATCOM control (case 1A) to ride through low voltage condition. Case 1A shows better performance than case 2. This can be proved through Figure 4-55; the comparison of the voltage profile of case 1A and case 2 at bus 2. Case 1A has a drop value of not less than 0.7p.u whereas case 2 involves a voltage drop of 0.6p.u.

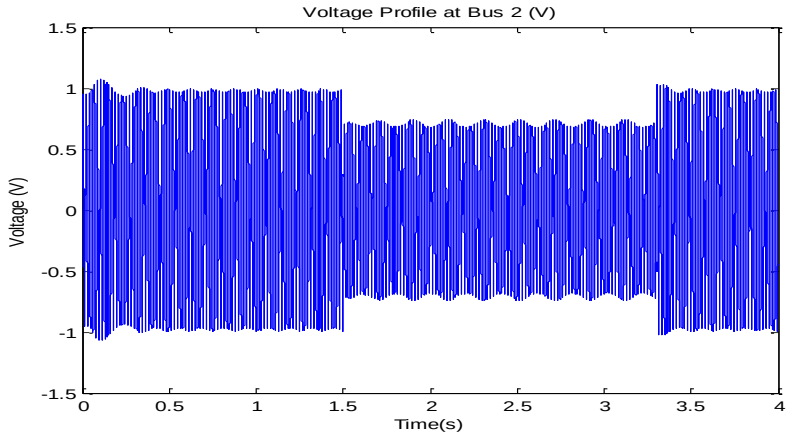

Figure 4-53: Voltage profile at Bus 2 for synchronous generator with STATCOM compensation (Case 1A)

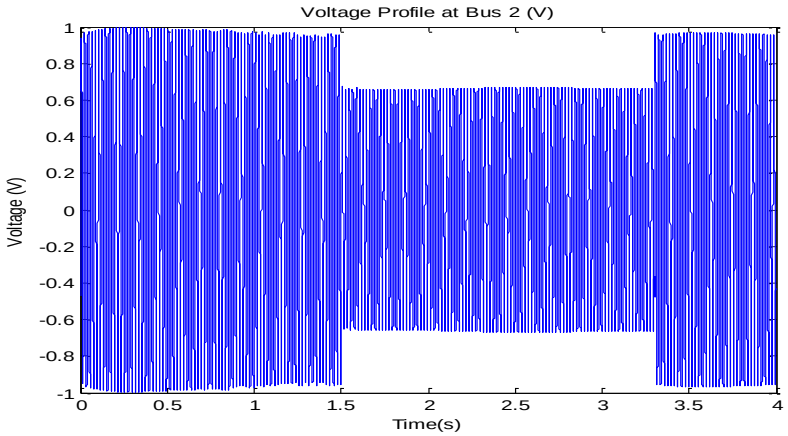

Figure 4-54: Voltage profile at Bus 2 for DFIG (Case 2)

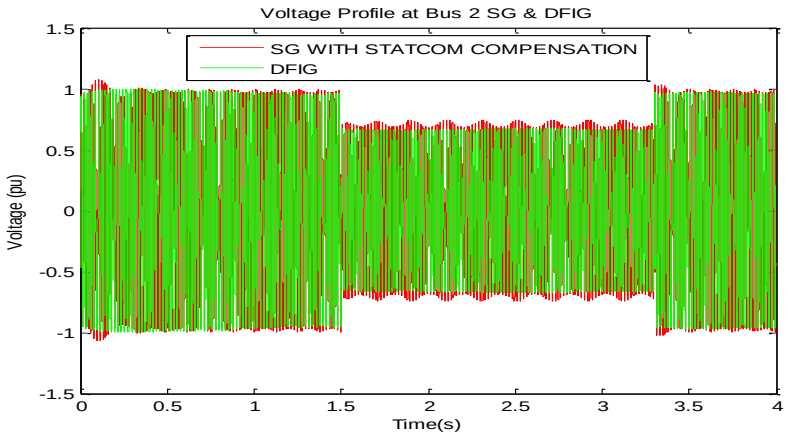

Figure 4-55: Voltage profile comparison at Bus 2 for synchronous generator with STATCOM compensation and DFIG (Case 1A and 2)

Considering voltage profiles at bus 3, case 1A shows the low voltage ride through capability. The voltage profile deviates from the rated voltage (1p.u) due to the STATCOM compensation of reactive power. The deviation from the rated voltage (1p.u.) as seen in Figure 4-56 can be noted to be +/- 20% during low voltage condition. The voltage profiles at bus 3 for case 1A Figure 4-56 and case 2 – Figure 4-57 are compared. It can be seen that the voltage drop for case 2 is still lower than case 1A as shown in Figure 4-58.

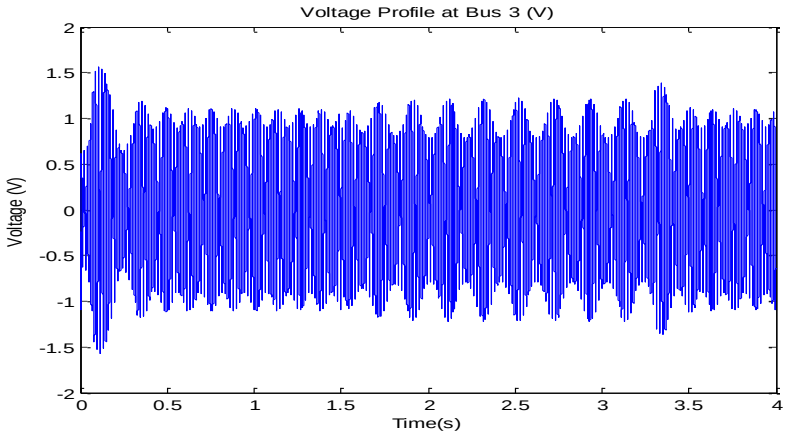

Figure 4-56: Voltage profile at Bus 3 for synchronous generator with STATCOM compensation (Case 1A)

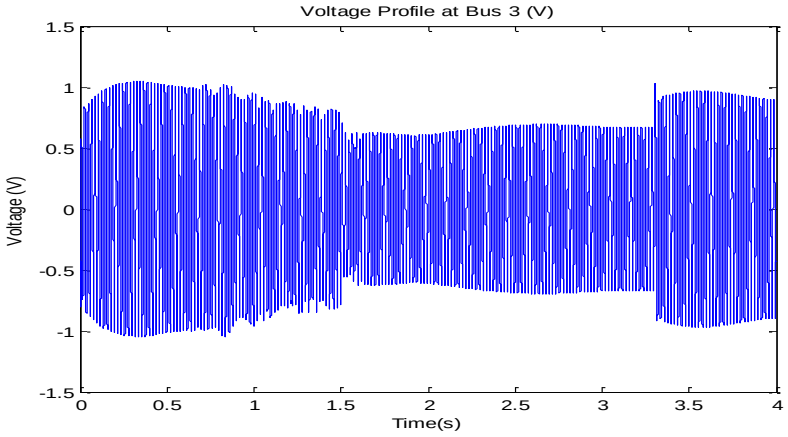

Figure 4-57: Voltage profile at Bus 3 for DFIG (Case 2)

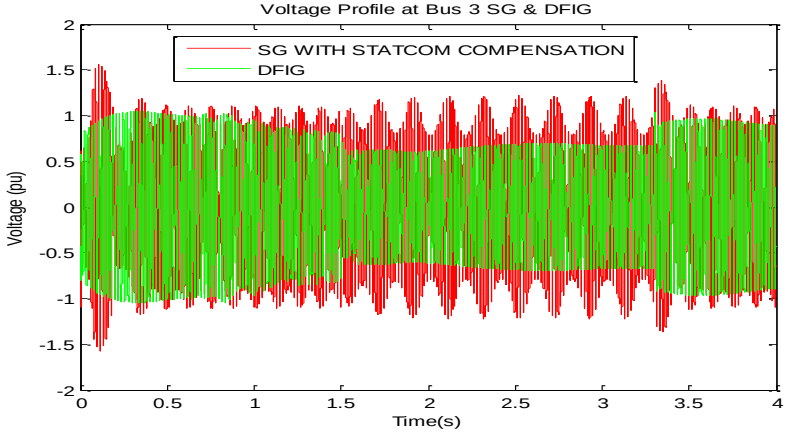

Figure 4-58: Voltage profile comparison at Bus 3 for synchronous generator with STATCOM compensation and DFIG (Cases 1A and 2)

The result figures as shown in Table 4-12 illustrate the capability of the synchronous generator with STATCOM compensation (case1A) to sustain low voltage condition. The results of case 1A are then compared to case 2 results and it is seen that the former provide a better performance in terms of voltage drop, thus active power generated and efficiency.

Table 4-12: Comparison values for Case 1A, 1B and 2

		Pre-fault value	During-fault value	Post-fault value
Active power (MW)	*Synchronous generator with STATCOM compensation (Case 1A)*	12 - 14	Fluctuates around 10 - 15	12 - 14
	DFIG with crowbar control	9	7-8	stabilises to 10
Reactive power (Mar)	*Synchronous generator with STATCOM compensation (Case 1A)*	0	0-2	almost 0
	DFIG with crowbar control	1	1.6	0
Voltage at bus 3 (p.u.)	*Synchronous generator with STATCOM compensation (Case 1A)*	1	0.7	1
	DFIG with crowbar control	1	0.6	1
Voltage at bus 2 (p.u.)	*Synchronous generator with STATCOM compensation (Case 1A)*	1	0.9	1
	DFIG with crowbar control	1	0.75	1

4.5 Discussion of Results

The result graphs presented in chapter 4 show the capability of the synchronous generator with STATCOM control to provide reactive power compensation to the PCC at the connection bus to be able to sustain low voltage condition and ride through. From the voltage and power graphs, it can also be seen that the synchronous generator with STATCOM control provides an enhanced Low voltage ride through than the DFIG with crowbar as the synchronous generator with STATCOM has a smaller voltage drop as compared to the DFIG with crowbar control graph. Moreover, the synchronous generator with STATCOM generates more active power than the DFIG during fault condition. The

comparison can be noted from the voltage profile graphs. As mentioned in the result sections 4.4.1 – 4.4.4, the voltage drop profile of the synchronous generator is higher than the DFIG voltage profile drop at both bus 2 and bus 3. The higher voltage drop during low voltage condition for the synchronous generator with STATCOM compensation can be explained; the rotor side converter of the DFIG is blocked during the complete low voltage time and the rotor windings are connected to the crowbar system. Only the Grid Side Converter is capable of injecting reactive power into the grid. Thus, the effectiveness of the voltage control is limited in the DFIG. However, the synchronous generator with STATCOM reactive compensation, allows the reactive power to be injected at the PCC of the bus during the complete low voltage condition. The LVRT characteristic graph as shown in Figure 2.1 in chapter 2 is respected.

The STATCOM compensation, allows the wind farm to operate to unity power factor generating around 13MW active power and almost zero reactive power. This is because the STATCOM injects reactive power during low voltage condition so that the rating of the STATCOM can be minimized. Thus, with the implementation of the STATCOM in the system, the power factor of the wind farm generated power can be controlled, which is as per the new grid code.

The disadvantages of the DFIG with crowbar should be considered. One of which is the lost in its controllability once the crowbar is triggered. The instability can be explained from the deactivation of the rotor side convertor and the DFIG absorbs a high amount of reactive power from the grid. This can lead to bigger voltage drop. We can thus conclude from the result discussion that the wind energy system with synchronous generator and STATCOM control can be used to replace the commonly used DFIG wind farm with crowbar control as it is more efficient. The results obtained clearly show the practability of the synchronous generator with STATCOM control as it operates as per the new grid code requirement depicted to achieve the fault ride through conditions.

5 CONCLUSION

This project research aim to show the effectiveness of the synchronous generator with STATCOM compensation in terms of the Low voltage ride through condition as per the allowed grid code shown in Figure 2-1 in chapter 2. The LVRT capacity of wind turbine brings large challenges to large scale wind plants connecting to grid with the introduction of new grid codes. Installed wind turbine capacity is in higher demand, thus creating a safer operation of the entire grid. This is because, when the grid fails as a result of grid voltage drop, the large-scale wind turbines cease operation and cause an unstable power system.

Significant voltage drop will induce rotor transient over current, damage converters and even cause wind generators to disconnect from the grid. Large scale disconnection of wind turbines will reduce the system frequency, leading to system stability problems. As the quest for higher performance, higher power wind turbines continues, newly proposed topologies must be measured with respect to their ability to react to grid anomalies. Regulatory agencies in South African and around the world have begun to set minimum standards for wind turbine performance with regards to Low voltage ride through capabilities.

5.1 Contributions

This project theoretically analyses the transient characteristics of a salient pole synchronous generator with STATCOM reactive power compensation as compared to a DFIG with crowbar when the power grid voltage sags. Most of the objectives stated in the initial phase of the project were fulfilled. The proposed ride-through scheme has been successfully tested through simulation on MATLAB/SIMULINK.

The focus of this thesis is mainly to show the ability of synchronous generator to ride through low voltage condition as per the grid code setup from authorities with the help of STATCOM control to provide reactive power compensation to the PCC at the bus of the transmission system. The performance of such synchronous generator is also compared with DFIG using crowbar control as DFIG is the most commonly used wind generator and is well known for its LVRT capability.

Three test cases are used as methodology for this thesis. The test cases are as follows:

- Case 1A: Synchronous generator with STATCOM control
- Case 1B: Synchronous generator without STATCOM control

- Case 2: DFIG with crowbar control

The three test cases are compared as per four test scenarios. The case studies are simulated for each test scenarios to confirm the ability of the synchronous generator to ride through low voltage condition and its better performance to DFIG with crowbar control. The test scenarios are listed in Table 5-1 below:

Table 5-1: Case scenarios 1 - 4

Case Scenario	Low voltage clearing time (s)	Time interval (s)	Voltage drop amplitude (p.u.)
1	*0.11*	*1.50 - 1.61*	*0*
2	*0.5*	*1.50 - 2.00*	*0.29*
3	*1*	*1.50 - 2.50*	*0.4*
4	*1.8*	*1.50 - 3.30*	*0.7*

Investigating the LVRT performance of the synchronous generator with STATCOM compensation as compared to DFIG with crowbar is illustrated and results in the form of graphs are shown.

The graphs clearly show a better performance of the salient pole synchronous generator in terms of low voltage ride through.

5.2 Results and findings

From the results and findings summarised in Table 5-2, the voltage drop during low voltage condition is always higher for the synchronous generator with STATCOM control. This is due to the limited effectiveness of the voltage control in the DFIG. It can concluded that synchronous generator with STATCOM has a better operation of the LVRT than the DFIG as the former has a better design than the latter. The grid side converter of the DFIG can only inject reactive power into the grid as compared to the synchronous generator which can inject reactive power during the whole low voltage period.

The design results show the viability of such STATCOM system implemented on a Synchronous generator and demonstrates the dynamic performance of the system. The STATCOM can achieve the Fault Ride Through conditions on a Synchronous Generator as per the grid code requirements. The objectives stated in the initial stage of the project are fulfilled.

Table 5-2: Case studies and findings

Case Scenario	***Low voltage clearing time (s)***	***Voltage drop (p.u.)***	***RESULTS***		
				Synchronous generator with STATCOM based wind farm (Case 1A)	***DFIG based windfarm (Case 2)***
1	0.11	0	Active Power (MW)	0	0
			Reactive Power (MVar)	8	4
			V at Bus 2 (p.u.)	0.15	0.03
			V at Bus 3 (p.u.)	0.3	0.23
2	0.5	0.29	Active Power (MW)	0 - 15	0
			Reactive Power (Mar)	2	1-6
			V at Bus 2 (p.u.)	0.65	0.29
			V at Bus 3 (p.u.)	0.2 - 0.3	0.28
3	1	0.4	Active Power (MW)	Drops to 3 then just before Low Voltage clearance rises to 28	4.4
			Reactive Power (Mar)	6.4	1 - 2.5
			V at Bus 2 (p.u.)	0.6 - 0.65	0.4
			V at Bus 3 (p.u.)	drops to 0.73	0.5
4	1.8	0.7	Active Power (MW)	Fluctuates around 10 - 15	7 - 8
			Reactive Power (Mar)	0 - 2	1.6
			V at Bus 2 (p.u.)	0.9	0.75
			V at Bus 3 (p.u.)	0.7	0.6

5.3 Suggestions for future work

As future work, various areas can be focused on, to demonstrate the benefits of STATCOM in relation to wind generator applications.

- Investigating through simulations, the impact of changing the size of the STATCOM and its relation on the performance of the LVRT.

- Implementing different strategies for reactive power compensation instead of STATCOM. A comparison can be made between them to show which one offers a better performance.

- Adding longer transmission lines and creating a large scale model, thus investigating the communication delay problems between the wind generator, the STATCOM and the transmission system operator.

- Different inputs to the wind generator can provide a better analysis.

REFERENCES

[1] C.Sourkounis, P.Tourou, “Grid Code Requirement for Wind Power Integration in Europe,” Institute *for Power System Technology and Power Mechatronics, Germany, March 2013*.

[2] International confederation of energy regulators, “Report on Renewable Energy and Distributed Generation,” *Pg17, February 2012*.

[3] S.M.Muyeen, “Introduction Wind Power,” InTech, *Available from* http://www.intechopen.com/books/wind-power/introduction.

[4] K.S.Latha, M.V.Kumar, “STATCOM for Enhancement of Voltage Stability of a DFIG Driven Wind Turbine,” Power *and Energy Systems Conference: towards Sustainable Energy, 2014, India 2014*.

[5] H.Qingjun, Z.Xudong, T.Li, K.Yong, Y.Xiugin, “An accurate transient analysis method for DFIG with crowbar protection under grid faults,” *Industrial Electronics Society, IECON 2013wer and Energy Systems Conference: towards Sustainable Energy, India 2014*.

[6] L.Gustav, H.Tobias, S. Maximilian, S.Peter, B.Martin, “Dynamic grid support in low voltage grids – fault ride through and reactive power r/voltage support during grid disturbances,” *Power systems computation conference, PSCC, Wroclaw, 2014.*

[7] J.Morgan, L.Moran, J.Rodroguez, R.Domke, “Reactive Power Compensation Technologies: State of the Art Review,” *Proceedings of the IEEE Volume: 93 Issue : 12, December 2005.*

[8] S.Ahsan, A.S.Siddiqui, S.Khan, “Reactive power compensation for integration of wind power in a distribution network,” *Pg. 1-4, IICPE, India, December, 2012.*

[9] R.Mittal, K.S. Sandhu, D.K.Jain, “Low Voltage Ride Through of Grid Interfaced Wind Driven PMSG, ” *ARPN Journal of Engineering and Applied Sciences, Volume 4, No5, July 2009.*

[10] P.Bousseay, F.Fesquet, R.Belhomme, S.Nguefeu, T.Chau Tai, “Solutions for the grid integration of wind farms – A survey, ” European Wind Energy Conference and Exhibition, London, 2004.

[11] G.Wenming, W. Yun, H. Shuju, X. Honghua, “A survey on recent Low Voltage Ride Through Solutions of large scale wind farm, ” *Power and Energy Engineering Conference, APPEEC, Asia Pacific, March 2011*.

[12] N.Aparicio, Z.Chen, H.Beltran, E.Belenguer, “Performance of Doubly Fed Wind Power Generators during Voltage Dips, ” *IWRES07, Seoul, 2007*.

[13] B.Singh, “Introduction to FACTS controllers in wind power farms: A technological review, ” *International Journal of Renewable Energy Research, Vol2, No2, 2012*.

[14] F.Blaabjerg, F.LOV, T.Terekes, R.Teodorescu, K.Ma, “Power Electronics – Key Technology for Renewable Energy Systems, ” *EPE-PEMC, Ohrid, 2010*

[15] J.V. Milanovic, Y.Zhang, “Modelling of FACTS Devices for Voltage Sag Mitigation Studies in Large Power Systems.” *Power Delivery, IEEE Transactions on Vol 25, Issue 4, pg 3044-3052, 2010.*

[16] D.Lijie, L.Yang, M.Yiqun, “Comparison of High Capacity SVC and STATCOM in Real Power Grid,” *Intelligent Computation Technology and Automation, ICICTA, USA, 2010.*

[17] P. Lipnick, T.M. Stanciu, “Reactive Power Control for Wind Power Plant with STATCOM”, *Master’s Thesis, Institute of Energy Technology, Aalborg University Denmark, Year 2010*.

[18] Y.Suresh, A.K.Panda,“Dynamic Performance of STATCOM under Line to Ground Faults in Power System”, *PEMD, Brighton, 2010*.

[19] B.Badrzadeh, S. K. Salman, “Enhancement of Fault Ride-through Capability and Damping of Torsional Oscillations for a Distribution System Comprising Induction and Synchronous Generators,” *International Conference on Sustainable Alternative Energy, SAE IEEE PES/IAS, pp. 1-7, 2009*.

[20] H.Li, Z.Chen, “Overview of different wind generator systems and their comparisons,” *Renewable Power Generation, IET, Vol2, Issue 2, 2008*.

[21] J.Morneau, “A comparative evaluation of low voltage ride through solutions in wind turbines using Double Fed Induction Generator,” *Master’s thesis, Dept Electrical and Computer Engineering, McGill University, Canada, May 2008.*

[22] X.Yan, G.Venkataramanan, P.S.Flannery, y.Wang, “Low Voltage Ride Through for DFIG wind turbines using passive impedance networks.” Sustainable Power Generation and Supply, SUPERGEN, Nanjing, 2009.

[23] C.Cho, S.Ryul Nam, S.Kang, S.Ahn, “Modeling of DFIG wind turbines considering fault ride through grid code,” International Conference on Advanced Power System Automation and Protection, Beijing, 2011.

[24] I. Erlich, H.Wrede, C.Feltes, “Dynamic Behaviour of DFIG Based wind turbines during grid faults,” Power Conversion Conference, PCC, Nagoya, 2007.

[25] Z.Zheng, G,Yang, H.Geng, “Short Circuit Current Analysis of DFIG type WG with crowbar protection under grid faults,” ISIE, Hangzhou, 2012.

[26] K.Ibrahima, Z.Chengyong, “Modeling of Wind Energy Conversion System using Doubly Fed Induction Generator Equipped Batteries Energy Storage System,” DRPT, Shandong, 2011.

[27] J.Morneau, C.Abbey, G.Joos, “Effect of Low Voltage Ride Through Technologies on Wind Farm,” EPC, Canada, 2007.

[28] H.EL Helw, A. Khaled, “Comparison Study between two dynamic breaking resistor techniques in protecting the doubly fed induction generator,” EEEIC, Wroclaw, 2013.

[29] G.Komurgoz, T.Gundogdu,” Comparison of salient pole and permanent magnet synchronous machines designed for wind turbines,” PEMWA, Denver, 2012.

[30] I.D.Margaris, N.D.Hatziargyriou,”Direct Drive synchronous generator wind turbine models for power system studies,” MedPower, Cyprus, 2010.

[31] H.S.Ramirez, R.S.Ortigoza, “*Control design techniques in power electronics devices*,” *1st* ed., Springer, 2006.

[32] http://www.wind-energy-the-facts.org/images/chapter1.pdf

[33] D.C. Aliprantis, S.A. Papathanassiou, M.P. Papadopoulos, A.G. Kaladas. 2000, ”Modeling and control of a variable-speed wind turbine equipped with permanent magnet synchronous generator,” *Proc. of ICEM. 3: 558-562, Helsinki, 2000.*

[34] C. Jauch, P. Sorensen and B. Bak-Jensen,” International review of grid connection requirements for wind turbines,” *Nordic wind power conference. Goteborg, March 2004*.

[35] J. Matevosyan, T. Ackermann, S. Bolik and L. Sder, ”Comparison of international regulations for connection of wind turbines to the network,” *Nordic wind power conference, Goteborg. March. 2004*

[36] M. B. C. Salles, A. P. Grilo, J. R. Cardoso, ” Doubly Fed Induction Generator and Conventional Synchronous Generator Based Power Plants: Operation during Grid Fault,” *ICREPQ,2011.*

[37] H. Slootweg, “Wind Power Modelling and Impact on Power system Dynamics.” *PhD thesis, Electrical Power Systems Laboratory, Delft University of Technology,2003.*

[38] S.Khajuria, J.Kaur, “Implementation of Pitch Control of wind turbine using Simulink (Matlab),” *International Journal of Advanced Research in Computer Engineering and Technology, Vol1 Issue 4, June 2012*.

[39] A. J.Baroudi, V.Dinavahi, A.M.Knight. “A review of power converter topologies for wind generators.” *Science Direct Renewable Energy, Volume 32, 2007*.

[40] “Mathworks technical documentation – Wind generation” *Matlab, USA, 2014*.

[41] P.O. Ochieng, A.W. Manyonge, A.O.Oduor, “Mathematical analysis of tip speed ratio of a wind turbine and its effects on power coefficient,”

International Journal of Mathematics and Soft Computing, Vol4, No1, pg 61-66, 2014.

[42] Dr D.B. Chair, Dr F.C. Lee, Dr D.K. Lindner, "Modeling and control of a synchronous generator with electronic load," *Master's thesis, Department of Electrical Engineering, VPEC, Virginia Tech, 1998.*

[43] E.Campero-Littlewood, G.Espinosa-Perez, R.Escarela-Perez, "Transient Analysis of a synchronous generator using a high order state space representation," *CERMA, USA, 2006.*

[44] M.Ravindra, D.G.Kumar, "Design of VSI based STATCOM for eliminating harmonic currents due to non-linear load and to compensate the reactive power in a grid connected system," *International Journal of Engineering research and Applications, IJERA, Vol 2, Issue 6, December, 2012.*

[45] I.H.Khan, "Design and Fabrication of single phase equivalent STATCOM that can absorb or generate reactive power viz. Improve power transmission efficiency," *New Horizons, Vol 11, Issue 1, pg11, January 2012.*

[46] K.E.Okedu, S.M.Muyeen, R.Takahashi, J.Tamura, "Wind Farms fault ride through using DFIG with new protection scheme*," Sustainable energy IEEE Transactions, Vol3, Issue 2, pg 242-254, 2012.*

[47] Z.Zheng, G.Yang, H.Geng, "Short Circuit Analysis of DFIG type WG with crowbar protection under grid faults," ISIE, pg 1072-1079, 2012.

[48] S.Li-ling, Y.Pu, W.Yi, "Simulation research for LVRT of DFIG based on rotor active crowbar protection," *SUPERGEN, pg 1-7, 2012.*

[49] A.Xu, L.Zhang, C.Gu, Y.Zhang, "Crowbar circuit in wind power grid low voltage ride through," CICED, pg 399-402, China, 2014.

[50] J. Matevosyan, T. Ackermann, S. Bolik and L. Sder, "Comparison of international regulations for connection of wind turbines to the network", *Nordic wind power conference, NWPC'04, Gothenburg, Sweden. March 2004.*